# Wood and Plywood as eco-materials for sustainable mobility:a review

B. Castanié, A. Peignon, C. Marc, F. Eyma, A. Cantarel, Joël Serra, R. Curti, H. Hadiji, L. Denaud, S. Girardon, et al.

▶ **To cite this version:**

B. Castanié, A. Peignon, C. Marc, F. Eyma, A. Cantarel, et al.. Wood and Plywood as eco-materials for sustainable mobility:a review. Composite Structures, 2024, pp.117790. 10.1016/j.compstruct.2023.117790 . hal-04337282

**HAL Id: hal-04337282**
**https://hal.science/hal-04337282**

Submitted on 12 Dec 2023

**HAL** is a multi-disciplinary open access archive for the deposit and dissemination of scientific research documents, whether they are published or not. The documents may come from teaching and research institutions in France or abroad, or from public or private research centers.

L'archive ouverte pluridisciplinaire **HAL**, est destinée au dépôt et à la diffusion de documents scientifiques de niveau recherche, publiés ou non, émanant des établissements d'enseignement et de recherche français ou étrangers, des laboratoires publics ou privés.

# Wood and Plywood as an eco-material for sustainable mobility: a review

**B. Castanié[1], A. Peignon[1], C. Marc[2], F. Eyma[1], A. Cantarel[1], J. Serra[1], R. Curti[1], H. Hadiji[1], L. Denaud[2], S. Girardon[2], B. Marcon[2]**

[1] Institut Clément (ICA), Université de Toulouse, CNRS UMR 5312, INSA, ISAE-Supaéro, INSA, IMT Mines Albi, UPS, Toulouse, France

[2] Arts et Metiers Institute of Technology, LaBoMaP, UBFC, HESAM Université, F-71250 Cluny, France

*corresponding author: bruno.castanie@insa-toulouse.fr

Wood has always been used by man for its means of transport. It is only since the beginning of the 20th century that it has fallen into disuse due to the industrial production of concrete, steal and plastic material. However, with an undeniable global warming, the societal challenge of decarbonizing transport may bring it back into the spotlight. In this article, after a brief historical review, arguments about its availability and durability in a bio-economic context are put forward. A review of the main mechanical properties of wood and plywood is then given, along with the main factors influencing both static and dynamic characteristics, the latter being important for the transport sector. Plywood is extensively detailed in this review paper, as it has been widely used in transport applications in the past, and presents potential optimized mechanical characteristics and eco-friendly resource utilization. Some mechanical models are also presented and put into perspective. A brief panorama of wood associations with natural or technical fiber composites is also proposed. Then, selected recent examples show that wood still has its place in naval, automotive, aeronautical, and even space applications. Finally, conclusions and numerous research prospects are offered in this vast and resurgent field.

## 1. Introduction

### 1.1 Objectives and general context

Wood has been used for human mobility since very ancient times for boats more than ten thousand years ago and when the wheel was invented. It is, in a way, the first bio-composite used by man in the field of transport. The first chariots are thought to have been created in the Eurasian Steppes in 4000 BC [1], before the technology spread to Asia Minor, China [2] and as far as the Sahara, as attested by numerous pictograms [3]. One of the earliest illustrations of chariots can be seen on the banner of Ur (a site located in Mesopotamia, today's Iraq) dated between 2700 and 2600 BC and on display at the British Museum [4]. It clearly shows a Sumerian chariot pulled by equids known as "kunga", hybrids between female domestic donkeys and male hemippes, as horses were not yet domesticated at the

time [5]. One of the most famous uses of chariots is the Battle of Kadesh (1247 BC) between the Hittites and the Egyptians, which involved several thousand chariots on both sides, making it probably the largest chariot battle in history (Figure 1). Egyptian chariot technology was remarkable, as shown in the article by Rovetta et al [6]. According to the authors "In fact, they are very similar to the technical and scientific principles used in machine mechanics with some of the modern concepts of today's applications". The aim of this article, however, is not to provide an exhaustive description of the use of wood in mobility over 6,000 years of human history, but rather to present, in the current context of ecological transition, the challenges of using this natural and renewable material for transport applications. Indeed, even if this use is not usually identified in studies, it fits naturally into the context of the bioeconomy and responds to the industrial decarbonization policies advocated by Europe [7]. Europe has set a target of reducing greenhouse gases by 80-95% by 2050, compared to 1990 levels [8]. According to [7], Europe has defined a policy for the forestry industry which aims, among other things, to promote rural development, energy efficiency and the sustainable use of forest products. In particular, the aim is to develop "new and innovative forestry and added-value products". On this last point, the use of wood in the transport sector could be the best candidate to meet this political and societal objective.

**Figure 1. Ur's banner and the battle of Kadesh (Wikipedia commons [4])**

In the second part of this introduction, the availability and durability of wood, as well as its carbon impact and life cycle, will be discussed. This is followed by a review of the main mechanical characteristics of wood and plywood, to illustrate the remarkable properties of this material and its many complexities. Particular emphasis will be placed on dynamic characteristics, an important issue

in the field of transportation. This will be followed by a selection of recent research on wood structures or wood in combination with other materials. Finally, a review of applications showing the evolution of wood uses in the naval, automotive, aeronautical and even space fields will be proposed.

**1.2 Affordability of wood for transportation in the context of bioeconomy and sustainability.**

In this paragraph, the objective is to make an evaluation of the resource to estimate in a rough way if the wood can be used in the field of transport. To this end, selected examples documented in the northern hemisphere and in the southern hemisphere are presented.

At European and American level, wood resources are correctly estimated, as are annual production. According to Eurostat 2021 [9], the wood-based industries employed 3.1 million persons across the EU in 2020 or 10.5% of the manufacturing total. It should be noted that, except for pulp production, which requires large structures, sawmilling, furniture and wood-energy activities are carried out by small, medium-sized, and rural companies. In 2020, the Gross Added value of wood-based industries in the EU was €136 billion or 7.2% of the total manufacturing industry. The roundwood production in Europe was 507 million $m^3$ (with 69% conifers). Production is 25.6% more than at the beginning of 2000. The total resource is estimated at 28.3 billion $m^3$. Production is therefore 1.78%, which is perfectly sustainable. The stocks of timber in forests increased in every Member State, giving a 30.6% growth at the EU level in the period of 2000-2020 which is more than what was harvested.

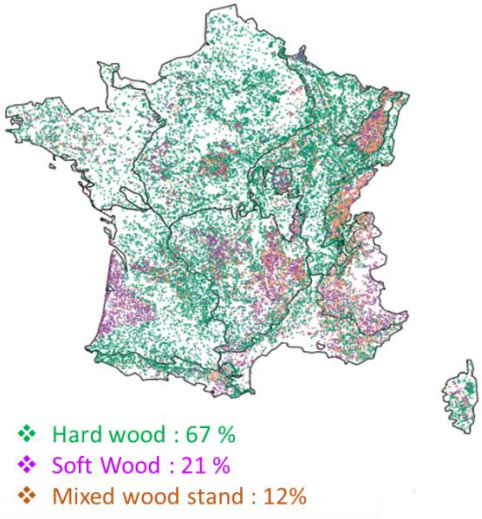


**Figure 2 – Composition of forest stands in metropolitan France [10]**

The total area of woodland in Europe is 159 million hectares, which means that 39% of the EU is covered with forests. In the case of France, forest cover has been steadily increasing over the last century [10]. In 1840, it represented 8.9 million hectares, in 1908 it became 10 million hectares, and today, the French forest covers 31% of the territory with 17.0 million hectares. Forest cover in France has therefore more than doubled in 180 years. The post-war rural exodus and agricultural revolution,

the afforestation of land supported by the National Forestry Fund (1947-1999: 2 million hectares planted) and ongoing reforestation in mountainous areas have all contributed to this expansion. Since 1985, when forest cover stood at 14.1 million hectares, growth has been sustained at almost 80,000 ha per year. Metropolitan France's forests are predominantly hardwood, accounting for 67% of the total forest area (9.9 million hectares). The volume of standing timber in metropolitan France is 2.8 billion cubic meters. The stock of standing timber has risen sharply, from 1.8 billion cubic meters in 1985 to 2.8 billion cubic meters today. That's an increase of almost 50% in just thirty years! The annual volume of abstractions averages 50.1 million cubic meters ($Mm^3$/year) over the period 2011-2019, or 1.78% of the resource. On average, 24.2 $Mm^3$ of hardwood and 25.9 $Mm^3$ of coniferous trees are cut down each year. In metropolitan France, annual mortality averages 10.0 +/-0.4 million cubic meters ($Mm^3$/year) over the period 2011-2019, or 0.4% of the resource. Mortality has increased by 35% in recent years. This increase is due in particular to repeated dry periods and climatic conditions favorable to xylophagous insects, notably bark beetles.

Germany, Europe's largest wood producer, also has similar figures [11]: In Germany, woods cover an area of approx. 111 billion $m^2$, about 31 % of the entire country. Thus, with approx. 3.4 billion $m^3$, Germany has one of the biggest timber resources in Europe. In addition, this amount increases by about 107 million $m^3$ every year whilst the total annual cut is about 56.8 million $m^3$ (mean value of the years 2003 to 2012). Sustainability is embedded safely in the German forest management values, thus, the cultivation and cut cannot be increased to an endangering limit, even if the demand on wood should increase. Another well-documented example is the USA. It is the world's 4th largest country in terms of forest cover, occupying 33% of its territory. Forest cover has remained generally stable over the last 100 years [12]. While U.S. forest land area remains stable, the current forest inventory (volume) has increased by ~60% (Figure 3b) from 1963 because of higher growth (about 3%) and lower removal (about 1.5

A priori, the impact of global warming on European forests will have contrasting effects [13]. A significant reduction in productivity is expected in Mediterranean regions, due to increased drought and fire risk. Climatic risks (storms, droughts, fire and floods) are also increased across the continent. However, it seems possible that other forests will grow faster by absorbing more $CO_2$, expanding northwards or to higher altitudes, and creating more summer wood. According to [10], "Utilizing such benefits, even if they are only of temporary nature, could increase the adaptive capacity of the sector and support long-term adaptation and innovation to better cope with climate change."

Although the overall resource is increasing in the northern hemisphere, it is decreasing dramatically in the southern hemisphere. To illustrate this point, we can focuse on the case of Madagascar. In this country, the forest has shrunk by 40% since 1950 [14], leading to further soil degradation [15]. According to Rajemison [16], the direct causes of deforestation are conversion to agricultural land, the

local collection of wood for energy and clearing for pasture. Indirect causes include changes in export prices for wood products, migration and land ownership. For Madagascar, the main direct factors contributing to this loss of forest cover are agricultural clearing, fires and irrational exploitation. Deforestation and resource degradation are essentially due to these uses. These generally relate to goods such as timber and non-timber products, forest space as an economic production medium for agriculture and livestock farming, and forest subsoil through mining. Added to this is the proliferation of illegal harvesting in the country in recent years, which has led to significant degradation of resources. The development of this type of activity can be explained by the growing demand for wood on internal and external markets. In addition to this decline in the productive potential of Madagascar's forests, there are also major threats to forest resources. The causes are the degradation of exploitable areas, amplified by the population's growing need for wood products, which is keeping pace with demographic growth (2.8% per year) and market requirements. The causes of deforestation identified in the case of Madagascar can be generalized [14-16]: demographic factors, institutional factors, local economic factors, the type of local resource and wood extraction (mainly fuelwood for local use), and the expansion of agriculture. Nevertheless, the cases of countries and continents are very diverse: for example, there has been virtually no decrease in forest cover in Gabon in recent years [17].

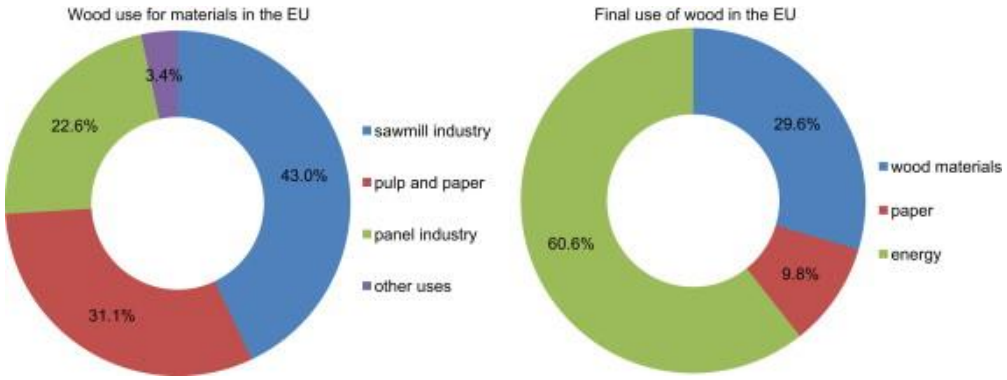


**Figure 3. The use of wood in the European Union (Reproduced from [9])**

In conclusion, there is great potential in Europe for the use of wood in innovative applications, as the resource exists and is largely available. Today, wood production flows in Europe can be seen in figure 3 [7, 18]. It can be noted, for instance, that 31.1% of production is dedicated to the paper industry, while worldwide use of wood has reached a plateau and is declining. It should be noted that wood is also used in cascades, i.e. recycled several times in various forms [7, 18]. At the end of the cycle, 60% of it is used as wood energy (see figure 3).

An additional benefit is the low energy cost of wood processing compared with other materials, as shown by Kolh et al [11], figure 4. Finally, increased use of wood enables better $CO_2$ sequestration, as shown by Negro et al [19] for the furniture and construction industry. For an average European

apartment, the quantity of carbon stored is estimated at 3531 kg, which corresponds to the $CO_2$ emitted by about 3 cars driving 10,000 km in a year and emitting 120 g of $CO_2$ per km. The fact that it is also a local resource and essentially processed locally greatly reduces the need for transport, which induces a positive feedback. Studies such as that by Bergman et al [20] on the $CO_2$ impact of wood use conclude that in all the cases they studied "The reduced carbon emission impacts associated with woody biofuel use and storage of carbon in long-lived wood products result in lower net carbon emissions of wood products compared with non-wood product alternatives. For the cases we evaluated, the combined GHG emissions reductions due to biofuel usage, carbon storage, and avoided fossil emissions are always greater than the wood product manufacturing carbon emissions". However, the authors point out that this result is only valid in the case of rational forest use. In [21], Peskinen et al summarize 51 studies on substitution factors. They conclude that "Overall, the 51 reviewed studies suggest an average substitution effect of 1.2 kg C / kg C, which means that for each kilogram of C in wood products that substitute non-wood products, there occurs an average emission reduction of approximately 1.2 kg C".

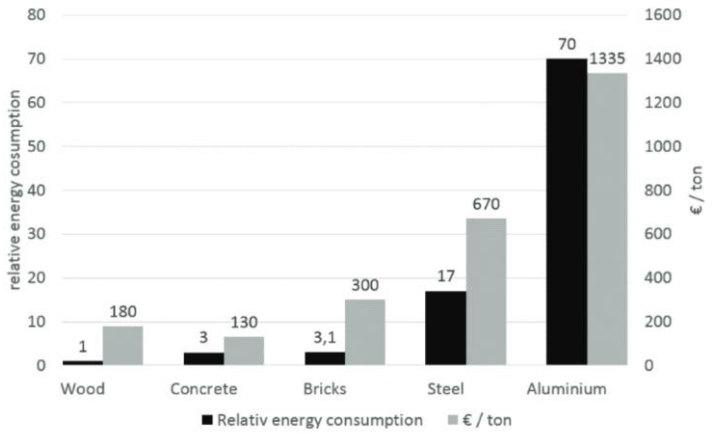


**Figure 4 – Costs and energy consumption of usual construction materials processing relative to cost and energy consumption of wood processing [11].**

All in all, while detailed studies are needed on the potential impact of widespread use of wood in means of transport, the authors can venture to consider the wood-based family car as an additional piece of furniture or part of the frame of the house. This use seems compatible with the scenarios for the use of forest resources in Europe (high, medium or low mobilization scenario [9]).

## 2. Wood structure and material remarkable properties

### 2.1 Overview and internal structure

Wood is a natural material with three main functions: conduction of sap, mechanical support of the tree, and reserve tissue. As a natural material made by a living tree, wood is heterogeneous and

variable at different scales. So, it is important to study it at several scales in order to understand its macroscopic mechanical properties. By its very nature and mode of growth, the tree is an oriented heterogeneous material, with a main stiffness direction toward the fiber direction (main axis of the tree). To describe it, we'll use three main directions (see figure 5) in a cylindrical coordinate system:

- the longitudinal direction (L), which corresponds to the main axis of the trunk,
- the tangential direction (T), corresponding to the growth-ring axis,
- the radial direction (R), perpendicular to the other two directions (L and T), and therefore oriented from the pith to the bark.

These directions give rise to three planes that can be seen in Figure 5 to describe the internal structure of the wood: the transverse plane (RT) formed by the radial and tangential directions, the radial plane (LR) oriented by the longitudinal and radial directions, and the tangential plane (LT) defined by the longitudinal and tangential directions.

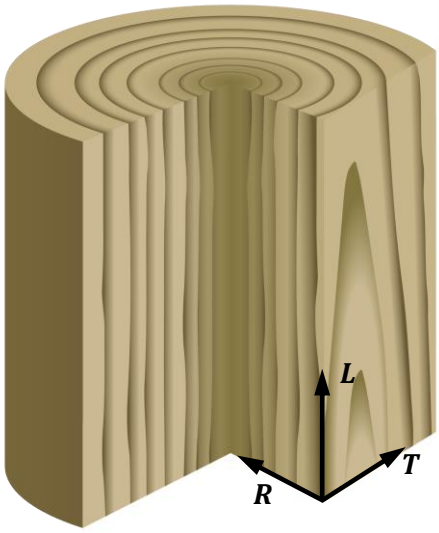


**Three directions :**

- **Longitudinal (L)**
- **Tangential (T)**
- **Radial (R)**

**Three plane :**

- **Transverse (RT)**
- **Radial (LR)**
- **Tangential (LT)**

**Figure 5 - Illustration of the three planes and directions used to describe wood [22].**

There are two main classes of tree: hardwood and softwood:

- softwoods are gymnosperm plants, i.e., plants whose ovule is bare and borne by leaf parts grouped on a twig. Unlike hardwoods, these plants have almost no differentiated cells, and their sap-conducting and mechanical-supporting roles are performed by the same cells called tracheids. Spruce, Douglas fir and fir are examples of softwoods,
- hardwoods are angiosperm plants, commonly known as flowering trees, which produce leaves. They are characterized by the presence of vessels in their wood, which are cells dedicated to the sap transport. So, in the case of deciduous trees, cells are specialized. Mechanical support and sap conduction are not carried out by the same cells. Beech, poplar and oak are examples of hardwoods.

On a macroscopic scale, wood is made up of several elements, listed from the inside out [23]:

- the heartwood, also known as “perfect wood”, in which all cells are dead. This is the central part of the tree, contributing to its rigidity. It's also what's generally sought after in industry,
- sapwood or newly-formed wood, in which the parenchyma cells are alive. It may be lighter (with a few exceptions) or darker in color than the heartwood depending on the wood species, in which case the wood is said to have differentiated sapwood,
- the cambium is made up of a set of generative cells that allow the wood to grow,
- the liber, also known as inner bark, which conducts the elaborated sap,
- the outer bark, composed of cork and phelloderma, which protects the tree from the outside environment.

These elements can be seen in Figure 6, which shows a cross-section of a tree trunk.

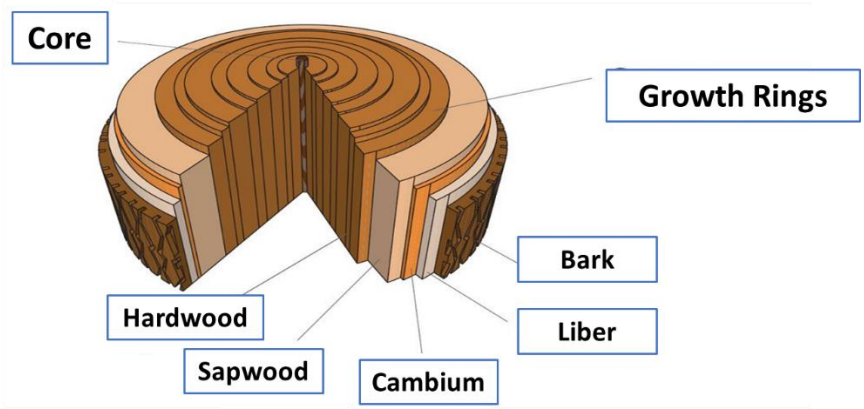


**Figure 6 – Cross section of a tree trunk.**

In temperate regions, during wood formation, there is a difference between wood formed in spring called earlywood, and that which formed in summer called latewood. Spring wood needs larger cells for the transport of nutrients and water by the sap, so it will be lighter and less dense than summer wood, which has thinner cells because the need for nutrients and water is less at the end of the growing season. These two kinds of woods form an overlapping cylindrical layer known as the annual ring or growth ring. There is also a difference between juvenile wood (the rings closest to the core), which is less rigid than mature wood (the rings closest to the bark). Those elements, regarding engineering wood products as shown by Rahayu et al [24] have shown that, in the case of poplar, the stiffness and elastic modulus of plywood or veneers made from mature wood is 15 to 20% higher, on average, than that of panels or veneers made from juvenile wood. This was also shown by Gaborik and Kacerova on poplar LVL made with juvenile and mature wood [25]. In addition to the heterogeneity of mechanical properties, wood density can differ significantly between initial and final wood for certain species (Table 1).

| Species | Kind | Density of earlywood | Density of latewood | Earlywood longitudinal Young's modulus (GPa) | Latewood longitudinal Young's modulus (GPa) |
|---|---|---|---|---|---|
| Douglas | Softwood | 0.29 | 0.82 | 18.24 | 45.51 |
| Scot Pine | Softwood | 0.30 | 0.92 | 11.38 | 21.58 |
| Spruce | Softwood | 0.30 | 0.60 | 29.33 | 35.41 |
| Poplar | hardwood | 0.40 | 0.48 | - | - |

**Table 1 - Average density and Young's modulus of earlywood and latewood of various wood species [26]**

The wood cells are also oriented, either longitudinally, for sap conduction in the direction of the wood fibers, or radially. The latter are known as wood rays. The microstructures of hardwoods differ from those of softwoods [22]. The cells that make up wood are mainly composed of celluloses (40%), hemicelluloses (30%) and lignin (30%) [27]; the relative percentage kind slightly change depending on the wood specie considered. Cellulose, in the form of microfibrils, acts as reinforcement. Hemicelluloses and lignin act as the matrix in which cellulose is found [26].

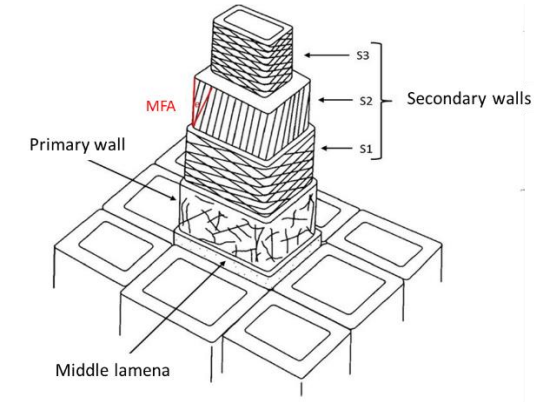


**Figure 7 - Schematic of a wood cell [31].**

The cell wall is made up of the following elements, visible in Figure 7:

- the middle lamella, which acts as intercellular cement. It is common to two neighboring cells and non-fibrillar. It contains no cellulose,
- primary wall made up of a network of cellulose microfibrils, making it extensible,
- S1 secondary wall: cellulose fibrils are horizontal,
- S2 secondary wall, where the cellulose fibrils, namely the microfibrils, are almost vertical and all parallel. This is the thickest wall, and therefore has the greatest influence on the wood's mechanical properties. The angle formed by these fibrils is called the micro-fibril angle (MFA). The smaller the angle, the stiffer the wood. This explains the difference in flexibility between juvenile and mature wood [28].
- secondary wall S3 looks like secondary wall S1 [29, 30].

**2.2 Main mechanical properties**

Due to its structure presented in the previous paragraph, on the scale of a thin wooden board, wood behaves like an orthotropic material in the reference frame $(\vec{L}, \vec{T}, \vec{R})$. Its elastic behavior is thus represented by the following symmetrical Hooke's stiffness matrix:

$$\begin{pmatrix} \varepsilon_L \\ \varepsilon_R \\ \varepsilon_T \\ \gamma_{RT} \\ \gamma_{LT} \\ \gamma_{LR} \end{pmatrix} = \begin{pmatrix} \frac{1}{E_L} & -\frac{\nu_{RL}}{E_R} & -\frac{\nu_{TL}}{E_T} & 0 & 0 & 0 \\ -\frac{\nu_{LR}}{E_L} & \frac{1}{E_R} & -\frac{\nu_{TR}}{E_T} & 0 & 0 & 0 \\ -\frac{\nu_{LT}}{E_L} & -\frac{\nu_{RT}}{E_R} & \frac{1}{E_T} & 0 & 0 & 0 \\ 0 & 0 & 0 & \frac{1}{G_{RT}} & 0 & 0 \\ 0 & 0 & 0 & 0 & \frac{1}{G_{TL}} & 0 \\ 0 & 0 & 0 & 0 & 0 & \frac{1}{G_{RL}} \end{pmatrix} \begin{pmatrix} \sigma_L \\ \sigma_R \\ \sigma_T \\ \tau_{RT} \\ \tau_{LT} \\ \tau_{LR} \end{pmatrix} \qquad \text{Equation 1}$$

where:

- $\mathrm{E_L}, \mathrm{E_R}$ et $\mathrm{E_T}$ are the Young Moduli along the three axes,
- $\mathrm{G_{RT}}, \mathrm{G_{TL}}$ et $\mathrm{G_{RL}}$ are the Shear Moduli along the three planes,
- $\nu_{\mathrm{TR}}, \nu_{\mathrm{LT}}, \nu_{\mathrm{RL}}, \nu_{\mathrm{RT}}, \nu_{\mathrm{TL}}$ et $\nu_{\mathrm{LR}}$ are the Poisson's Ratios.

Due to the symmetry of the matrix : $\frac{\nu_{\mathrm{LR}}}{\mathrm{E_L}} = \frac{\nu_{\mathrm{RL}}}{\mathrm{E_R}}$, $\frac{\nu_{\mathrm{LT}}}{\mathrm{E_L}} = \frac{\nu_{\mathrm{TL}}}{\mathrm{E_T}}$ et $\frac{\nu_{\mathrm{RT}}}{\mathrm{E_R}} = \frac{\nu_{\mathrm{TR}}}{\mathrm{E_R}}$. This explains why, expressed in the orthotropic reference, the stiffness matrix is resumed by only nine independent elastic constants. The properties of wood depend on the direction of stress, but also on the species through the ligneous plane and therefore the microstructure specific to each species. For many species, certain stress directions offer better mechanical properties; namely: for the moduli of elasticity: $\mathrm{E_L} >> \mathrm{E_R} > \mathrm{E_T}$ , for the shear moduli: $\mathrm{G_{RL}} > \mathrm{G_{TL}} > G_{\mathrm{RT}}$, and for the Poisson's ratios: $\nu_{\mathrm{TR}} > \nu_{\mathrm{LT}} > \nu_{\mathrm{RL}} > \nu_{\mathrm{RT}} > \nu_{\mathrm{LR}} > \nu_{\mathrm{TL}}$. Table 2 presents the elastic constants of some species of wood.

The strength of wood also depends on the sign of stress. There is a significant difference in stress at break between tensile and compressive stresses. Overall, tensile strength is twice as high as compressive strength in the L-axis, but tensile strength in the L-axis is the quarter of compressive stress in T or R-axis. It's also important to note that in compression, wood exhibits significant deformation: it behaves like a ductile material, which is not the case in tension, where wood is considered a brittle material (Figure 8). The dispersion of these properties remains significant due to the heterogeneity of the wood material. Table 3 shows the mechanical strengths of various wood species in relation to

different mechanical stresses. These mechanical properties differ from one species to another, but also within the same species [24].

| | Softwood | | | Hardwood | | |
|---|---|---|---|---|---|---|
| Properties | Pine | Fir | Sequoia | Poplar | Balsa | Birch |
| Moisture contents (%) | 12 | 12 | 12 | 12 | 12 | 12 |
| Density (g/cm$^3$) | 0.51 | 0.35 | 0.38 | 0.46 | 0.16 | 0.62 |
| $E_L$ (MPa) | 12,300 | 10,000 | 9,200 | 10,900 | 34,000 | 13,900 |
| $E_R$ (MPa) | 959.4 | 390 | 818.8 | 468.7 | 510 | 695 |
| $E_T$ (MPa) | 1389.9 | 1020 | 800.4 | 1002.8 | 1564 | 1084.2 |
| $G_{RL}$(MPa) | 996.3 | 580 | 708.4 | 752.1 | 1258 | 945.2 |
| $G_{RT}$(MPa) | 1008.6 | 700 | 607.2 | 817.5 | 1836 | 1028.6 |
| $G_{TL}$(MPa) | 159.9 | 60 | 101.2 | 119.9 | 170 | 236.3 |
| $\nu_{RL}$ | 0.292 | 332 | 0.346 | 0.392 | 0.488 | 0.451 |
| $\nu_{TR}$ | 0.328 | 0.341 | 0.36 | 0.318 | 0.229 | 0.426 |
| $\nu_{LT}$ | 0.362 | 0.336 | 0.4 | 0.329 | 0.231 | 0.426 |

**Table 1 - Elastic mechanical characteristics of some softwoods and hardwoods [22]**

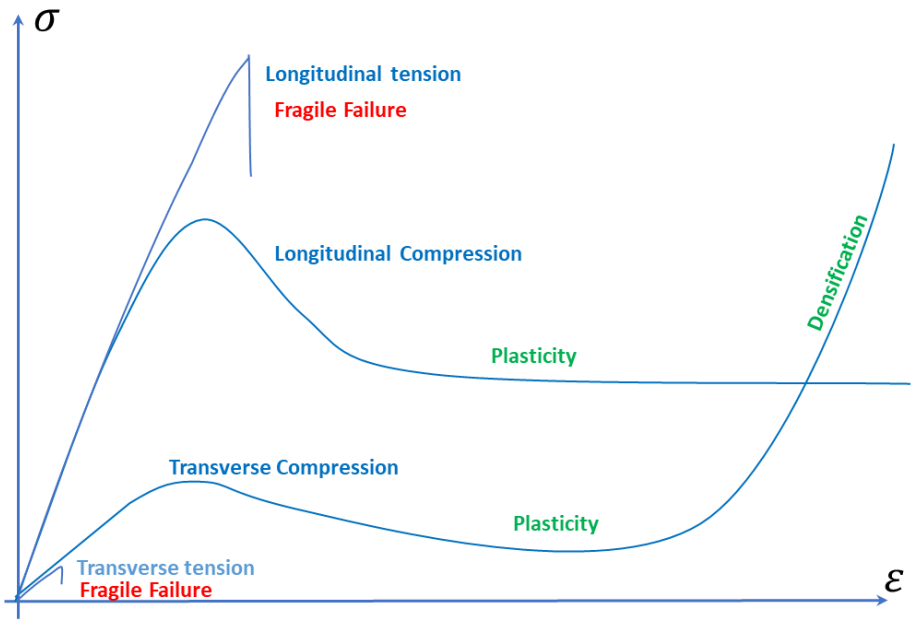


**Figure 8 – Typical stress-strain curve for wood loaded in tension and compression [22].**

| | Species | | | |
|---|---|---|---|---|
| | Fir, spruce | Pine, Douglas fir, larch | Oak | Iroko |
| Average density at H = 12 % moisture content | 0.40 | 0.45 | 0.65 | 0.65 |
| Axial Compression (MPa) | 35 - 45 | 40 - 50 | 50 - 80 | 40 - 60 |
| Axial tension (MPa) | 90 - 100 | 100 - 120 | 120 - 150 | 100 - 120 |
| Bending (MPa) | 50 - 70 | 80 - 90 | 100 - 150 | 80 – 1,300 |
| Transverse Compression (MPa) | 6 - 8 | 7 - 8 | 18 - 20 | 12 - 15 |
| Transverse Tension (MPa) | 1 - 1.5 | 1.5 - 2 | 3 - 5 | 3 - 4 |

**Table 2 - Average strengths of some species [32, 33]**

The failure mode in tension is generally brittle, whereas the modes of failure in compression and shear are more complex. Depending on the direction in which the wood is loaded in compression (longitudinal, radial or tangential), its failure scenario differs, in line with the wood's orthotropy. For longitudinal loading (L), three successive phases are observed (Figure 8), which are very common in cellular structures (foam, honeycombs [33, 34]):

- an initial elastic phase in which stress evolves linearly with strain; the modulus of elasticity in tension is equal to that in compression,

- a load peak followed by a drop in stress, corresponding to local buckling of the wall, and then a progression of the buckling wave,

- a region of consolidation and densification, where stress increases sharply. The lobes of the buckled walls are superimposed (Figure 8).

When subjected to radial (R) or tangential (T) compression, the stress-strain curves are similar (Figure 8), but the failure mechanisms are different. This explains why the stiffness of wood under this type of load is lower than under longitudinal compression [35, 36]. These behaviors depend on a number of factors, such as wood density, moisture content, external temperature, and type of loading [37]. Six cases of failure in longitudinal compression can be identified [30] (Figure 9). Kinking is a local buckling of wood fibers (Figure 9, f), very similar to that observed in composite materials [38]. In addition, 4 case of failure in longitudinal tension are showed Figure 9.

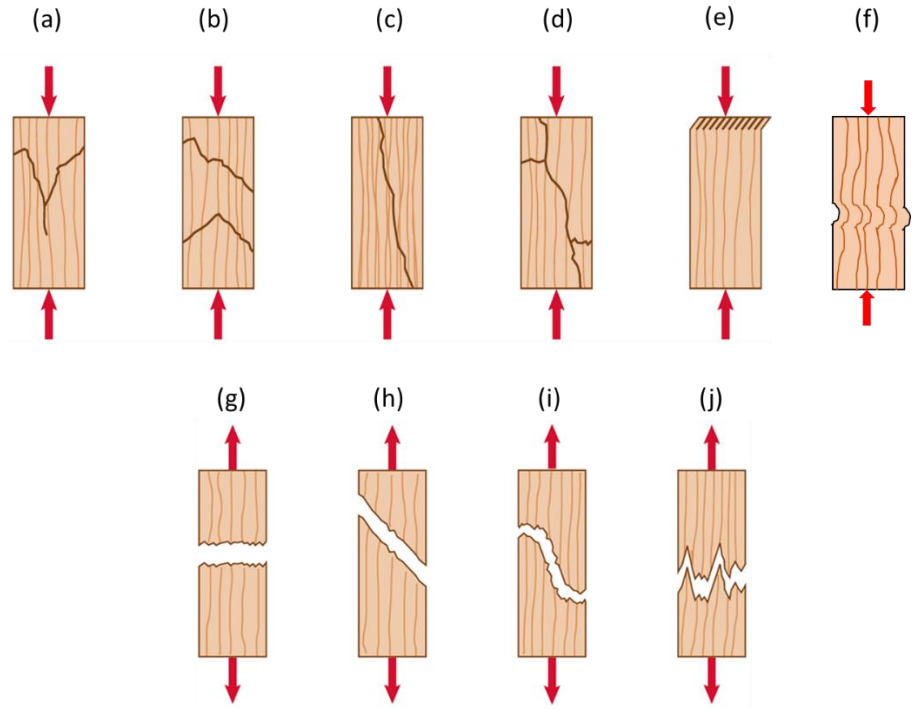


**Figure 9 – Failure in longitudinal compression: (a) failure by fiber crushing, (b) bevel splitting, (c) simple splitting, (d) splitting by transverse failure, (e), extremities crushing, and (f) kinking. Failure in longitudinal tension: (g) pure tension, (h) shearing, (i) tension + shearing, (j) tension + splitting**

To conclude this overview of the usual mechanical properties of wood, it is noticeable that a crucial mechanical property for the development of structured materials is the specific rigidity, i.e. rigidity (Young's Modulus) divided by density.

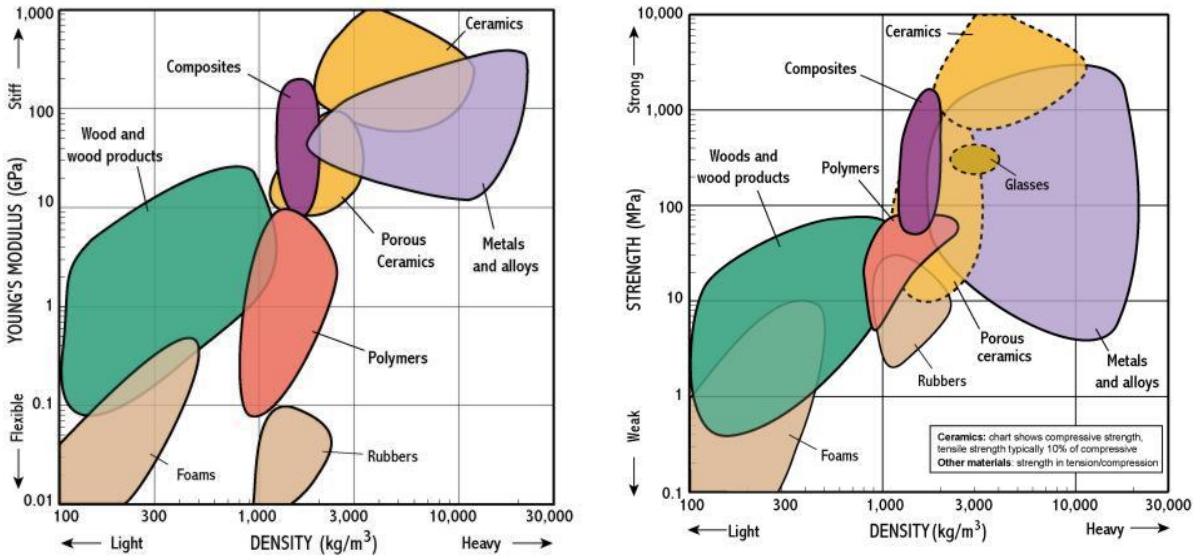


**Figure 10: modulus–density chart for common mechanical construction materials (left) and strengh-density chart (right) [39].**

This is even of greater concern for the design of parts dedicated to being integrated into vehicles, where the minimization of the overall mass is primordial. Indeed, regarding this criterion, thanks to its

low density and average mechanical properties, wood performs very well. It has a high rigidity/density and strength/density ratios when loaded parallel to the grain and a rigidity/density$^3$ ratio higher than most other mechanical construction materials (the later ratio being related to the flexural modulus per unit mass). An illustration of the position of wood among the other usual materials is shown in Figure 10 with the form of an Ashby diagram [40] commonly used today for material selection.

## *2.3 Main factors influencing the mechanical properties of wood*

### *2.3.1 Wood density*

Wood density is a function of many parameters, such as the presence of porosity in the wood, the presence of knots or various defects, the presence of resin or extractives, the ratio between final earlywood and latewood or between sapwood and heartwood, temperature or moisture content. Density also depends on the species of wood [32]. It is directly correlated with the wood's mechanical properties: the denser the wood, the more rigid and resistant it is, whatever the applied stress. This property applies to all wood species for which a linear evolution between mechanical properties and wood density can be observed (Figure 11) [22].

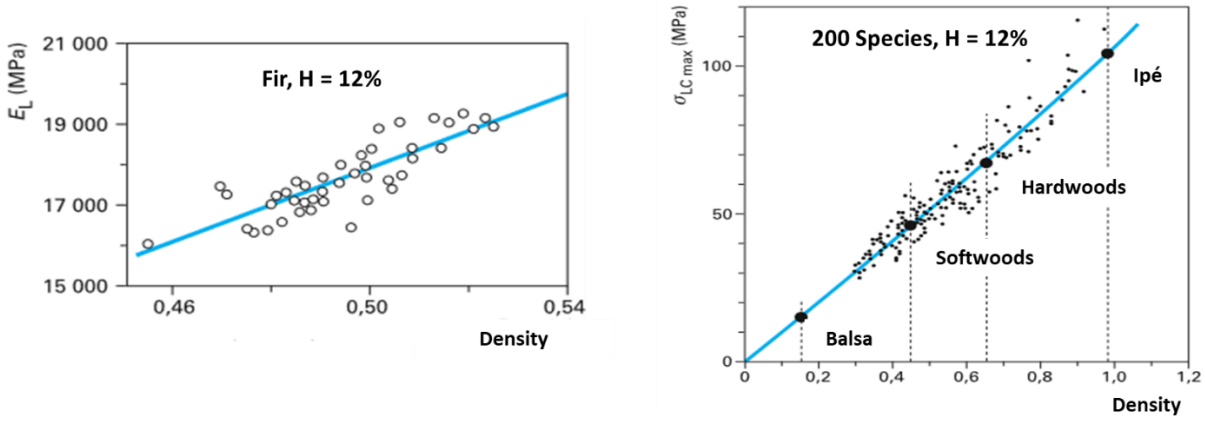


**Figure 11 – Evolution of longitudinal Young's modulus for fir (right) and compressive stress at break for several species (left) as a function of wood density [22].**

The linear relationship between the mechanical properties of wood and its density is reliable [23]. As we'll see later for moisture content and temperature, corrective formulas can be used to determine wood properties for a given density. Moduli of elasticity can then be calculated from a wood's density as shown in Table 4:

| Modulus | Elastic modulus (MPa) versus density d | |
|---|---|---|
| | Hardwood H = 12% | Softwood H = 12% |
| EL | = 14 400 (d / 0.65)1.03 | = 13 100 + 41 700 (d - 0.45) |
| ER | = 1 800 (d / 0.65)1.3 | = 1 000 + 2 370 (d - 0.45) |
| ET | = 1 030 (d / 0.65)1.74 | = 636 + 1 910 (d - 0.45) |
| GTL | = 971 (d / 0.65)1.26 | = 745 + 989 (d - 0.45) |
| GLR | = 1 260 (d / 0.65)1.14 | = 861 + 2 080 (d - 0.45) |
| GRT | = 366 (d / 0.65)1.74 | = 83.6 + 228 (d - 0.45) |
| EL | = 14 400 (d / 0.65)1.03 | = 13 100 + 41 700 (d - 0.45) |
| ER | = 1 800 (d / 0.65)1.3 | = 1 000 + 2 370 (d - 0.45) |
| ET | = 1 030 (d / 0.65)1.74 | = 636 + 1 910 (d - 0.45) |
| Domain of validity | 0.1 < d < 1.2 | 0.3 < d < 0.6 |

**Table 4 – Elastic Modulus (MPa) versus density d [23].**

### *2.3.2 Moisture effects*

Wood is an hygroscopic material, meaning that it absorbs or loses moisture depending on the external conditions of its environment, i.e. temperature and relative humidity of the ambient air (noted RH). Depending on external conditions, the moisture content (MC) of wood will stabilize at an equilibrium moisture content (EMC), as described in Figure 12 [23]:

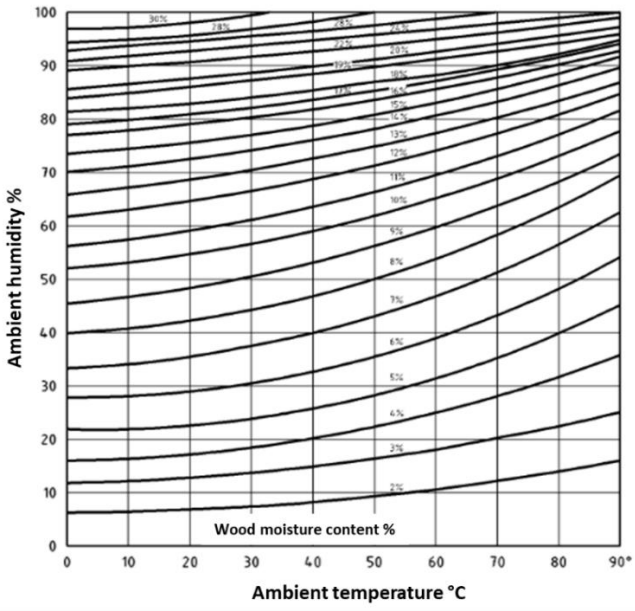


**Figure 12 - Hygroscopic balance of wood as a function of temperature and relative humidity of the ambient [23].**

When the humidity of the ambient air is close to 100% and the temperature is around 20 °C, the wood tends to stabilize around a moisture content called the “Fibre Saturation Point” (FSP). FSP is around 30% for almost all wood species. The moisture content of wood having influences on its mechanical properties, one will generally find in the literature the characteristics of wood for a reference moisture content of 12% corresponding to the average moisture content of wood in use (indoor building etc); to simplify, this moisture content of 12% is generally observed for external conditions of 65% RH and 20 °C. When the moisture content of the wood is below the FSP, there is an effect of the moisture content on the mechanical properties of the wood, i.e fracture properties and elastic properties (Figure 13 and Figure 14) are depending on inner moisture content. Beyond the FSP, these properties remain stable depending on the moisture content of the wood. It can be seen that the lower the moisture content of the wood, the more its mechanical rigidity and its resistance to various mechanical stresses increase (except for the tensile tests (longitudinal and transverse direction) which present an optimum breaking strength for a certain humidity level (Figure 13)).

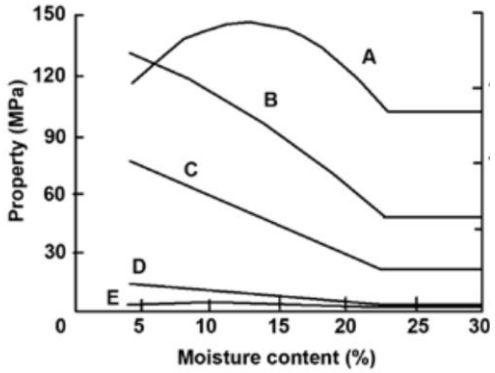


**Figure 13 - Effect of moisture content on the strength properties of wood. A: tension parallel to the grain; B: bending; C: compression parallel to the grain; D: compression perpendicular to the grain; and E: traction perpendicular to the wire [32].**

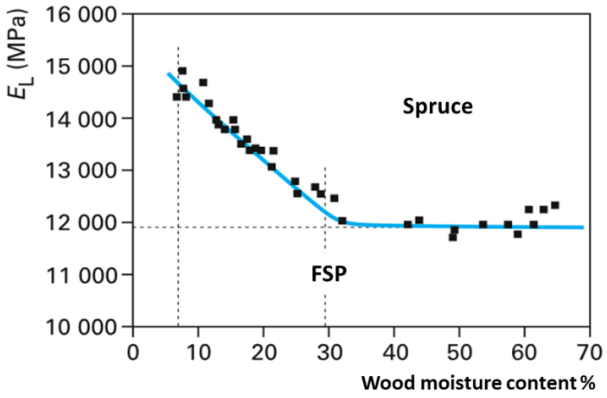


**Figure 14 - Influence of the moisture content of spruce wood on its longitudinal modulus of elasticity [23].**

The moisture content also influences the wood geometry, deforming in proportion to the change in moisture content only below the FSP (< 30%); above the FSP no dimensional change is observed. As

moisture content increases, wood tends to swell, and conversely, as moisture content decreases, it tends to shrink. This phenomenon depends also on wood direction (i.e. L, T and R). These differences in shrinkage/swelling coefficients between wood directions can lead to anisotropic deformations (Figure 15). Axial (or longitudinal) shrinkage is the smallest among the three directions, and is generally neglected. The tangential shrinkage is the most important, approximately two times higher than the radial shrinkage and twenty times higher than the axial shrinkage. These values will be different for each species, but also for each species as for all the wood properties already studied. Values for these shrinkages can be found in Trouy [22].

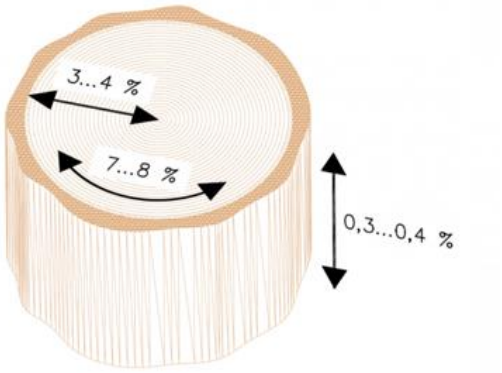


**Figure 15– Shrinkage values as a function of wood direction [29]**

These differences in shrinkage in the same wood generate deformations on a macroscopic scale. Figure 16 illustrates the main deformations that can be observed when the moisture content of wood boards varies.

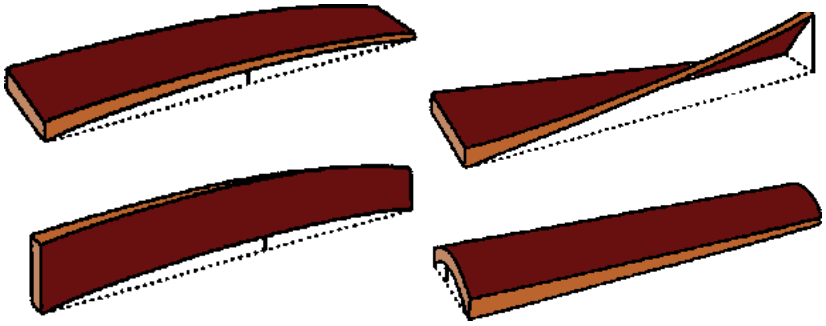

**Figure 16 – Main deformations of wooden boards due to moisture content modification, from its green state to its dry state for instance [41]**

### *2.3.3 Temperature.*

The cellulose, hemicellulose and lignin that make up wood are biopolymers, composed of macromolecules and derived from low-molecular-weight molecules. Polymers and biopolymers have a temperature that defines the transition from a glassy (solid) state to a rubbery state. This latter temperature is called the glass transition temperature, usually noted $T_g$. It depends, for example, on

the nature of the wood and its species, the density of the wood or its relative humidity [23], and as common polymers (wood being composed of biopolymers) of the speed of solicitation (or dynamic excitation) for instance during dynamical mechanical tests (Hopkinson bar, vibrational, AFM…). In addition, cellulose, hemicellulose, and lignin have their own glass transition temperatures. " The glass transition temperature is 40 °C for hemicelluloses, 50 °C to 100 °C for lignin, and above 100 °C for cellulose [41, 42]. At constant moisture content and below 150 °C, the mechanical properties of wood are approximately linearly related to the temperature. Below 100 °C, a rapid temperature change will result in essentially reversible property changes [32]. At a constant moisture content, an increase in temperature causes a reduction in the mechanical properties of the wood by softening it. The curves in Figure 17 show the relationship between elastic modulus and stress at break in relation to wood temperature. Corrective coefficients such as those proposed by Palka et al [43] can be used.

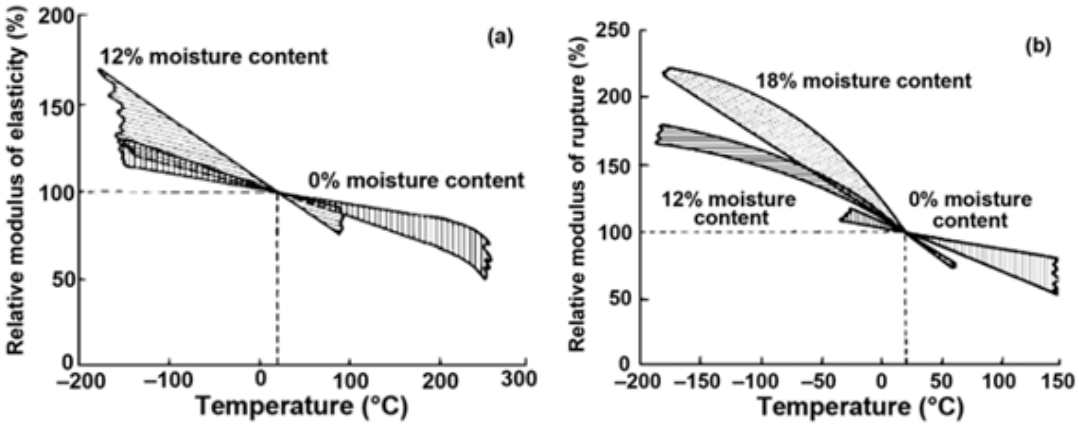


**Figure 17 – Summary of several studies linking the influence of temperature on the properties of wood: elastic modulus (a) and breaking stress (b) [32].**

Where temperatures are high and wood is exposed to them for long periods, irreversible effects are observed on its mechanical properties. These include loss of mass and stiffness, degradation of the wood constituents, and the creation of a charcoal layer on the material outer shell. These irreversible degradations depend on factors such as wood moisture content, temperature, exposure time, heat

source, species and sample size (Figure 18). This point should be borne in mind, for example, when bonding composite or metal skins to wooden cores [44].

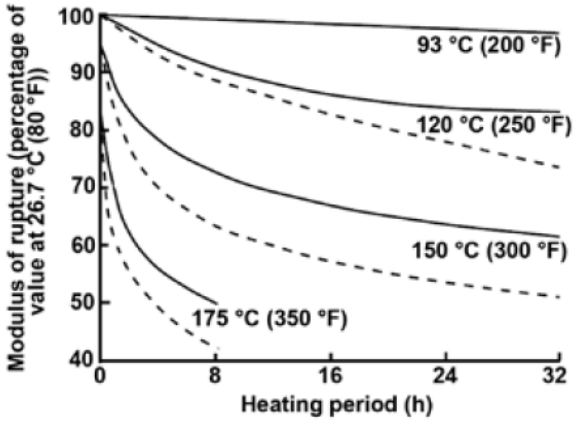


**Figure 18 – Relative modulus of rupture of wood as a function of irreversible damage caused by heating with water (solid lines) and steam (dashed lines) [32]**

### *2.3.4 The singularities in the wood.*

Since wood is a natural material, it contains a variety of heterogeneities, such as its irregularly distributed density, growth singularities or defects, and the diversity of cell natures and shapes that make it up. These singularities can give rise to three main defects in wood [27]:

- the grain slope, or wood grain, which designates the deviation of wood fiber orientation either from the longitudinal axis of the wood, or from the long axis of a machined part. The angle of deviation is never zero. This inclination of the grain can cause local stresses, leading to premature wood failure (Figure 19, left),
- knots are a modification of the wood caused by the growth of a branch. This causes local deviation of the wood's grain fibers around the knots as shown firstly by Shigo et al. [45], and more recently with very advanced and accurate imagery technics Hu et al. [46]. This local irregularity of the grain around a knot leads to mechanical weakening of the wood [47, 48, 49, 50] (Figure 19, right). The density of the knot is also greater than that of the wood. Billard et al. measured an increase in average knot density compared with average wood of 83% for white fir, 92% for Norway spruce and 64% for Douglas fir,
- splits are narrow openings in the wood, mainly due to the wood humidification/drying cycles during more or less abrupt changes in humidity or temperature. They create a void in the material, reducing its mechanical properties,
- reaction wood which is formed when a trunk is exposed to a mechanical stress due to wind or soil inclination grows with a different anatomy to ensure the stability of the whole structure. It results in different mechanical and biochemical local properties [51].

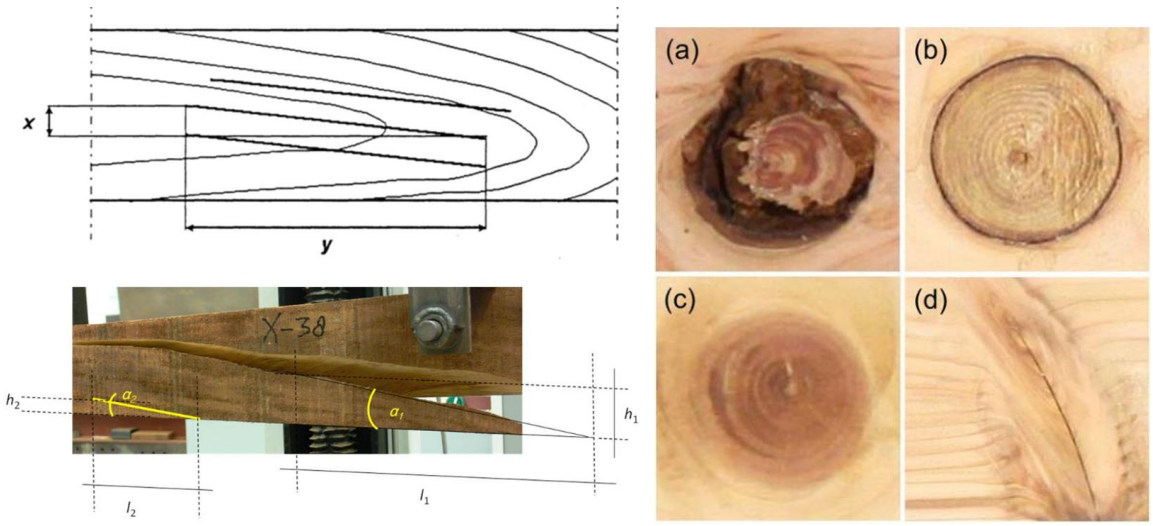


**Figure 19 – Left: Definition of the slope of the grain angle according to standard EN 1310 (Top), Angle of the grain and associated slope of the fiber angle measured during a bending test (Bottom). Righ: Four types of wood knots: (a) rotten knot, (b) coated knot, (c) sound knot (d) sharp knot [49, 50].**

## 3. The case of plywood and Laminated Veneer Lumber (LVL)

### 3.1 Overview and Manufacturing

Laminated Veneer Lumber (LVL) is made of thin sheets of wood, called veneers, joined together with an adhesive. They are manufactured by two means, rotary peeling of splitting and their fibers are mainly oriented in a single direction leading to sheets mainly in the LT plane for the rotary peeled ones, and L- and a mix of R ot T plane for the spitted ones. Wood laminates can be cross-ply laminated, meaning that longitudinal and transverse veneers alternate throughout the laminate. When the veneers main orientation alternate, this laminate can be referred to as plywood.

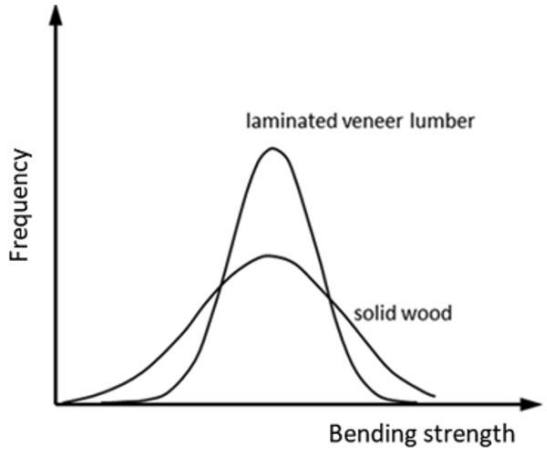


**Figure 20 – Representation of the comparison of the failure stress in bending between a solid wood and an LVL of the same species [53, 54].**

Because of the way it is manufactured and the possibility of removing defects, by choosing the veneers that make it up and their orientation, LVL has mechanical properties that are comparable or even superior to those of solid wood, while at the same time reducing the dispersion of its mechanical properties. The reduction in the variability of wood mechanical properties can be explained by a better volumetric distribution (random or eventually optimized [CC] of its natural defects, such as knots, grain slope or splits (Figure 20 and [52-54]). Veneers are manufactured by peeling logs (Figure 21). Between each veneer, also known as a ply, an appropriate resin or adhesive (such as epoxy, phenol, formaldehyde, melamine, urea formaldehyde, polyethylene, reactive polyurethane, ...) is incorporated. The manufacturing process involves steps such as steaming, uncoiling, ply drying, ply positioning and orientation, gluing, pressing and planing. In some cases, laminates are manufactured under heat, with press temperatures of around 140 °C, to ensure that the thermoplastic adhesive fuses with a heated press. The panel is then cooled to room temperature and pressurized to prevent twisting or warping of the laminate due to thermal expansion and internal stresses associated with uneven cross-layer deformation. Figure 22 shows a peeling machine, and figure 23 shows the manufacturing process and the final structure of the LVL. Once the wood panel has been obtained, it is cut to the desired dimensions [55].

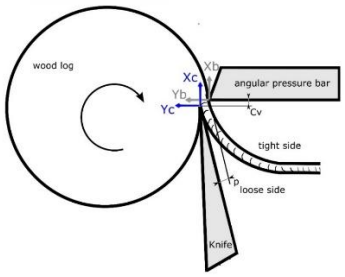


**Figure 21 – Schematic diagram of the process for peeling a wooden log.**

The peeling process is a complex machining process that has a significant effect on the quality and condition of the veneers, and therefore on the resulting LVL. This is machining in 0-90 T mode shown in Figure 24 (where the first number corresponds to the angle between the edge of the tool and the grain of the wood, the second corresponds to the angle between the direction of cut and grain of the wood, and the letter corresponds to the direction of the cut; nomenclature proposed by McKenzie to describe the methods of cutting wood [55]). This cut of the wood makes it possible to limit the cutting forces while offering a low damage to veneers.

**Figure 22 – logwood peeling platform, LaBoMaP (Arts et Métiers, Cluny, France)**

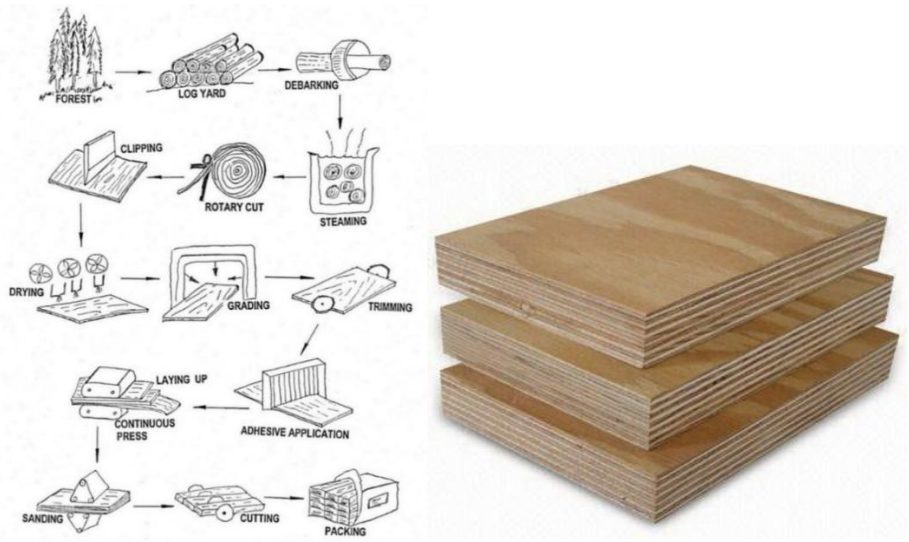


**Figure 23 – Processes for manufacturing an LVL panel [55] and finalized LVL plate.**

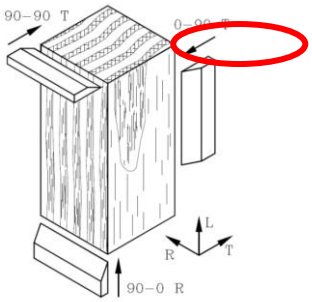


**Figure 24 – Main modes of cutting wood [55, 56], rotary peeling cutting mode 0-90 T highlighted with the red ellipsoid**

To optimize the veneer production using the peeling process, a wide range of settings need to be taken into consideration, depending on the species and the type of veneer to be produced: he geometric parameters of the peeling tools, cutting speed, log steaming temperature, and eccentricity also have an impact on veneer quality. Tools and their geometries play a key role in the peeling process. In particular, the knife has a cutting angle of between 18 and 22°. To prevent premature damage, the edge can be locally reinforced with a micro-bevel or rounded. The tool clearance angle, which remains the main setting for this part, is variable during the peeling process. The angle increases from a positive value at the start of the process to form a chip as quickly as possible, then stabilizes before decreasing at the end of the cut to limit log vibration [56, 57,58].

Another device complements the knife in the peeling process: the pressure bar. It creates a stress field by compressing the wood to limit the appearance of peeling cracks (see next subsection and Figure 27). The pressure bar has a beak angle greater than 90°, so that the stress field is upstream of the knife. The rate of compression applied to the wood depends on the horizontal position of the bar. For veneer peeling, compression rates ranging from 10% to 20% of the veneer thickness are usually used [56, 57,58]. Log temperature is a parameter to be considered too when manufacturing veneers. Some species, such as poplar, can be peeled at room temperature or even frozen (poplar), but others require the logs to be steamed (beech, Douglas fir). Wood that is too cold will produce cracked, rougher veneers, while wood that is too hot will produce "fluffy" veneers. This ideal peeling temperature, providing the best veneer qualities, is specific to each species and some authors are suggesting that the Tg plays a role in that phenomenon [59]. To obtain the desired temperature before machining, the log is steamed in saturated steam or boiled in hot water.

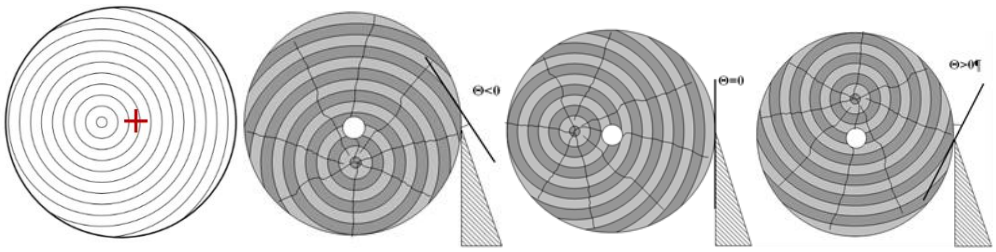

**Figure 25 – Representation of an eccentric log [59]**

Log eccentricity also influences veneer quality. Indeed, a log centered on its core will produce veneers of better quality than an eccentric log (Figure 25) [60]. When peeling a centered log, the knife will pass over a longer distance through locally homogeneous wood (summer wood, summer/spring wood transition, spring wood, spring/summer wood transition). In this case, the tool will encounter more transitions due to the eccentricity of the log. However, this recommendation runs counter to the practices of veneer manufacturers who, to optimize material yield, look for the geometric center of the log rather than its core. Furthermore, veneer quality differs according to its distance from the log

center, which is explained by the difference in mechanical properties between juvenile and mature wood. It should be remembered that the rigidity and strength of mature wood is greater than that of juvenile wood. The mechanical properties of the veneer are therefore influenced by where, in the radius of the log, the veneer has been extracted.

### 3.2 The cracks inside the veneers after manufacturing

These cracks, generally mentioned as lathe checks, which occur during the peeling phase (Figure 26) and run parallel to the veneer fibers, are characterized in the literature by two parameters: their spatial frequency (or distance between two cracks), and their average depth [61]; among those two, a third one can be introduced, the angle formed between the surface of the veneer and the crack path within the veneer thickness (sometime the crack can change suddenly its path direction creating two diverse angle of propagation). The main factor influencing the crack formation, for a specific wood specie, is the thickness of the unwound veneer: the thicker the veneer, the deeper the cracks, but they are less frequent (Figure 26) [62, 63, 64]. However, veneer thickness is not the only parameter to be considered when characterizing crack formation: other parameters such as wood local density, the log steaming temperature before peeling, the pressure bar compression ratio, the peeling radius, or the peeling speed also have a greater or lesser influence.

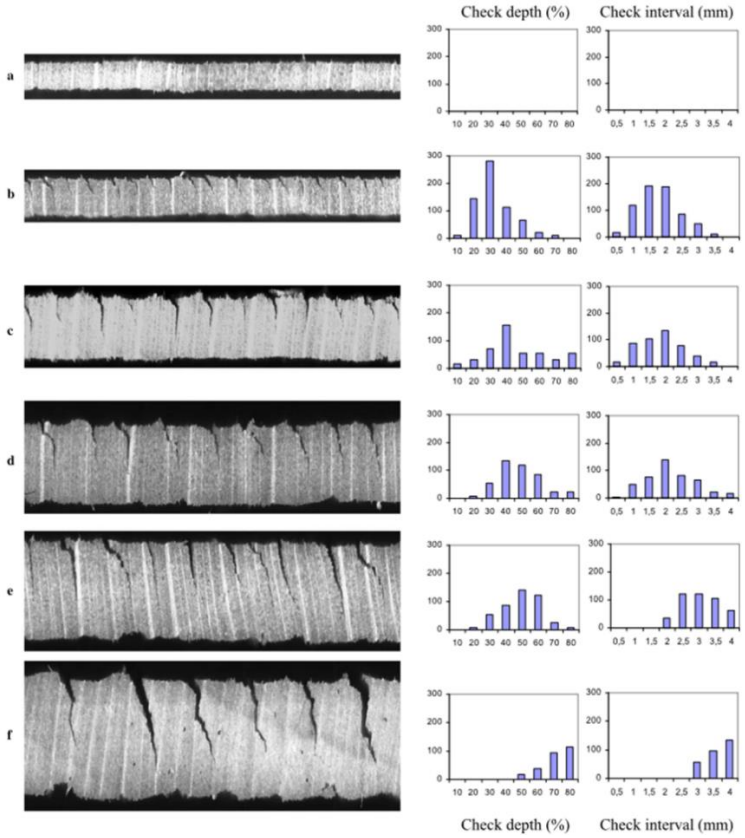


**Figure 26 – Lathe checks on beech veneer of different thicknesses: 0.7 mm (a), 1.0 mm (b), 1.5 mm (c), 2.0 mm (d), 2.5 mm (e), 3.0 mm (f), presented with histograms (number of control occurrences on a 1 m long veneer) of control depths per turn (in % of the thickness) and intervals [65].**

Lathe checks have a non-negligible effect on the veneer mechanical properties. The deeper they are (and therefore the less frequent they are), the lower the elastic moduli and stresses at break. The effect of cracks is mainly studied at the LVL scale in the literature. Bekhta et al. [66] show, using tensile tests parallel and perpendicular to the grain of a 5-ply LVL, that the presence of cracks, and especially their depth, leads to a reduction in the stresses at fracture of LVL compared with solid wood. They found a reduction of around 23.7% in stress at break in the longitudinal direction and 86.9% in the transverse direction. This loss of properties can also be observed in the longitudinal and shear elastic moduli of LVL, due to the depth of the cracks [67, 68, 69]. Crack orientation and position play an important role in the properties of laminated timber, particularly in the case of shear stresses. Rohumaa et al. [70] show the effect of crack depth and the direction in which cracks are loaded (crack-opening or crack-closing shear) on the shear strength of their plywood (Figure 27).

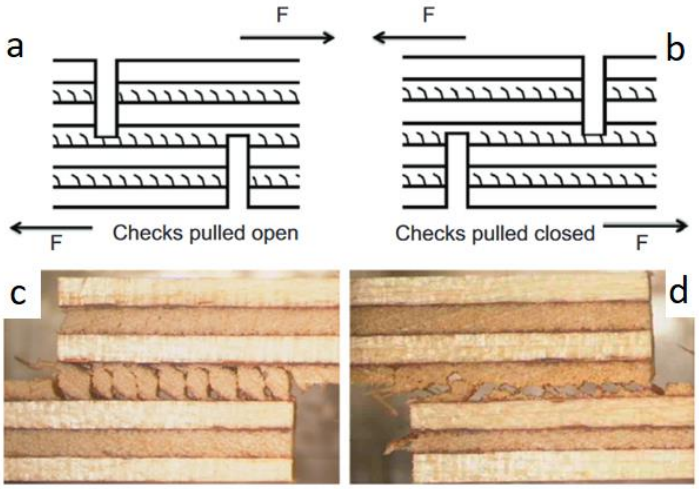


**Figure 27 – Intermediate ply with crack opening (a) Intermediate ply with crack closure (b) Failure of plywood in crack opening (c) Failure of plywood in crack closure (d) [70].**

The way in which the plies are bonded together, and therefore the positioning of the cracked faces in relation to the sound faces, also has a bearing on the shear properties of LVL (Figure 28). The worst case is when the cracked faces are bonded together, and the best case is when the sound faces are bonded opposite to each other [71]. In industry, the faces of LVL panels are bonded so that the cracked faces face the sound faces [72].

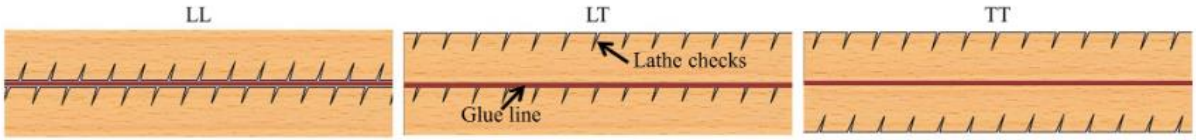


**Figure 28 – Three different LVL bonds for shear tests [71]**

Pot et al propose [73] a finite element model (FEM) to describe and to analyze the influence of veneer lathe checks on the elastic properties of LVL. The results show that the longitudinal modulus of

elasticity is marginally affected by checking, while the shear rigidity of the LVL beam is significantly reduced in edgewise bending if checks are not glued. Gluing checks, even under consideration of a low glue Young's modulus, highly reduces the effect of checking on the elastic global mechanical properties of LVL.

**3.3 Densification of veneers**

During the LVL manufacturing process, the use of pressure to bond veneers can tend to densify them. Densification occurs when the density of the veneer is artificially modified. Wood, and therefore wood veneers, can be mechanically densified in order to increase their stiffness and stress at failure. This process can also be carried out prior to LVL manufacture to improve certain properties of the final laminate. Densification is a means of improving the mechanical properties of wood up to a maximum density of around 1.5 g/cm$^3$, which corresponds to the cell wall density of dry wood [32]. Transverse or radial compression allows a significant reduction in cell void volume and is the most frequently used method for densifying wood. Wood densification can take place in several stages [54]:

- Softening of the cell wall: wood can be heated to a temperature above the glass transition temperature (Tg) of its amorphous polymers (hemicellulose and lignin) (160 to 200 °C [74]),
- Compression phase,
- Drying of compressed wood to improve dimensional stability,
- Fixation of compressed wood. The densification achieved under these conditions is, however, partly reversible if the wood is re-exposed to high humidity [75].

In order to improve the mechanical properties of wood-based composites, numerous densification processes have been developed since the beginning of the twentieth century. However, we will only deal here with thermo-mechanical densification, which most closely resembles the veneer densification observed when bonding plies under press for LVL manufacture. In this process, the softening of the wood can be initiated by the rise in temperature if the LVL is hot-pressed prior to the application of a compressive force in the transverse or radial direction [76]. This densification has an effect on the mechanical properties of LVL. Indeed, ply densification increases the stiffness as well as the stress at break of LVL in bending, tension and compression [66, 77, 78, 79]. Table 11 summarizes the tensile stresses at break of 1.5 mm birch and alder veneers. Tensile stress at break is higher for densified veneers than for non-densified veneers in the case of fiber-direction tension. For tensile tests perpendicular to the fibers, densified veneers have a lower stress at break [66].

| | | Birch | Alder |
|---|---|---|---|
| Tensile strength in the fiber direction (MPa) | Non densified veneers | 128.2 | 63.5 |
| | 5% densified Veneers | ~130-135 | ~64-90 |
| | 25% densified Veneers | ~150-164 | ~82-113.6 |
| Tensile strength perpendicular to the fiber direction (MPa) | Non densified veneers | 1.42 - 1.5 | - |
| | 10% densified Veneers | ~1.35 - 1.98 | - |
| | 20% densified Veneers | ~0.76 | |

**Table 5 – Tensile strength of 1.5mm birch and alder veneers [66]**

Other methods for densifying veneers include thermo-hydro-mechanical densification processes. These processes overcome the fact that, in a simple thermo-mechanical compression process, densified wood largely recovers when re-exposed to high humidity and temperature [75]. In this case, wood samples are softened with steam, mechanically compressed and finally post-treated with saturated steam [54]. In addition to improving mechanical properties for an equivalent geometry, viscoelastic thermal compression processes enable equal or even better bonding performance to be achieved with phenol-formaldehyde adhesives compared with non-densified veneers [54, 80, 81]. Wood can also be delignified before pressing. As reported by Shams et al [82], extracting the lignin reduces the transverse rigidity of the cell wall and therefore facilitates cell compression during densification. This leads to gentle compression of the bulk cellulose, with almost no cracking of the cell wall [54, 82].

### 3.4 Veneer bonding glue effect

Bonding is a crucial step in the manufacture of LVL. The choice of glue and the quantity used have an effect on the properties of LVL. What's more, in engineered wood products, glue doesn't just create an interface, in could affect the global stiffness and strength of the final product compared to solid wood. In the case of glued wood joints, three different zones can be clearly identified: the adhesive-only interface (orange line in Figure 29), an interface in which the wood cells are partially filled with adhesive (yellow zones in Figure 29), and solid wood clear of any glue (Figure 29) [83, 84]. Knowing the elastic properties of wood and adhesive, the elastic properties of the interface can also be calculated by applying simple mixture theory. In all cases, penetration of the adhesive into the wood leads to an increase in local stiffness and the formation of a wood-adhesive composite [85, 86].

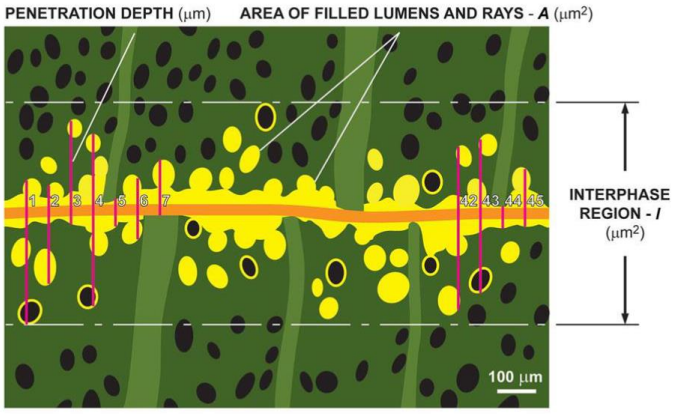


**Figure 29– Diagram representing the penetration of glue into the wood [87]**

Many parameters play a part in the adhesion performance between wood and glue such as the formulation and type of glue, the quality and quantity of adhesives used, the gluing pressure applied, the heating temperature during pressing, the thickness of the glue joint, the penetration of the glue into the wood, and so on. However, it's important to note that it's impossible to compare the adhesion performance of different types of glue on the basis of glue penetration alone. Penetration may only have a secondary effect on adhesion performance, whereas the effects of cohesive strength or covalent bonds, which will differ depending on the adhesive formulation, may have a greater impact [88]. In the case of LVL, glue penetration into peeling cracks and damaged cells on the ply surface improves adhesion performance. In addition, penetration promotes better stress distribution between the adherends when they are subjected to load [88].

It should be noted, however, that the thickness of the glue joint and the penetration of the glue into the wood depend on several parameters, such as the amount of glue put between each veneer (often referred to as GS for "Glue Spread" rate), the pressure at which the veneers are glued, the type of glue and the wood species and orientation [88]. In the process of pressing veneers for LVL production, the pressure exerted is directly related to the thickness of the final glue joint. The harder you press, the thinner the glue joint and the greater the glue's penetration into the wood. This is what Kurt and Cil [29] show on LVL, bonded with phenol formaldehyde (PF) adhesive that the glue joint thicknesses are diverse depending on the gluing conditions, as extracted in Table 6). However, it's not just the type of adhesive that matters. The type of glue, but also its viscosity, are parameters that have an effect on glue penetration into the wood [89]. This is also shown by Haas, who compares the average penetration of different glues on solid wood (Figure 30) [90].

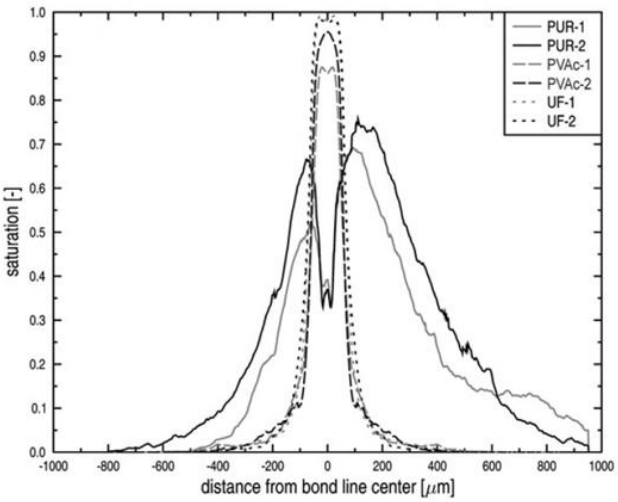


**Figure 30 – Average Saturation Value of Different Glues as a Function of Distance to Glue Interface [43]**

It should be noted, however, that in the case of LVL, higher pressure during gluing not only enhances glue penetration, but also densifies the veneers. Both phenomena have an effect on the mechanical properties of LVL. Table 6 summarizes the mechanical properties of LVL and the thickness of the glue joint as a function of the pressure used during LVL pressing from [79].

| | Pressure exerced ($kg.cm^{-2}$) | | | | |
|---|---|---|---|---|---|
| | 2.5 | 5 | 7.5 | 10 | 12.5 |
| Thickness of the bonded joint (μm) | 141 | 121 | 88 | 68 | 47 |
| Density | 0.35 | 0.36 | 0.38 | 0.40 | 0.44 |
| Compression ratio | 1.09 | 1.13 | 1.19 | 1.25 | 1.38 |
| Bending elastic modulus (MPa) | 5339.73 | 5496.22 | 5818.76 | 5946.67 | 6211.73 |
| Bending failure stress (MPa) | 54.23 | 60.65 | 62.54 | 63.88 | 69.15 |
| Compression failure stress in fiber direction (MPa) | 63.60 | 71.00 | 73.11 | 80.05 | 89.41 |

**Table 6 – Mechanical properties of LVL as a function of bonding pressure [79]**

### 3.5 Grain Angle

As it has been showed before, the peeling of a log is complex and generate a slope of the grain. It has an influence on the mechanical properties of the wood material. A non-zero fiber orientation in the direction of stress weakens the wood and the veneers. On solid wood, Kollmann [26] observed that a deviation of 15° from the load axis results in an almost 50% reduction in tensile stress at break (Figure 31).

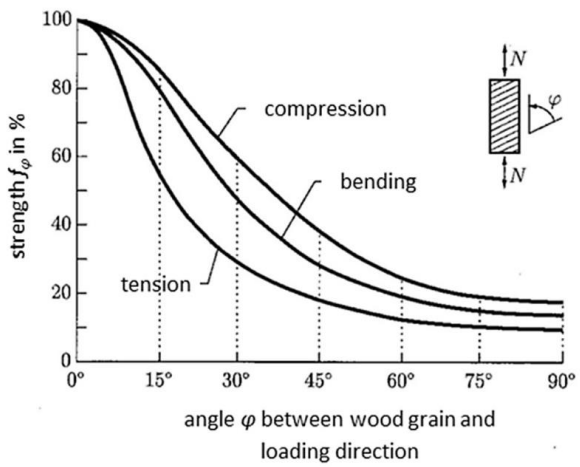


**Figure 31 – Schematic curves of the loss of strength of wood in tension, bending and compression as a function of the angle $\varphi$ between the fibers and the direction of the loading $\overrightarrow{N}$ [26].**

In the case of veneers, fiber deflection has been shown to be one of the most influential properties when it comes to tensile stress at break. However, measuring this deflection is not easy. Several non-destructive measurement methods exist to measure the grain angle, but these methods are not infallible and have their advantages and disadvantages. It should also be borne in mind that grain angle deviation does not occur solely in the plane, and that it could display an out-of-plane component to this deviation, as illustrated in figure 32.

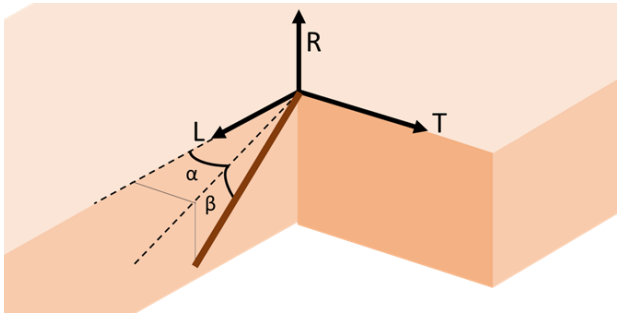


**Figure 32 – Possible deviations of the fiber in the wood: α describes the in-plane deviation and β describes the out-of-plane deviation angle of the veneer.**

It is possible to use fracture criteria to calculate an equivalent fracture stress as a function of the grain angle. A widely used criterion in the wood characterization literature is Kollmann's criterion, which is described below [26]:

$$\sigma_\varphi = \frac{\sigma_l \times \sigma_t}{\sigma_l \times sin^n(\varphi) + \sigma_t \times cos^n(\varphi)} \quad \text{Equation 2}$$

where

- $\sigma_\mathrm{l}$ and $\sigma_\mathrm{t}$ are the longitudinal and transverse failure stresses,
- $\varphi$ is the grain angle measured with respect to the direction of stress (Figure ),
- $\sigma_\varphi$ is the breaking stress of the studied material having a grain angle $\varphi$,
- $n$ is an empirical parameter introduced by Kollmann [26] to generalize Hankinson's formula where n=2 [110].

Kollmann's formula can be generalized to calculate many mechanical parameters based on wood grain deviation. Table 7 summarizes the values of $n$ according to the properties studied as well as the values of the ratio $\sigma_t/\sigma_l$ calculated in the literature for solid wood [22] If the formula is generalized to other mechanical properties, $\sigma_l$ and $\sigma_t$ are no longer the breaking stresses, but the properties studied in the longitudinal and transverse directions.

| Property to determine | $n$ | $\sigma_t/\sigma_l$ |
|---|---|---|
| Failure stress in tension | 1.5 – 2.0 | 0.04 – 0.07 |
| Failure stress in compression | 2.0 – 2.5 | 0.03 – 0.4 |
| Bending Failure stress | 1.5 – 2.0 | 0.04 – 0.10 |
| Young Modulus | 2.0 | 0.04 – 0.12 |

**Table 7 – Parameters of the Kollmann's formula [26]**

Although Kollmann's formula is easy to use and enables wood properties to be calculated when the grain angle is known, it does not take shear into account and is not directly applicable to cross-laminated composite woods such as plywood [111]. For this reason, some authors use different fracture criteria or formulas to account for this phenomenon. One example is the Tsai-Hill's criterion:

$$1 = \frac{(\sigma_\varphi \times cos^2(\varphi))^2}{{\sigma_l}^2} - \frac{(\sigma_\varphi \times cos^2(\varphi)) \times (\sigma_\varphi \times sin^2(\varphi))}{{\sigma_l}^2} + \frac{(\sigma_\varphi \times sin^2(\varphi))^2}{{\sigma_t}^2} - \frac{(\sigma_\varphi \times cos(\varphi) \times sin(\varphi))^2}{{\sigma_{lt}}^2} \quad \text{Equation 3}$$

where $\sigma_{l\mathrm{t}}$ is the in-plane shear stress. Using laminate theory, one can obtain the elastic properties of a veneer as a function of its grain angle. For example, the following relationship can be used to determine Young's modulus:

$$\frac{1}{E_x} = \frac{cos^4(\varphi)}{E_l} + \frac{sin^4(\varphi)}{E_t} + sin^2(\varphi)cos^2(\varphi)\left(\frac{1}{G_{lt}} - 2\frac{\nu_{lt}}{E_l}\right) \quad \text{Equation 4}$$

where

- $E_{\mathrm{x}}$ is the Young's modulus of the studied material having a grain angle $\varphi$
- $E_l \; and \; E_t$ are the longitudinal and transverse Young's moduli of the material
- $G_{\mathrm{lt}}$ is the in-plane shear modulus
- $\nu_{\mathrm{lt}}$ is the in-plane Poisson's ratio modulus

The orientation of the veneer fibers therefore has a non-negligible effect on its mechanical properties. During the manufacture of LVLs, it is therefore important to position the veneers precisely like for composite laminates and minimize the effect of defects.

**3.6 Measurements**

*3.6.1 Density measurement*

As previously mentioned, the wood mechanical properties are clearly correlated with its density. Density is highly variable, whether at the level of the same species, the same tree, or even at the level of a growth ring. Thus, accurately measuring this property is highly consequential to optimize in the view of sorting wood material. Two major families of methods can be distinguished for measuring this property: "physical/mechanical" methods and "spectroscopic" methods.

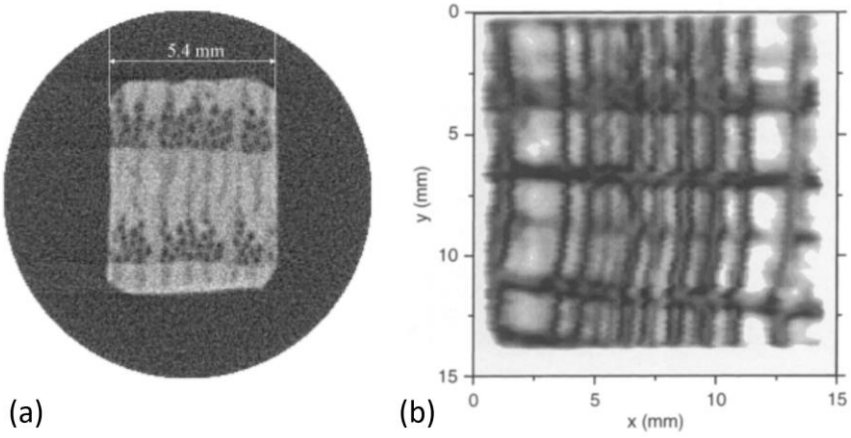


**Figure 33: (a) X-ray CT image (28.3 keV, spatial resolution = 0.1 mm) of an oak (*Quercus rubra* L.) sample 0 , and (b) THz image (spatial resolution = 0.3-0.5 mm) of a beech (*Fagus sylvatica* L.) sample 0**

Among the methods in the first category, the most classical is simply measuring the mass divided by the volume of the sample under study. There are also hardness probes such as the Pylodyn 0, the Resistograph 0 or ultrasonics 0, which can be used, for instance, on standing trees 0. These methods are all destructive or at least require contact with the measured element, which is not the case for

spectroscopic methods. For the latter, the existing interaction between the material and the radiation possessing a certain frequency is used. Among the different wavelengths, only particular ones are suitable for measuring the density of wood. Ultraviolet, visible, and infrared radiations cannot be used because wood is opaque to these wavelengths. X-rays, with wavelengths ranging from 0.03 nm to 10 nm, are currently the most commonly studied and used types of waves in the industry. The proportion of the wave's intensity absorbed by the medium it has passed through is related to its attenuation coefficient, thickness, and of course its density according to the Beer-Lambert law. This principle, used to perform 2D imaging and tomography 0 0 0, is also applicable in the context of spectroscopy by other types of radiation. However, the high penetration capacity of X-rays and their short wavelengths allowing them to detect very fine density differences explain their prevalence in both industry and research. Gamma rays (<0.01 nm) 0 0 have comparable properties, with even better penetration capacity allowing the treatment of thicker and denser woods, but their use requires even more expensive equipment than X-rays. While the use of high-frequency radiation is particularly satisfactory in terms of results, it is not without danger due to the ionizing nature of these radiations. Low-frequency radiation, such as microwaves (1-30 mm) 0 and terahertz (THz) (0.01-3.00 mm) 0 0, which are non-ionizing and therefore not harmful to health, can also be used for measuring density. The spatial resolution, according to Abbe's law 0, is proportional to the wavelength used. High-frequency waves such as X-rays have a particularly good spatial resolution, as illustrated in Figure 33-(a), while waves with lower frequencies such as terahertz or microwaves have a resolution on the order of millimetres to centimetres. However, it is possible to enhance this resolution significantly by manipulating other factors such as optical components or imaging methods, as shown in Figure 33-(b).

### *3.6.2 Lathe checks measurement*

Lathe checks due to the peeling process, as mentioned in section 3.2, have a significant effect on the veneer’s mechanical properties. For their measurement, two main parameters are to consider: the depth of the checks and their frequency. At present, there is no online measurement of cracks, with existing methods being mostly either destructive or contact based. The basic procedure involves impregnation, with a coloring ink to help the checks observation and crack tip detection, of veneers and observation under a microscope **Erreur ! Source du renvoi introuvable.**. As these measurements are cumbersome and tedious, new methods had to be developed.

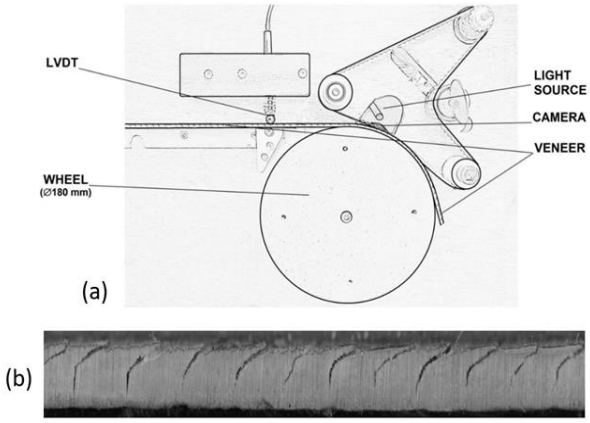


**Figure 34: (a) SMOF, optical lathe check measuring system (LVDT = linear variable differential transformer)** Erreur ! Source du renvoi introuvable.**, and (b) an image of Douglas fir veneer obtained with it**

Several methods have been developed to measure cracks in veneers, including acoustic measurements **Erreur ! Source du renvoi introuvable.** . Denaud et al. 0 employed this approach by recording sound and cutting forces during the peeling process and comparing predicted crack frequencies with actual measurements of veneer profiles. While this study produced promising results, it did not provide depth information for the checks. This limitation prompted the development of the SMOF (Optical Crack Measurement System) 0, shown in the Figure 34-(a). This measurement is performed on the edge of veneer strips (Figure 34-(b)), and to make cracks more easily detectable, they are slightly opened by passing the strip over a wheel whose diameter is chosen according to the thickness of the veneer, to limit over enlarging the cracks leading to their propagation or creating new ones. This system allows for a good mapping of the cracks, but only in 2D in the RT plane. Antikainen et al. 0 observe a laser passing through a veneer by transmission, and by processing the images, they are able to obtain the mapping of cracks in the LT plane as well as their depths using the area of each crack on the processed images.

### *3.6.3 Grain angle measurement*

The simplest method for identifying the grain slope angle in the veneer plane is the one presented for solid wood, i.e. visual determination of this angle. Although this method is very simple, it is not very accurate and provides only an idea of the average grain slope angle on a specimen [112].

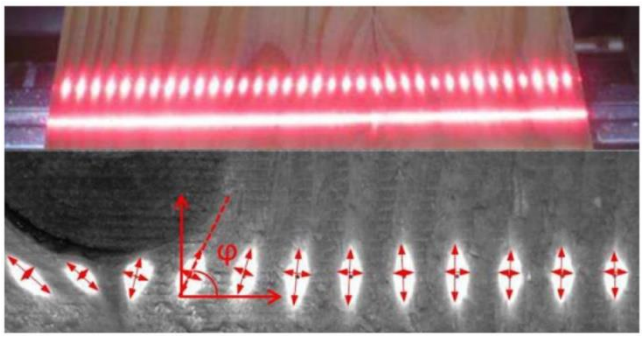

**Figure 35 – Tracheid effect by projection of a l laser beams line over a Douglas fir beam surface. Example of grain angle deviation around a knot [48]**

Another way of measuring the grain angle slope is a scattering method based on the "tracheid effect". When condensed light, such as a laser beam, is shone onto the surface of wood, the beam is diffracted by the wood's fibers and tracheids. The result is an elliptical spot oriented in the same direction as the slope of the grain. The latter is then calculated from the ellipse formed by the observed light (Figure 35). Based on conduction at the wood surface, researchers have used a similar set-up, but instead of measuring the reflected laser beam, they now measure the temperature at the wood surface, which also provides the grain angle [48]. These measurement methods can then be automated to map the grain slope on a veneer (Figure 36).

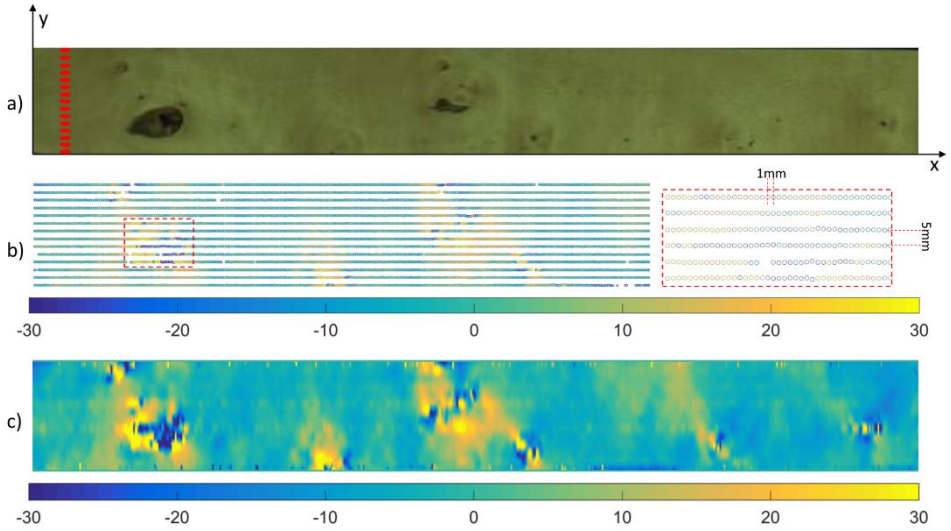


**Figure 36 – Local grain angle measurement: (a) photograph, (b) raw data, and (c) interpolated data [113]**

The use of image analysis also makes it possible to identify the woody rays and thus the deviation of the wood grain, with the aim of mapping these deviations in 2D (Figure 37). This method, which is relatively simple to implement, also fails to provide information on the out-of-plane component of grain deviation [114, 115]. Out-of-plane deflection can be measured using methods such as wide-angle X-ray scattering (WAXS) characterization. By adjusting the positioning of the veneer under study, both in-plane and out-of-plane deflection can be measured [62, 63]. Other methods are based on measurements using radio waves of various frequencies [116]. The major disadvantage of these characterization methods remains the measurement time, which is much longer than for the methods discussed above.

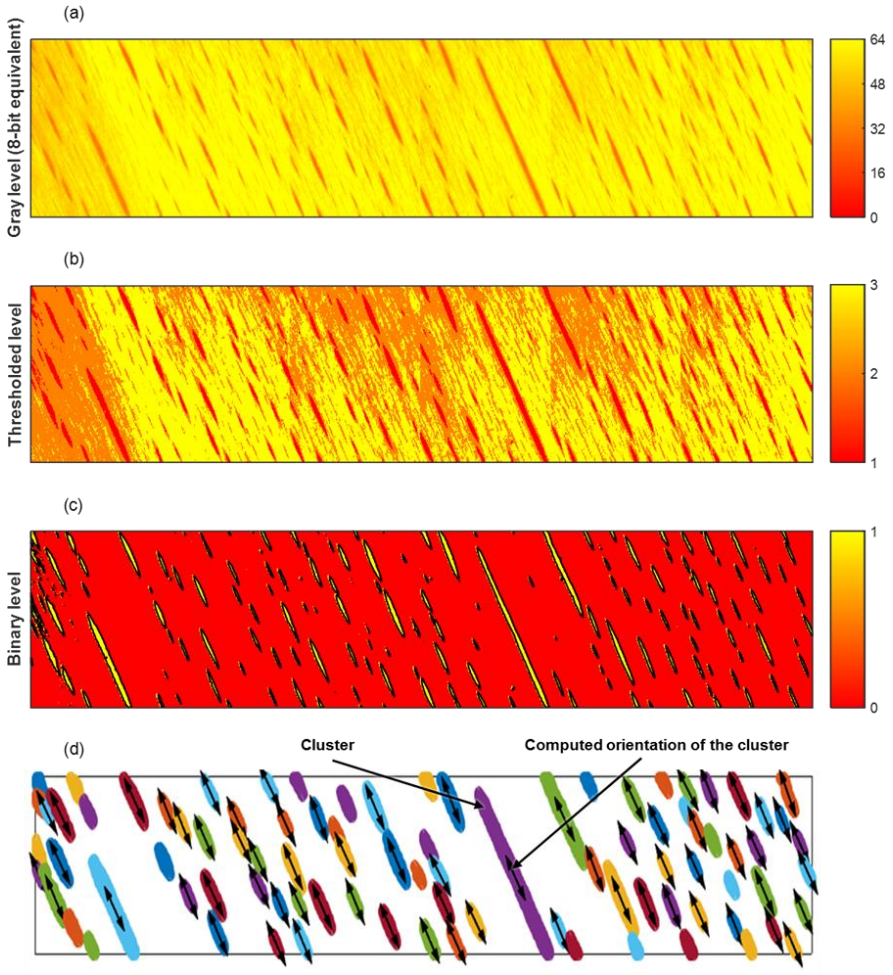


**Figure 37 – Image processing state during the grain direction computation: (a) initial image (grayscale converted to 8-bit), (b) 3-level thresholded image, (c) binarized image on which medullar rays contours were detected and drawn (black contour), and (d) clusters and their main directions indicated by the corresponding double-arrow. Clusters where no arrow is associated were not considered in the computation (area too small or shape not elongated enough (Reproduced from [114])**

## 4. Simulating the behaviour of wood

### 4.1 Composite laminate theory vs Modelling of plywood

The behavior of the plywood ply is more complex than the behavior of a classic laminate ply made from technical fibres. It is particularly influenced by the wood densification during manufacture, the lathe checks spatial repartition, and the impregnation/penetration of the glue in the wood and lathe checks. As a result, the theory of laminates [117] cannot be applied directly. Preliminary results on 0° I214 poplar specimens with 1 to 8 layers under tension carried out by the authors are shown Figure 38.

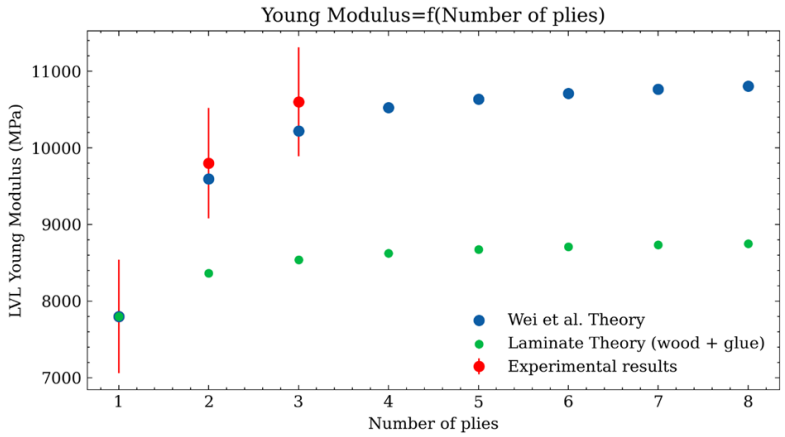


**Figure 38 – Longitudinal Young's Modulus of I214-poplar LVL vs the number of plies composing it in tension**

In the literature, Okuma [117] proposes a laminate model considering the effect of the glue. To do this, he considers the part of the veneer where the glue penetrates as a ply with different mechanical properties. Wei et al [86, 118] propose an improvement to this model by considering the intake of glue to the wood composite, this model also considers the densification of the plies linked to the design of the LVL by press-fitting. The global Young's modulus of the laminate in a given direction can therefore be predicted using Equation 5.

$$E_{compressed} = \frac{(n-1)GS.E_g}{t_0.\rho_g(1-CR)} + \frac{E_w}{1-CR} \qquad \text{Equation 5}$$

where:

- $E_{compressed}$ is the Young's modulus of the laminate in a given direction
- $n$ is the number of plies composing the LVL
- $GS$ is the glue rate per m² between each ply (glue spread)
- $E_g$ is the Young's modulus of the glue
- $E_w$ is the Young's modulus of the wood in a given direction
- $t_0$ is the thickness of a veneer before compression
- $\rho_g$ is the density of the glue
- $CR$ is the compression ratio of the veneers

Wei et al [119] also show, via their model and a test campaign, that the glue influence becomes negligible if the LVL is manufactured with thicker veneers, since its relative quantity in the composite material will be less for the same geometry. The authors have shown that this theory appears to give good results for 1, 2 and 3 plies (Figure 39), but further, more systematic investigations are in progress. To the best of our knowledge, only one publication has proposed the complete consideration of real veneer geometry without resorting to homogenization. Pot et al [18] model a beech LVL beam made up of plies with different peeling crack frequencies and depths. In addition, the model considers whether or not the crack is closed by the glue joint. This model enables us to take a quantitative look

at the influence of peeling cracks and their interaction with glue on flexural and shear modulus (Figures 39 and 40).

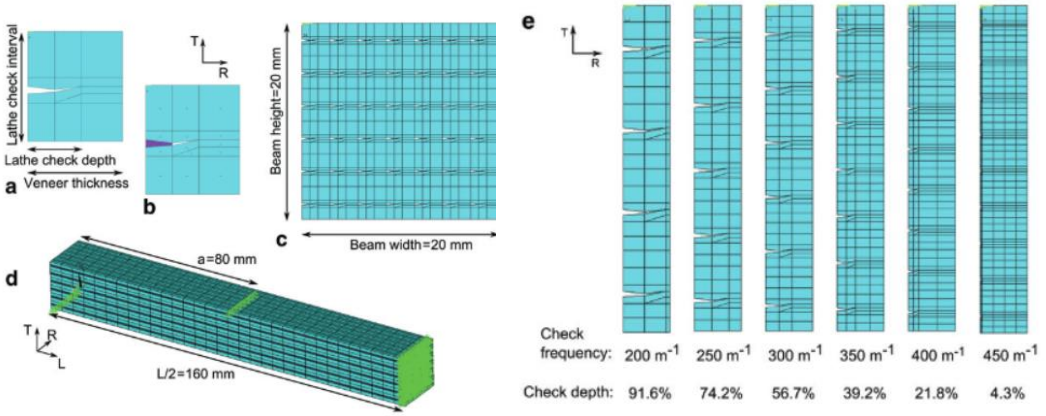


**Figure 39 – Finite element model of an LVL beam. (a) Base Pattern; (b) base pattern with glued cracks (the glue is purple in color); (c) beam cross-section (crack frequency 300 $m^{-1}$); (d) half of the beam (the green triangular symbols represent the boundary conditions); (e) finite element model of the six cracked veneers used in the numerical model [120].**

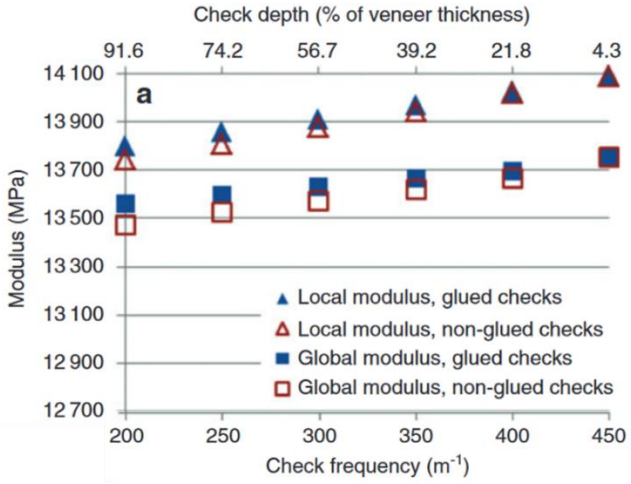


**Figure 40 – Mechanical properties of an LVL beam obtained by finite element modeling as a function of crack depth, frequency and bonding: Local and global modulus obtained in 4-point bending [120]**

## *4.2* ***Wood failure modelization and simulation***

### *4.2.1 Solid wood models*

In view of the above, the behavior of wood is complex, not only because of its orthotropy, but also because of the many factors that influence its behavior, such as temperature, moisture content, type of load, defects and, when considering LVL, the manufacturing method. In the case of static or quasi-static loading, it is considered linear and brittle in tension in the fiber direction, and ductile in compression in the fiber direction (see Figure 8, [121]). As the loading rate increases, the cell walls begin to deform locally, and the wood's behavior becomes non-linear. For all these reasons, the development of numerical models to model wood is still an important research topic. One of the most

widely used models, already implemented in LS-DYNA (MAT_143), is the Murray et al. model [122]. In this model, transverse isotropic behavior is considered with a modified Hashin failure criterion. In this criterion, compressive and shear stresses are assumed to be mutually weakening, so a compressive parallel and perpendicular criterion similar to that for tensile loading can be assumed. Damage evolution is computed through parallel and perpendicular mode fracture energy parameters, which are obtained from stress intensity factors in modes-I and -II in the parallel and perpendicular directions. The details of this complex model can be found in [123]. Despite its complexity and the large number of parameters to identify, it makes it possible to model complex phenomena such as the impact on sandwiches with Balsa cores [124, 125].

Other materials present in LS-DYNA can be used to model wood: MAT_143, MAT_126 and MAT_026. It should be noted that the last two models are based on honeycomb materials whose macroscopic architecture can be compared to that of wood. A comparison of these different models was carried out by Maillot et al [125]. Using unit test simulations, the authors conclude that the current state of wood models (MAT_143) do not seem capable of representing balsa wood in confined compression and shear. They also conclude that MAT_MODIFIED_HONEYCOMB gives more appropriate results for the loads studied by these authors. Baumann et al [126, 127] also compare material models under LS_DYNA, including MAT_143, MAT_126. Although these models may be representative of tests on solid wood, the authors conclude that additions are necessary, such as the inclusion of strain rate or damage modeling. In addition, the orthotropic nature of wood requires a large number of characterization tests. A small number of authors have adapted and implemented nonlinear behavior laws from the mechanics of continuums and other materials. For example, Oudjene and Khelifa [128] have implemented an orthotropic elastoplastic constitutive law which makes it possible to consider for solid wood: (1) Ductile compressive behavior with densification perpendicular to the grain; (2) Brittle tensile failure parallel and perpendicular to the grain; (3) Compressive failure with softening parallel to the grain. They identified the parameters of the law using simple compression and bending tests on spruce wood.

### *4.3.2 LVL models*

Various numerical approaches to modeling LVL are presented in the literature. A first approach is linear modeling using Finite Element Methods (FEM), considering the veneer as a layer of the laminate (plate or volume) to simulate the linear part of tensile, compression or bending tests [129, 130]. The addition of failure criteria such as the maximum stress criterion, Tsai-hill, Hashin or Puck, makes it possible to set up simple LVL models for tensile, compression or bending tests [131, 132, 133]. In addition to these linear models, inhomogeneities in wood and the same for veneers can also be considered. Zerbst et al [134] add wood mapping to their modeling, playing on the type of wood (winter wood or spring wood)

to account for veneer inhomogeneity (note that they model sliced veneer, not peeled). The grain angle [135] or the consideration of defects such as knots can also be considered by modifying the local stiffness of the model [136]. In addition, scaling factors can be considered to account for different geometries between simulations and material property identification tests [137].

However, it is important to note that the weakness of some modeling strategies may stem from the lack of input data, and also from the variability of mechanical properties for a particular tree species. To consider the variability of mechanical material properties, some authors propose 3D stochastic finite element models and Monte Carlo simulations to analyze stress states in bending, tension and compression tests [138]. However, these linear models, even when coupled with failure criteria for LVL, fail to account for experimentally observed failure modes. Indeed, using failure criteria, we obtain the force at failure in the weakest element during the applied stress. Nevertheless, the initial fracture of the specimen does not necessarily correspond to its final failure. In such cases, a non-linear or more complex model is required to dissociate initial damage and specimen failure (Figure 41) [131, 132].

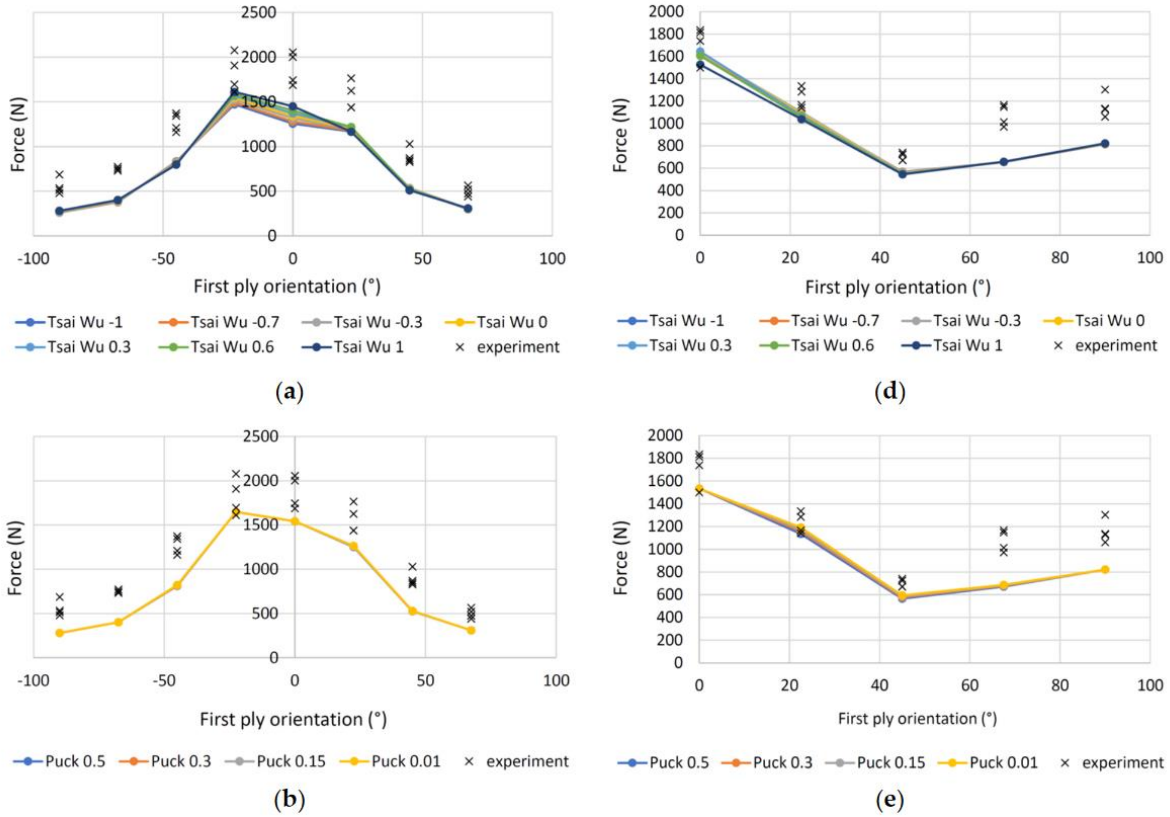


**Figure 41 – Failure forces measured and calculated on 7-ply specimens (7A and 7P) LVL loaded in 4-point bending: (a) 7A specimens, Tsai-Wu criterion; (b) specimens 7A, Puck criterion; (d) 7P specimens, Tsai-Wu criterion; (e) 7P specimens, Puck criterion [131, 132]**

For example, Susainathan et al. [123] used an LS-DYNA MAT_143 model to model low-velocity, low-energy impact on a sandwich with a plywood core. Due to the large number of materials contained in the plywood and skins, only a rough estimate of material properties was made to implement this

model. Despite this, the model correctly predicts sandwich behaviors, particularly for 5 Joules and 10 Joules impacts, where damage is limited. Most of the discrepancies observed between experimental and numerical results, notably in terms of initial slopes, maximum loads and maximum deflections, are less than 20%. However, significant discrepancies were observed for permanent indentation, energy absorbed by the sandwich and 15 Joules impacts. The explanation put forward is that the material damage model in LS-DYNA does not sufficiently incorporate the effects of softening in the damage process.

Models including the interfaces are also proposed in the literature. By adding cohesive elements between plies, delamination between LVL plies or cracking within plies can be considered [139, 140, 141]. However, although some authors use cohesive elements to model the bonded interface between LVL plies, some authors note that it may have its limitations on bonding with solid wood. Muller et al. [142] carried out a shear simulation of the glue joint and found that in certain study areas, the shear strains obtained by simulation and those measured experimentally differed (Figure 42). The authors conclude that a more complex approach is needed to model glue joints due to the structural complexity of bond lines and the uncertain mechanical properties of adhesives. One difficulty in modeling glue joints resides in being able to describe the mechanical behavior of adherent wood and the wood-glue interface line [143]. Indeed, as the glue penetrates the wood, it locally modifies these mechanical properties. However, the model developed by Müller et al [142] is on average comparable with experimental measurements.

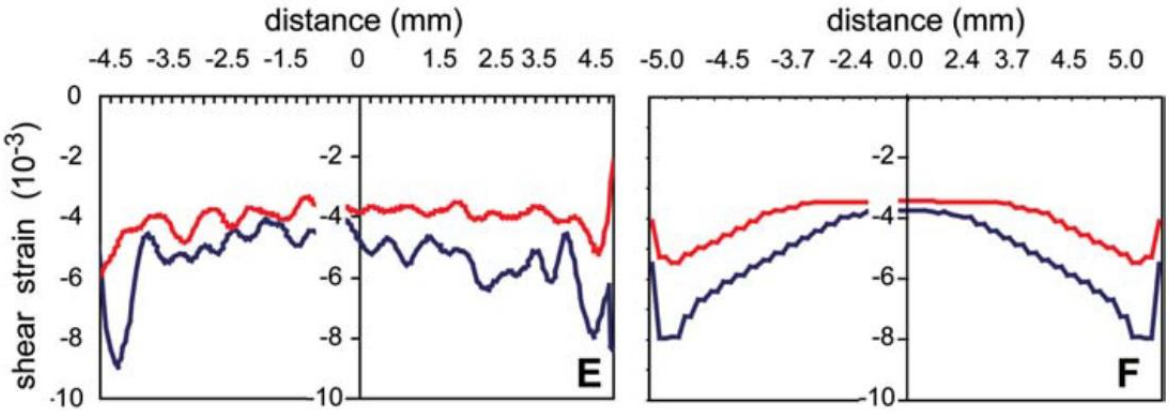


**Figure 42 – Experimental shear deformations along the glue line (E) and shear deformations obtained by simulation (F) (PRF glue: red line and PUR glue: blue line) [39]**

Non-linear laws linking strain and stress are modeled to account for the nonlinear behavior of the material in compression [141]. A comparison between the numerical and experimental results of Gilbert et al. is shown in Figure 43, and the law used is illustrated in Figure 45. Gilbert et al [141] present also a numerical model to capture the structural response of circular LVL hollow-section beams loaded in bending. The model uses an orthotropic elastic-perfectly plastic material to simulate

ductile failure modes in compression. It is based on Hill's anisotropic plasticity criterion. The average ratios between experimental and numerical results for beam flexural strength and stiffness were 1.02 and 0.93, respectively. However, in this model, the LVL is modeled only as a solid element and bonded interfaces and various veneers are not considered.

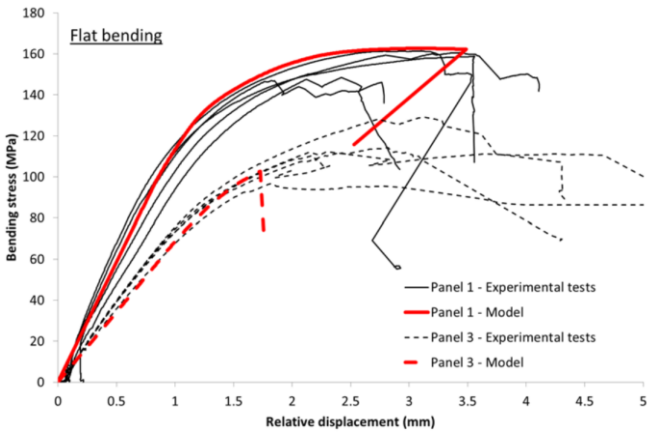


**Figure 43 – Comparison between experimental and numerical results for a two-panel configuration in flat bending [141]**

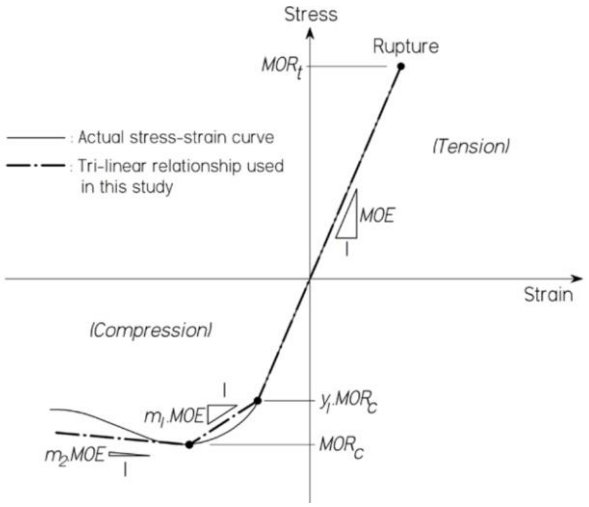


**Figure 44 – Relationship between stress and strain for wood loaded parallel to the grain [141]**

Saavedra Flores et al [144] proposed an interesting model but for CLT timber and investigated the rolling shear failure in cross-laminated timber structures by homogenization and cohesive zone models. Despite its high numerical complexity this model is relevant and captures quite well the failure mode as shown in Figure 45. There are few dynamic models of wood. Sebek et al [145] modeled European birch tested with Hopkinson bars. The model considers anisotropy, elasticity, plasticity, and failure. Moreover, the asymmetry for failure in tension and compression was addressed as well. The continuum damage mechanics approach was adopted through a simple material weakening but the model does not consider the strain rate dependency.

On balance, this selection of articles shows that significant modeling work remains to be done and that the intrinsic complexity of the material and its natural dispersion are difficult to model. However, there is an abundant literature of composite fracture models like the Discrete Ply Models [146, 147, 148] which could be adapted including wood imperfections [149, 150].

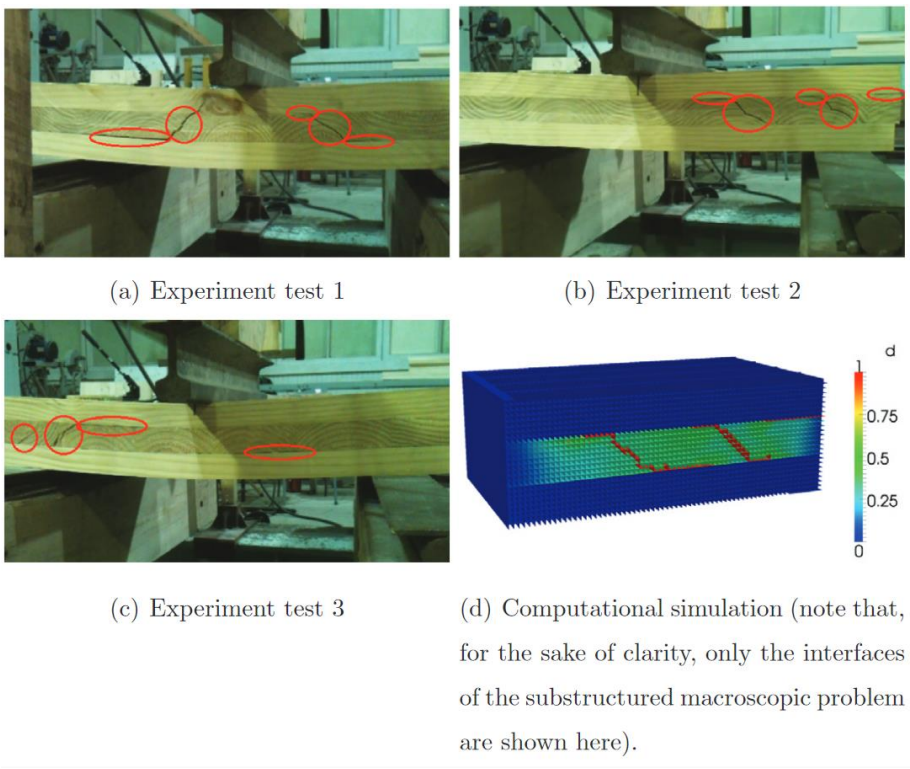


(a) Experiment test 1 (b) Experiment test 2

(c) Experiment test 3 (d) Computational simulation (note that, for the sake of clarity, only the interfaces of the substructured macroscopic problem are shown here).

**Figure 45: Shear Crack in three experimental tests vs numerical simulation (reproduced from [144])**

**5. Wood or plywood merged with composite materials**

For its use in means of transport, wood will certainly be used in conjunction with other materials, in particular long-fibre composites, as has already been done in aviation (see Figure 70). The aim of this section is to provide a non-exhaustive overview of some of the studies carried out on this subject.

Susainathan et al have studied sandwich structures with a wood core and skins made of aluminum, carbon, glass and linen respectively [44]. The manufacturing issues and static bending response of these structures have been studied. The quality of the bonding between skins and plywood core can vary with the manufacturing method (vacuum molding or thermo-compression). Susainathan et al have used epoxy resin from aeronautic with a high curing temperature which can degrade the wood properties during the manufacturing process. The bending tests performed showed that the mechanical characteristics were very interesting by comparison of an aeronautic carbon Nomex used for flooring of aircraft. Among others, the sandwich with plywood core and carbon skins provides the best bending stiffness while the sandwich with plywood core and glass skins provide the best

resistance. On the other hand, these solutions are too heavy with a ratio of 2-3 with the reference used in the study. Nevertheless, many optimizations exist to improve the specific resistance of such structures knowing that the price is 20 times lower than the current solution used for aircraft flooring. Then, Susainathan et al have used the same structure to study their low-velocity, low energy impact behavior [151] and their residual strength with compression after impact (CAI) [152] following the testing methods used in aeronautic [153, 154]. The impact absorbing capacity depends on the quality of adhesion between core and skins. The sandwich with carbon skins shows weak results in terms of energy absorption but has the lowest indentation dent and the highest contact force. The sandwich with aluminum skins has a very energy absorption but is penalized due to his high mass and a very depth indentation which can be undesirable in some applications. With glass fiber reinforced composite skins, the behavior is quite different. The perfect adhesion and the spring back effect of the skin prevents delamination but decohesion occurs in the first ply of the plywood core. The flax skin provides good results. There is minimum delamination and debonding between skin and core due to the moderate elastic spring back effect while the absorbed energy is comparable to sandwiches with aluminum skins. The compression after impact is one of the main sizing criteria in aeronautic composite structures [155] and must be analyzed. A great result was obtained with the configuration with a strength reduction with is less than 10% for the configuration with aluminum or flax skins. This result is surprising since for classical aeronautic structures the reduction can reach 50%. Moreover, these sandwiches have a large plateau area in the force/displacement curves which is very favorable for crash absorption. Basha et al [156] also studied the compressive behavior after impact of sandwiches with cores made of either balsa (oriented perpendicular to the skins) or birch with plies oriented parallel to the skins. Post-impact behaviour showed an abatement of 40 %, comparable to the abatements observed by Susainathan et al [152], except for the aforementioned materials.

There have been numerous studies of sandwiches with Balsa cores, due to their widespread use in naval applications [157], but wood sandwich cores with very different geometries have also been used [158]: honeycomb core; I-shaped core; interlocking lattice core; corrugated core; molded core; pyramid lattice core; single-layer fiber core; single-layer strand core; multi-layer fiber core. Some authors have also merged the wood with foams to make cores [159]. Wood has also been identified as a component of eco-based sandwich structures [160]. Hybrid sandwiches with a foam core, rubber-cork and E-glass intermediate composite layers and wood skins have been tested by Demircioğlu et al [161].

As far as laminates are concerned, the mixing of veneer with other materials was studied as early as the 1960s [162, 163] with the fibers available at the time, namely glass fibers. It has also been possible to use carbon plies for this purpose [164, 165, 166] and, more recently, basalt fibers [166, 167]. More

specifically Zhou et al [168] studied experimentally the effect of elevated temperature on the bond integrity of aramid, basalt and carbon fiber reinforced polymer bonded to wood systems. This study among others shows the very capacity of wood to be bonded efficiently to a wide variety of materials.

There has also been a recent development in studies on the hybridization of wood with natural fibers. Pereira Acosta et al. have studied wood/jute laminates manufactured by infusion [169]. These hybrid laminates were shown to have better mechanical performance than wood-only laminates in compression and bending. Jorda et al [170] have studied a molded plywood formed part reinforced with flax fibers. This way of reinforcement generates a significant increase in load capacity and stiffness by respectively 76% and 38% on average. Moezzipour et al [171] have studied the reinforcing effect of date palm and kenaf fibers on mechanical properties of plywood by hand-laying these fibers between the wood layers while Wand et al used ramie fibres [172]. Karri et al [173] studied the bond quality of plywood reinforced with short hemp fibers and bonded with lignin phenol-formaldehyde adhesives for structural applications in construction engineering.

This limited number of examples shows that solid wood or plywood is perfectly compatible with composite materials, metals or natural fibers, opening up very broad prospects for structural design by incorporating it as a core material in sandwich structures or directly as a laminated element [174].

**6. Dynamic behavior and Crash capabilities**

Many authors show that wood behavior is not the same according to the speed at which it is subjected to stress, especially in compression, the wood being dry or with a high moisture content. Therefore, this parameter is important to consider when designing wood parts for the transport industry. This viscous behavior has been highlighted for several mechanical properties of wood: Higher is the strain rate, higher is the modulus of elasticity [175, 176, 177], so is the stress at failure [178].

The level of stress in compression between the elastic deformation and the densification is also higher when the strain rate is high. To reveal clearly this relation, the range of strain rate tested must be large enough, from quasi-static to highly dynamic loading. For instance, Targarielli et al. [179] compared experiment with a range of strain rate going from 0.0001 to 4000 $s^{-1}$ (Figure 46). Vural and Ravichandran have also shown that the densification phase occurs at a lower strain with a high strain rate [180].

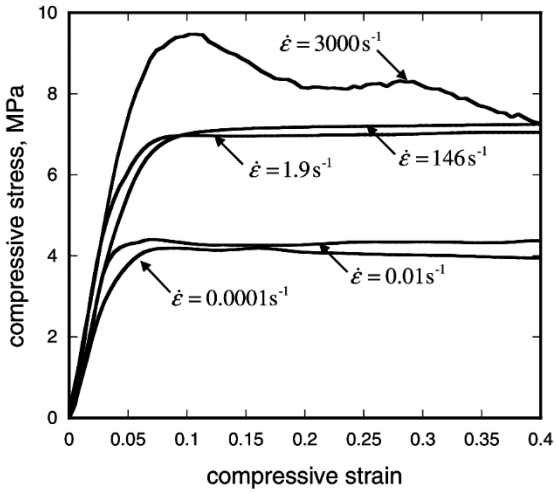


**Figure 46: A comparison between 5 different strain rates compressive responses of balsa wood [179].**

In the previous paragraph, the good post-impact compressive strength of some sandwich specimens was highlighted [152, 156]. The aim of this section is to highlight the little-known shock-absorbing properties of wood and its behavior during and after impact. The positive effect of wood on shock absorption has been known empirically for some time. In the supplementary material, an extract from "Les corsaires barbaresques" (The Barbary Corsairs) shows the extraordinary impact resistance of the hull of the USS Constitution. It is composed of three layers, with white oak for the two outer layers and Virginia oak for the core. It was successfully used during the Tripoli War of 1812. To the authors' knowledge, no scientific studies have been carried out on this subject to find explanations. More recently, wood has been used as a shock absorber in the transportation of nuclear waste [181, 182, 183] or as a crash barrier for freeways [184, 185]. Generally speaking, the dynamic behavior of wood has been studied for many practical applications according to [186]: atomic blast [187]; 19th century warship [188] or wooden buildings [189]. Recently, Ding and Binienda [190] studied the dynamic behavior of birch trees to analyze the crashworthiness of an aircraft in a birch forest. Many authors have also analyzed the dynamic properties of wood, for example with the Hopkinson bar [191, 192, 193], but the aim was not to highlight the interesting natural absorption properties of wood.

Naturally the coconuts have developed an energy absorbing capacity. Therefore, the coconut wood crashworthiness was analyzed by several authors [194, 195, 196]. Nguyen et al. [194] made many quasi-static compression tests in the 3 directions of the coconut wood. Nevertheless, the Specific Energy Absorption (SEA) remains low with an order of magnitude of 5 kJ/kg. A relation with its hierarchical microstructure and the internal fibers directions was identified by Lu et al. [196]. More recently, Guelou et al have studied the crash behavior of a number of tube configurations made with wood veneers of different species (poplar, birch and oak) with or without confinement by glass or carbon fabrics [197 – 202]. In [197], poplar tubes are crushed statically and dynamically, with varying

stackings ([$0_6$], [90/$0_4$/90], [$90_2$/02/$90_2$], and [$0_4$/$90_2$], 0° corresponding to the longitudinal axis of the tube. The belt effect known from composite laminates is found here, and the best drape is [90/$0_4$/90], which achieves a correct SEA of around 30 kJ/kg. In [198, 199], the influence of the number of poplar plies at 0° inside sandwich tubes with skins made of carbon or glass fabric plies is studied. In Fig. 47, for all tube configurations, both static and dynamic, the absorbed energy increases linearly with the number of plies, and increases by a factor of around 2 when the number of poplar plies increases from 2 to 6. This result shows the significant contribution of wood plies to energy absorption. However, the SEA remains more or less constant, with a very good level of 60 kJ/kg for poplar carbon tubes under static conditions. It should also be noted that poplar plies cost around 40 times less than carbon plies. Then, the same authors compare 3 species: poplar, birch and oak with or without composite skins [200, 201, 202]. In all cases, birch gave the best results, with a birch/carbon tube absorbing 7,000 J over 80 mm. The confinement effect was also demonstrated in another configuration by Zhang et al [203]. These authors showed that the gain in SEA for timber cut in the longitudinal direction with an aluminium alloy containment cylinder is, for example, + 380 %. Figure 48 shows that the SEA of tubes made of wood or with wood as the core have very interesting SEA values, and that these materials are perfectly suited to energy absorption, at low economic cost and with a low carbon footprint, and are perfectly renewable. The fact that plywood has good energy-absorbing capacity was also corroborated by Naghizadeh et al [204] in a comparative study with solid wood and OSB (Oriented Strand Board) under high velocity impact. In [205] Heyner et al studied the crash behavior of mixed wood/steel beam structures that could be used as automotive door impact beams. According to the authors, the result of hybridization is interesting, even if the weight of the prototype beams is comparable to that of the reference steel beam. On the whole, wood has a much better crash behavior thanks to the metal component, and makes a significant contribution to energy absorption.

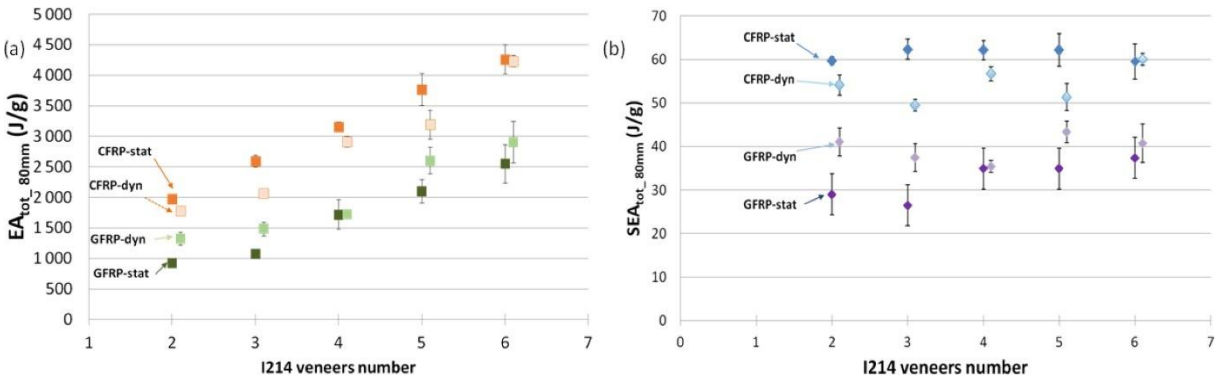


**Figure 47. Evolution of (a) EAtot_80 mm (b) SEAtot_80 mm according to the number of poplar layers, the nature of the skins (CFRP: Carbon Fiber Reinforced Polymer; GFRP: Glass Fiber Reinforced Plastic), and static and dynamic conditions. Reproduced from [199]**

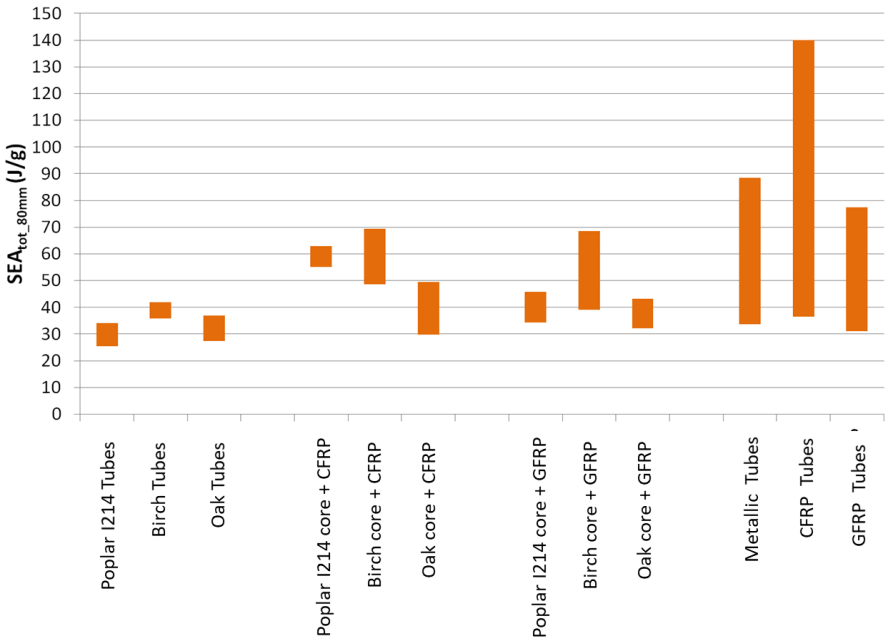


**Figure 48. SEAtot_80mm for the wood species tested and for others materials (Reproduced from [202]).**

## 7. Some chosen examples of wood and plywood in the naval industry

It would seem that very early on, navigation was a means of exchange and transport for men and that the first ships appeared around 50,000 years ago. The first ships dating from prehistoric times were dugout canoes dug directly into tree trunks or dugout canoes [206]. The means to dig these rudimentary boats were varied, excavation using tools or by controlled combustion of the internal part. The oldest example of these canoes appears to be the 10,000-year-old Scots pine canoe from Pesse found in 1950 (see figure 49) in the Netherlands and dated to around 8243-7582cal. BC [207].

**Figure 49: The dugout canoe from Pesse, Netherlands, 8243-7582 cal. BC. Length: 2.98m; width: 0.44 m; depth. 0.31m; pinus sylvestris [207].**

These boats will be used for a long time and models found over a long period, for example the 22 canoes found on Lake Sanguinet (Landes-Frances) are dated from 1732 BC for the oldest to 1621 AD [208]. They were mostly pine but some were oak. Later, structures in several caulked elements for sealing [206]. The most striking examples are the solar boats of Egypt. The artifact solar ship of Khufu

(2550 BC) is one of the oldest and the largest boats of the ancient times. It is 43.6 meters long and 5.9 meters wide. It is a masterpiece of the ancient craft of shipbuilding and this boat is composed of more than 1600 different pieces, some of which are marked with mounting indication. It was discovered into a sealed pit carved out of the Giza bedrock [4]. During antiquity these ships were perfected to allow navigation in the Mediterranean: Thalassa. Two notable types of ships developed, merchant ships and warships. Phoenician merchant ships are emblematic of the first category, the Gaulos appear around 2000 BC (figure 50), the Greek and Roman triremes with their sails, their rows of rowers and their spur are a perfect example of the second category (figure 51). On the other hand, no wreckage has been found with certainty and little information on their method of construction remains, we just know that they were made of local wood, namely fir, pine, or cedar [210]. There are very few wrecks because its ships being made of wood, they did not sink and when they did, the wood is quickly eaten away in the sea and disappears in a few decades.


**Figure 50: Phoenician Gaulos, merchant ship, 2nd millenium BC [2010]**

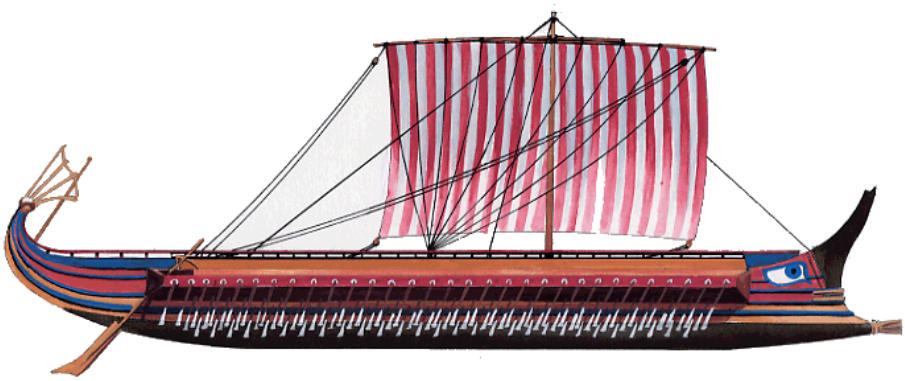

**Figure 51: Athenian trireme in the years of the Peloponnesian War, half of the 5th century BC [210].**

In the Middle Ages, construction techniques evolved and envelopes were mounted on structures like Viking ships (4th to 13th century). They had a T-shaped keel in one piece (or even two) and articulated

couples on the keel to keep a certain flexibility and elasticity. The drakkars or snekkar are real sea serpents which slide and deform along the waves following the swell. The sides are in plank assembled with clapboard (with an overlap). Hulls, mostly oak or pine, were caulked with tar-coated hemp. They did not have a bridge but beams went from one side to the other and served as a thwart [211].

The Vasa, launched and sunk in 1628, is an emblematic wreck because it was refloated almost intact in 1961 and is now on display in Stockholm [212]. It allows you to study the construction techniques of the time. The Vasa is a hybrid type three-master between the galleon and the carrack. Her sails included three tiers of square sails on the foremast and on the mainmast, two square sails on the bowsprit, a lateen sail and a square sail on the mizzenmast, the ship had 4 decks and was made of oak, Sparred length: 69 m, between perpendiculars 47.5 m, beam 11.7 m, height 52.5 m, Draft 4.8 m. This type of ship is built from a structure, i.e. the planking is fixed afterwards (Frame first). Frame-first construction involves laying down the framework of the vessel before attaching the planks to the boat. This is done by erecting a master frame in the center of the keel, and the ribs and after deriving the shapes of the other frames using a curved piece of wood stretched between the frame and the end posts, or through a geometric curve. This type of assembly appears during the 5th century AD.

The Endeavor is an emblematic 18th century ship aboard which explorer James Cook set out in 1768 to explore and map New Zealand and part of Australia, a replica of which was built in 1988 using plans kept at the Greenwich Maritime Museum [213]. The 19th century saw maritime exchanges intensify across the Atlantic as ships capable of traveling the oceans and defending fleets were built. Precise plans exist from this period and the manufacturing techniques are well known, which facilitates the production of replicas. One of the most famous is certainly the Hermione (3 masts, 65 meters long), the frigate that took Lafayette to America to support the American Independence Army in 1870. She accidentally sank off Brittany in 1793. The replica, whose construction began in 1997, was launched in 2014. construction techniques used were identical to the original and the materials also used, in particular the use of 2000 oaks for the construction of the hull [214, 215].

During the end of the 19th century and until the end of the first half of the 20th century, many leisure or racing boats were built in wood and many in mahogany (mahogany). Sailboats will gradually give way to motor boats. Chris Craft factory is a perfect example [216]. It began in 1861 by building small mahogany boats for family trips on the lakes, then equipped its boats with increasingly powerful motors at the beginning of the 20th century (figure 52 (a)) and became one of the largest manufacturers of dayboats and runabouts. During World War II, it built more than 12,000 patrol boats, utility launches, and rescue vessels for the United States Navy and Army (figure 52 (b)). During the 50th

they lineup but they manufacture their first fiberglass boat and in 1971 they their last mahogany boat. The maintenance of wooden boats was becoming too expensive compared to composite ones.

(a)  (b) 

**Figure 52: (a) Chris Craft runabout mahogany boat 1935; (b) Chris Craft landing craft 1944 [216]**

Many wooden boats were built during the World War II. Splinter fleet was a nickname given to the United States wooden boats used in World War II. The boats served in many different roles during the war (figure 53). These boats were built in small boatyards everywhere on the American coast. They could be built quickly, in just 60 to 120 days. Most of the boats were built by boatyards that already had the tools and knowledge from building yachts, sailboats and motor boats. Many were built by craftsmen in family-owned small businesses. These wooden boats have lighter weight and are easier to repair than steel hull boats and there was a shortage of steel and steel shipyards. Many of these boats used plywood for their manufacture especially for the hull [217].

**Figure 53: wooden PT-105, 24m long, build in 1942 [217]**.

From the beginning of the 20th century, steel will replace part of the wooden structures in sailboats. During the 60th years, fiberglass will gradually replace wood for the hulls of pleasure boats. Maintenance is greatly simplified but the charm of the wood disappears, or remains in the form of veneer. Nowadays, only the fittings, in plywood or solid wood, and the covering of the decks, in teak, are still made of wood. There are very few wooden boat manufacturers left and they are mainly

sailboat builders. Spirit Yachts manufactures pleasure sailboats and motor yachts in a very traditional way (figure 54) [218].

**Figure 54: Spirit Yachts classic building [218].**

Other shipyards offer plywood constructions, one of the best known is the RM Yacht shipyard [219]. The marine plywood elements are delivered as a kit. These elements will then be assembled by gluing with epoxy fillets. The plywood structure is then mounted around the metal structure which takes up the main forces of the keel and the shrouds, the whole will contribute to the rigidity of the hull (figure 55). The glass/epoxy-infused, plywood-clad deck is then assembled to the hull (Figure 11b). The junctions are reinforced with GFRP epoxy. The assembly is then covered with an epoxy paint to protect the wood from the marine environment (figure 11a). Units are up to 14 m long [10,11]. The advantage of these boats is mainly the lightness of the structure, its structural rigidity and the silence during navigation.

**Figure 55: Plywood structure of an RM sailboat [219]**

(a)  (b) 

**Figure 56: (a) Painted structure of an RM; (b) sailboat deck [219]**

**8. Some chosen examples of wood and plywood in the automotive industry**

In 1769, military engineer Nicolas Cugnot built the first vehicle capable of doing without animal traction - in the truest sense of the word, an "auto-mobile". Initially, this was a military project, as the vehicle had to be able to move heavy loads, in particular artillery pieces. For this reason, Cugnot obtained the support of the Duc de Choiseul, Louis XV's Minister of War, for the development of his project. A steam boiler alternately powers two cylinders installed on either side of a single driving wheel. Designed to reach 15 kilometers per hour, the fardier, which made its first test run in 1769, did not exceed 4 or 5 kilometers per hour. It had a reverse gear. Measuring 7.30 m, weighing 3.5 tons, the wheels and structure were made of wood. It didn't have a long career, however, as the prototype hit a wall without a braking system. Joseph Cugnot's research came to an immediate halt. Figure 57 shows a recreation of Cugnot's fardier.

**Figure 57: The first automobile with wooden chassis and wheels, the "Fardier de Cugnot"** (www.lefardierdecugnot.fr).

Many of the very first automobiles before 1914 had wooden chassis or body components. In a 1920 article, Ermendorf [220] explains the use of plywood in automobile construction. Firstly, thanks to its use in aeronautics, glues had really improved compared with the vegetable glues used before the 1914 war. Glues were perfected that enabled plywood to withstand 8 hours of boiling or 10 days of soaking in water without separation of the plies. He goes on to discuss the use and shaping of plywood for

body components. Although steel rapidly supplanted wood construction in the USA, some mass-produced vehicles, such as the Ford Model A Woody of 1929 [221], had wooden bodies. This phenomenon lasted well into the 1950s, although industrial production was limited, and some vehicles were still built by hand. An example is shown in Figure 58. Throughout history, there have been many one-off hand-built models, such as the Ray Russell plywood car of 1942 [222]. A survey of some of these products can be found in [223] and a brief review of the use of wood-based panels in the transport sector in [224] (Bus and Cars, Motorhomes and caravans, railways).

**Figure 58: 1929 Ford Model A (Reproduced from [221]).**

In this review article, we have chosen to focus on some of the lesser-known examples of industrial adventures involving automobiles with working wooden structures. First and foremost, the achievements of English engineer Frank Costin are a must [225, 226, 227]. Frank Costin, a former De Havilland engineer, was responsible for several plywood aircraft, including the famous DH 98 "Mosquito", which reached speeds of 612 km/h and was one of the best planes of the Second World War [155] With the experience he had acquired in aeronautics, Frank Costin was responsible for numerous prototypes of racing vehicles, most of them with plywood chassis. He was behind the Marcos brand, which he co-founded with Jem Marsh (MARsh and COStin), producing several hundred cars between 1959 and 1972. The GT (Figure 59 (a)), which existed with a wide range of engines, had an all-plywood chassis. It's made up of 386 separate plywood pieces that had to be cut out and glued together in a time-consuming process. This is probably why, despite its lower weight, the original plywood chassis was later replaced by a steel chassis. One model produced in only 12 examples was the Costin Nathan GT (Figure 59 (b)), which boasts an extremely light weight (around 400 kg) and a central plywood shell. On both ends a tubular subframe was mounted to support the suspension and mid-mounted engine. One of the main reasons for the extensive use of wood was that it offered a strong, lightweight construction at the fraction of the cost of a similar aluminium chassis [226]. It was entered at Le Mans in 1967, but its low engine (1000 $cm^3$) was a handicap on the Hunaudières straight, and it soon retired. However, the models produced went on to win various races in England over the years. Finally, a single example of the Mantis (Figure 59 (c)) was produced with a resolutely modern design that illustrates the adaptability of plywood design.



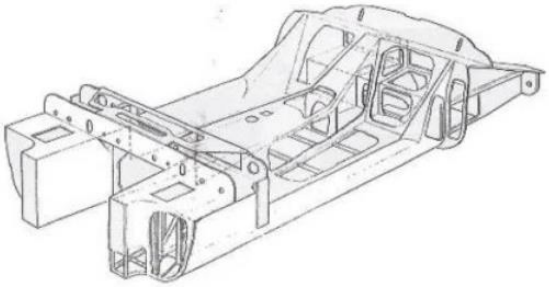

**(a) Marcos GT (1964-1972)**



**(b) The Costin-Nathan Le Mans GT (1967)**

**(c) Marcos Mantis XP (1968).**

**Figure 59: Some of the production of wooden cars designed by Frank Costin.**

The Africar was imagined, designed, tested and produced by a visionary Englishman by the name of Tony Howarth in the 1980s [228]. Inspired by the Citroën Mehari, but with a chassis and bodywork made of marine-grade epoxy resin-impregnated plywood. The aim was to create an all-terrain vehicle

that would be easy to repair and have a minimum lifespan of 30 years (see Figure 60). An expedition from the Arctic Circle in Norway to the Equator in Uganda was organized with the support of a TV channel. The films [229] and the book [230] show the performance of the three vehicles involved (a sedan, a pickup and a 6-wheel station wagon) over difficult terrain, crossing the Sahara, the Sahel and difficult tracks in Central Africa and Zaire. The plywood chassis remained pristine while some metal parts like the gearbox where cracked due to fatigue. Despite the quality of the prototypes and the chassis, the Africar company was poorly managed and soon disappeared.


**Figure 60: One of the 3 Africars crossing the Ubangui River and a plywood chassis [230].**

The English Morgan brand is an icon of car manufacturing [231, 234]. Since 1936, Morgan cars have been built with an aluminum or steel "ladder" chassis, consisting of two longitudinal beams and several crossmembers. The aluminum body is attached to an ash superstructure, which in turn is attached to the chassis. An excellent description of this structure is given by a restorer in [233], and is partially reproduced in Figure 5. These are the last cars still built according to this scheme; despite this old-fashioned method, the Morgans meet automobile safety standards. The latest evolution of this model (Plus 6, see Figure 61) uses more wood than previous versions [232]. Production, which has remained deliberately small-scale, stands at around 300 cars a year.

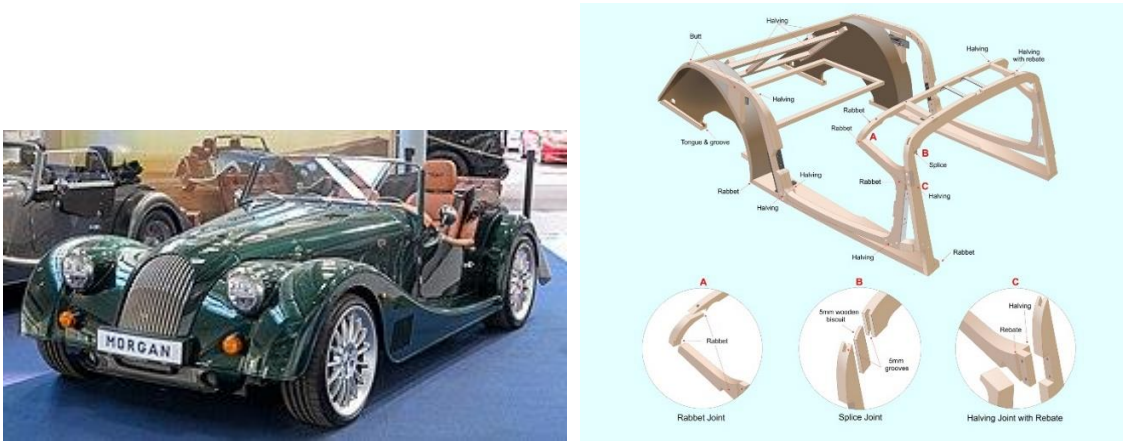


**Figure 61: The last model of Morgan cars, the "Morgan Plus Six" and its ash frame structure [231, 233].**

For the moment, major automakers have shown little interest in this material, but Toyota presented a highly original concept car at Milan Design Week in 2016, designed by chief development engineer Kenji Tsuji [235]. The Setsuna, which means "moment" in Japanese (Figure 6), is made entirely of wood, using the traditional Japanese carpentry technique of "okuriari" (no nails or screws). According to [235]: "As a functioning vehicle, it was important that different types of wood were selected for specific applications. For the exterior panels, Japanese cedar (*Cryptomeria japonica*) was chosen for its combination of vivid colour, refined wood grain, and overall flexibility. For the frame, Japanese white birch (*Betula platyphylla*) was selected for its strength and rigidity, while the floor uses Japanese zelkova due to its strength and durability. Finally, the seats are constructed in smooth-textured castor aralia (*Fatsia japonica*)". The Concept car is 3.03 metres long and 1.48 metres wide, with a height of 0.98 metres. The bodywork comprises 86 interchangeable elements, as shown in Figure 62. Its color changes over time according to weather conditions (humidity, temperature). It is electrically propelled.

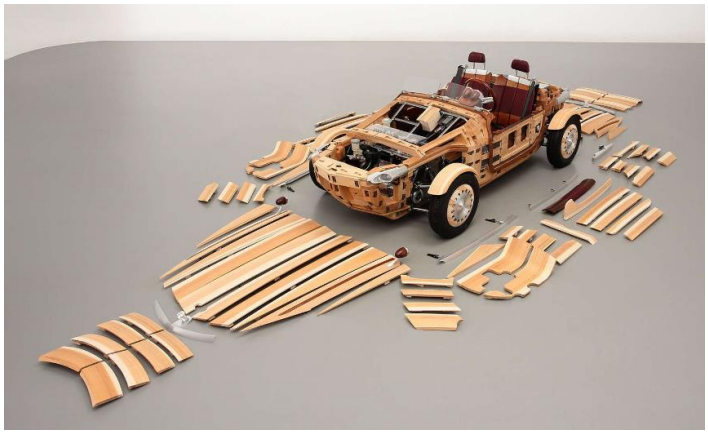

**Figure 62 : Toyota Setsuna Concept Car [236].**

Renewed interest in wood is reflected in a number of recent research programs. The most noteworthy is the Austrian WoodC.A.R. (Wood - Computer Aided Research) project. According to [237], "The vision of the K-Project WoodC.A.R. (Wood - Computer Aided Research) is to introduce Engineered Wood Products (EWP), Engineered Wood Components (EWC), and wood-based materials to the mobility sector, which follows the demand for improvement of environmental and economic sustainable materials in this branch. Key for the application of EWPs and EWCs in the engineering and the development process are reliable Computer Aided Engineering (CAE) models of wooden materials exposed to dynamic and static loads. Additionally, new production technologies for shaping, joining and bonding are required. Simulation tools as well as new technologies will open new markets within and beyond the mobility sector". Dynamic simulations were carried out on automotive structural components (subfloor, rear panels and front instrument carrier) based on a previous research program called CULT (Car Ultraligth Technologies) see Figure 63. An exhaustive species characterization program was carried out, involving over 5,000 tests to obtain the material maps required for crash

simulation. Some of these tests were even robotized [238]. A snowmobile structure was also designed and crash-tested. All in all, the program has shown that it is possible to simulate wood components for the transport sector [239,240]. Moreover, an economic comparison shows a clear advantage for wood solutions in terms of mass savings, unit part costs and tooling investment. For example, the cost of tooling to produce the aluminum floor is 1,400 k€, whereas it is only 100 k€ for the wood solution.

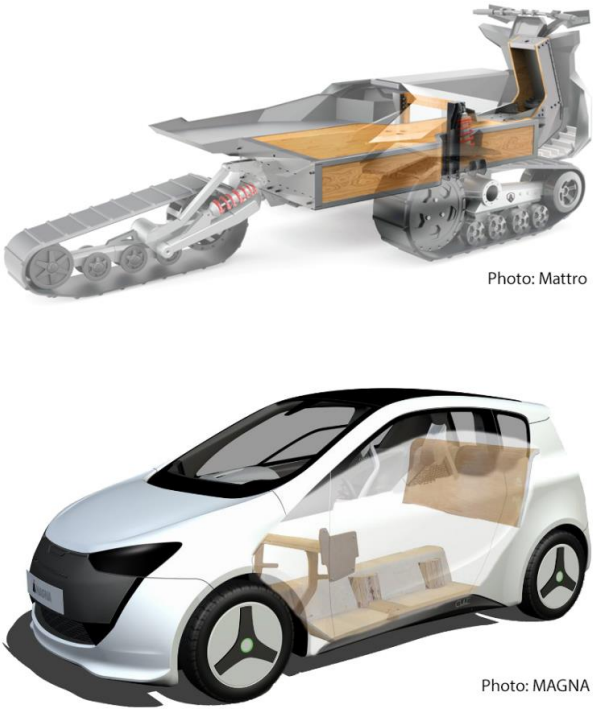


**Figure 63: (a) wood frame on a snow mobile; (b) Wood part on CULT Car project (Reproduced from [237]).**

**9. Some chosen examples of wood and plywood in the aeronautic industry**

As with the automotive industry, an exhaustive review of the uses of wood in aeronautics, especially in its early days, is impossible within the scope of this article. We will therefore focus on a selection of the most emblematic applications. With weight constraints, wood was the only viable material in the early days of aviation, and virtually all aircraft up to the 1920s had wood and fabric trellis structures, often stiffened by steel cables. Two typical examples from the period are presented:

- The Wright brothers' airplane, illustrated in Figure 64 (a), which made the first truly manned powered flight in 1903 [241, 242].
- The Blériot XI was the first plane to cross the English Channel in 1909 (see Figure 64 (b)), and was also the first military aircraft ordered by the armies of France, Italy, England, Switzerland, and Italy. Over eight hundred Blériot XIs were sold between 1909 and 1919, and were used in the First World War [243].

(a) 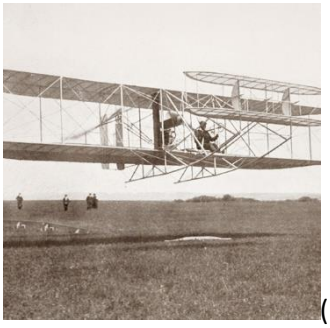 (b) 

**Figure 64: (a) Aircraft of the Wright brothers (Reproduced from [241]); (b) Blériot XI (Reproduced from [243])**

Although the transition to aluminum-alloy metal structures had begun in the 1920s [244], many aircraft continued to be built in wood until the Second World War. At the time, aluminum was a strategic and expensive metal, and less readily available than today. Structures were classically made of plywood, solid wood or sandwich with light wood as core. This last point was addressed in a previous review [155] and will not be repeated here in detail. A few significant examples are given below. Figure 65 illustrates the typical design principles of a wooden wing on the A.N.E.C. (Aeroplane Air Navigation and Engineering Company) aircraft of 1923. According to [245] "The spar is of triangular section, and is built up of three corner strips of spruce, joined under each rib by an internal triangle formed of thin spruce strips. The whole is covered with plywood. The entire leading edge is covered with plywood". In the inter-war period, new resins and glues were developed, enabling the development of more efficient assemblies [246]. As an application, the Hughes H-4 Hercules remained until recently the world's largest aircraft, with a wingspan of 97.54 meters, and is made almost entirely of wood [247].

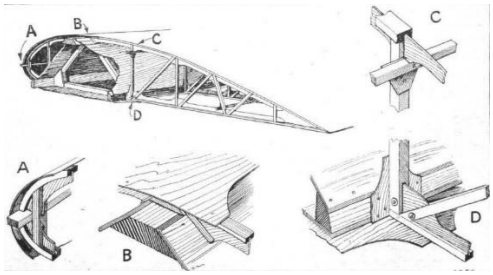


**Figure 65: Typical design of a wood wing and internal joints (reproduced from [7])**

**Figure 66: The Lockheed Vega, the concrete molds used to form the fuselage halves and components of the first Lockheed Vega 1 before assembly (Reproduced from [11])**

In [248, 249] a record-breaking aircraft is showed: the Lockheed Vega (Figure 66). It was a four-passenger (plus pilot) aircraft that was one of the fastest aircraft of its era. Using a wooden monocoque fuselage, plywood-covered cantilever wings and the best engine available, the Vega delivered on the promise of speed. The fuselage was built from sheets of plywood, skinned over wooden ribs. Using a large concrete mold, a single half of the fuselage shell was laminated in sections with glue between each layer and then a rubber bladder was lowered into the mold and inflated with air to compress the lamination into shape against the inside of the mold. The two fuselage halves were then nailed and glued over a separately constructed rib framework. This solution, with two half-fuselages bonded and nailed, was also adopted by some of the best aircraft of the Second World War (see Figure 67), such as the De Havilland Mosquito DH-98 [155], nicknamed "the wooden wonder". The following figure shows a view of the construction The Mosquito is a good example of the possibilities offered by wooden structures (here a sandwich structure with birch or Douglas-fir skins with a balsa core), since it reached a speed of 618 km/h and was produced in 7,781 units. Like the Lockheed Vega, this is a "one-shot" composite solution. It is interesting to note that composite methods were already in use in the 40s, with the use of autoclaves (see Figure 68) for the production of plywood parts [250].

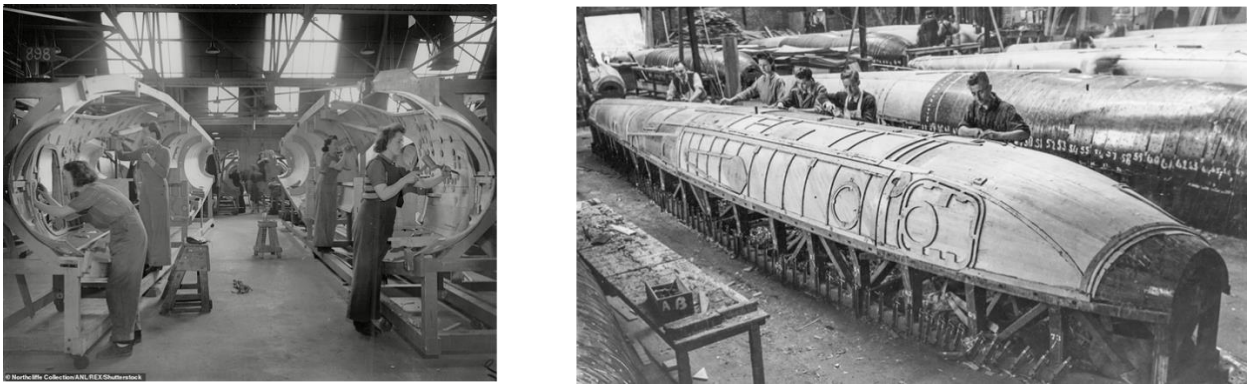

**Figure 67: The De Havilland Mosquito ([6])**

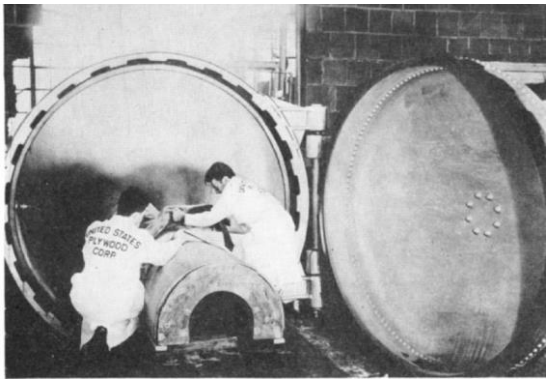

**Figure 68: An early Autoclave (1944) used for the forming of plywood (Reproduced from [250])**

During the Second World War, the US Forest Product Laboratory gave considerable impetus to the design of timber structures [251]. Among other things, it led to the drafting of design manuals [252,

253]. It is also a little-known fact that very common test methods for aeronautical structures, such as the deformable square [254], originated from work carried out by the US Forest Product Laboratory on aeronautical plywood. To conclude this section on the Second World War, one present two aircraft among others for which wood structures were used to cope with shortages of metal materials. The first is the Russian Yakovlev series (Figure 69 (a)), for which the Soviet authorities imposed the use of wood as early as 1936. The second highly original aircraft was the Heinkel He 162, which, along with the twin-engine Messerschmitt Me 262, was one of the first operational jet fighters in history. It was designed and built in 90 days, in a last-ditch effort to prevent Germany's defeat at the end of the Second World War. As conceived, the Heinkel He 162 was to be an inexpensive fighter, capable of being built by semi-skilled labor from non-strategic materials such as wood (Figure 69 (b)). The aircraft is made of wood, except for the light-alloy fuselage. Finally, to conclude this section, although widely available, wood proved an indispensable resource for the war effort and aviation in particular, as the poster in (Figure 69 (c)) from [20] shows.

(a)

(b)

(c)


**Figure 69: (a)The yakovlev YAK -1 (Reproduced from [255]); (b): the Heinkel He 162 (Reproduced from [256]); (c): a poster on the need for wood during the second world war for aircraft [257].**

After the Second World War, the golden age of wood use clearly came to an end, with the spread of aluminum construction and the arrival of the first composite materials [155, 244]. However, a few specific applications remained, such as fuselage skins, ailerons and flooring. Today only a limited number of wood aircraft are produced. Most are simple and inexpensive aircraft that could be built by amateur builders for education or recreation and not for large production. One good example among dozens is the Varieze and Vari-Viggen planes made by Burt Rutan in the 1970s [258], and inspired by

the Saab Vigen Fighter, shown in Figure 70. The main structure was made of plywood and was easy to build using normal techniques. Spruce was used for spars and longerons, and aircraft plywood for the formers, ribs, and skin. The plywood skin was covered with lightweight Ceconite and finished with dope followed by polyurethane. In France, a tradition of wood construction has endured to the present day. The Mudry CAP 10 is an acrobatic aircraft made entirely of plywood, weighing around 530 kg. Around 300 have been built since 1968 (Figure 70). An improved and certified version, the CAP10 BK, incorporates carbon spar beams (Figure 70) for enhanced performance. The aircraft is now manufactured by Robin Aircraft. This company is well known in the aviation world for its DR 400, now the DR 401, made entirely of plywood, 2,700 of which have been produced since 1972 [259, 260]. In [259], the company demonstrates that when properly designed, bonded and protected, the structure's service life is very high.

(a) 

(b) 

(c) 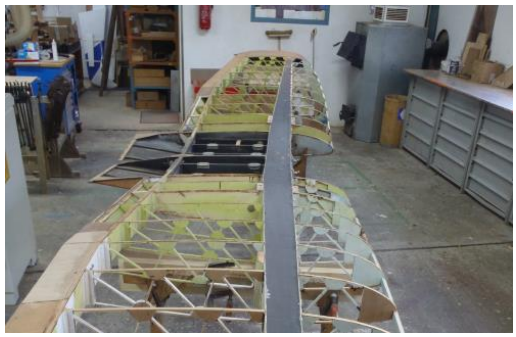

**Figure 70: (a): A Varrivignen (Reproduced from [21]); (b): the Mudry CAP 10 (Now Manufactured by Robin Aircraft); (c): The CAP 10 BK carbon spar inside the wood wing.**

Two new French companies are also involved in the design and production of lightweight aircraft incorporating wood structures. Aura Aéro is in the process of certifying a wood-carbon aerobatic aircraft (the Integral R, see figure 71 and ref [261]). Avions Mauboussin is also developing an all-wood light aircraft with electric or hydrogen propulsion, based on the DH-98 "Mosquito" with a sandwich under the trade name Y. The wood species used in the manufacturing process of YGDRASIL (Scandinavian birch, French poplar and ash, balsa) inspiration from the Mosquito [262].


**Figure 71: Two new wooden light aircraft in France: Aura aero Integral R and its carbon-wood structure and the forthcoming "Avion Mauboussin" and a picture of a wing made with a wood-based sandwich "YGDRASIl".**

**10. Wood and plywood in the space industry.**

It may seem surprising to find wood in this field too, but its use in specific applications has been known since the beginning of the space adventure. Wood's ability to absorb dynamic loads is well known, and balsa impact attenuators have been studied for various applications. It was used for the Rangers missions to moon in the early sixties (see figure 72). According to [263] "The sphere was 65 cm in diameter, and it surrounded a transmitter and a seismometer instrument that was designed by the Caltech Seismological Laboratory. The sphere would separate from the spacecraft shortly before impact and survive the rough landing on the moon. The capsule was also vacuum-filled with a protective fluid to reduce movement during impact. After landing, the instrument was to float to an upright position, then the fluid would be drained out so it could settle and switch on." It was used to measure the hardness of the lunar soil, which was unknown at the time.

**Figure 72: Rangers 3, 4, and 5 each had a seismometer encased in balsa wood to limit the impact loads for moon exploration (1962), [263].**

In 1965, a space probe project for a Mars landing was studied with an impact attenuator "which consists of a spherical payload contained within a thick spherical shell of balsa wood. The spherical balsa shell will be constructed of segments of balsa in sufficient number so that the approximate grain direction throughout the balsa sphere is radial" [264]. In 1966, a specific study of environmental effects on the crushing response of balsa was published by NASA [265]. The effect of vacuum, moisture content in the wood (between 0 and 20%), density (80 kg/m$^3$ to 240 kg/m$^3$), and temperature (-87 °C to + 150 °C) on mean crushing stress were studied. [265].

Cork, mixed with phenolic resin, is the most widely used, and has been since the 1960s [266]. It bonds perfectly with today's composite structures and is used on civil and military launchers' fairing as a thermal protection system [265]. Wood is used for thermal protection during re-entry into the Earth's or Mars' atmosphere. During these phases, friction on upper level of atmosphere cause the wood to burn and char, leaving behind a layer of charcoal. Both the wood and the charcoal are great insulators. Then the burned layer is blown away during the descent and the cycle repeat. Finally, very little heat is transmitted to the spacecraft. According to [266], some Chinese satellites may probably use solid oak as thermal protection during these re-entry phases. Among all the published applications, a recent study for a European Mars lander (Schiapparelli Module) caught our attention (Figure 73). The Descent Module is shown entirely covered in cork [267], and a posteriori heat flow calculations have been carried out [268, 269], showing good prediction and the effectiveness of the NORCOAT LIEGE® coating. It is truly surprising to see that wood has been transported to Mars, proving its intrinsic effectiveness in this field. A recent study details the physical mechanisms at work [270]. Many of the above points are presented in an interesting popularization video [271].

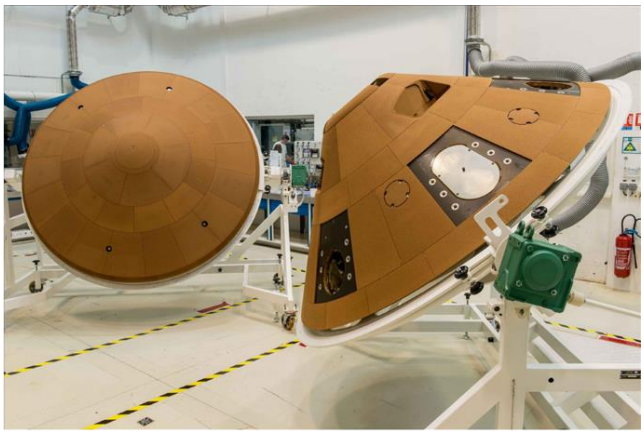

a

b

(c)

**Figure 73: (a),(b) views of the Schiaparelli Front and Back Heat Shield TPS during assembly. Copyright: Airbus Defence and Space SAS 2014 A. Gilbert. The images are available on the ESA Exploration web site http://exploration.esa.int/; Reproduced from [267]. (c) The transformation of cork in charts after a burning test with a plasma torch (reproduced from [269]).**

To conclude this quick tour of wood in space, it's interesting to note that two studies are currently underway, in Japan and Europe (Finland), to use wood as a structural material for small satellites. According to [272], for the Japanese study, “The idea of a ‘WoodSat’ as an answer to the growing problem of space debris in low Earth orbit… Here’s one possible plus for a wooden satellite: wood is largely transparent to radio waves, meaning you could keep most of your communications and research antennas internal: no more unfurling bulky instruments after achieving orbit. In fact,”failure to deploy” once orbit is achieved has doomed many a satellite… and this wouldn’t be a problem with

WoodSat". This satellite will use magnolia wood. According to [273] "The high durability of wood in space was recently tested and confirmed at the International Space Station (ISS) by an international group of scientists led by those from Kyoto University. Their experiments showed wood samples tested at the ISS for durability underwent minimal deterioration and maintained good stability. Preliminary inspection, including strength tests and crystal structural analyses, of the wood samples was also done once they were brought back to Earth from the ISS by Japanese astronaut Koichi Wakata." ([274] and Figure 74 (a))

The European satellite (Figure 74 (c)) is made of Finland birch plywood [275], but with some additional elements to help it withstand space conditions. A camera is deployed like a selfie pole to film the behavior of the wooden structure, which is the main objective of this mission. According to [276], "The base material for plywood is birch, and we're using basically just the same as you'd find in a hardware store or to make furniture," explains Woodsat chief engineer and Arctic Astronatics co-founder Samuli Nyman. "The main difference is that ordinary plywood is too humid for space uses, so we place our wood in a thermal vacuum chamber to dry it out. Then we also perform atomic layer deposition, adding a very thin aluminum oxide layer—typically used to encapsulate electronics. This should minimize any unwanted vapors from the wood, known as "outgassing" in the space field, while also protecting against the erosive effects of atomic oxygen. We'll also be testing other varnishes and lacquers on some sections of the wood."

(a)

(b)

(c)

**Figure 74: (a): sample sent to ISS for testing; (b): Japan Lignosat and (c): Wisawoodsat.**

## 11. Conclusion and perspectives

Wood has accompanied the mobility needs of human beings for 6,000 years. If during the last century its use in this field has greatly decreased, the examples chosen in the naval, automotive and aeronautical fields clearly show the potential of wooden structures in the field of mobility. The carbon footprint of these structures is only a fraction of that of metal structures while achieving significant reductions. Contrary to popular belief, the crash behavior can be excellent and the problem is all the less severe as the structures can be lightened. Another important advantage of wood is its ability to be mixed with other materials, which puts “the right material in the right place”. The question of the resource is delicate because the sensitivity of forests to global warming is great. For the Northern hemisphere the resource exists and is available. For the Southern hemisphere, deforestation is massive. However, a use with high added value such as the transport industry could lead to more reasoned management or even replanting for this purpose for local use.

From a structural calculation point of view, wood and plywood are very complex, even compared to composites. The literature is poor concerning plywood and the need is important to have models that are both exhaustive and predictive. Many points in particular must retain the attention of researchers for a practical purpose and applications to automotive and aeronautical purposes: the development of damage models adapted from those of composites to be able to carry out static calculations, in damage or crash tolerances for sizing common areas or junctions. The methods of identification of the parameters of these models will also have to be adapted to these materials. Finally, the significant variability of the veneers should be integrated in one way or another. A possibility studied in the French research program initiated in 2021 ANR BOOST [277, 278] is to measure in-process during and/or instantly after peeling the local characteristics (surface scanning) of the veneers to introduce them into a dedicated veneer and plywood model. Generally speaking, the research on wood or plywood for transportation has lost interest and there is a wide area of research to develop in terms of characterization and modeling, environmental effects and many others from the scale of coupons to real structures. In general, as during the Second World War, wood is a resource that can be strategic and contribute to the resilience of a society. Studies such as the preservation and sustainability of the resource must be given increased attention.

## Acknowledgments

The research that led to the results presented above received funds from the French National Research Agency under the BOOST project (ANR-21-CE43-0008-01).

## 12. References

[1] D.W. Antony, The Horse The Wheel and Language: How Bronze-Age Riders from the Eurasian Steppes Shaped the Modern World, Princeton University Press 2007, Princeton, USA, ISBN 9780691058870.
[2] L. Liancheng, Chariot and horse burials in ancient China, Antiquity. 67;257 (1993) 824-838. doi:10.1017/S0003598X0006381X.
[3] G. Camps, Les chars sahariens [Images d'une société aristocratique], Antiquités africaines. 25 (1989) 11-40. https://doi.org/10.3406/antaf.1989.1152.
[4] https://fr.wikipedia.org/wiki/%C3%89tendard_d%27Ur (accessed 16 july 2023).
[5] E.A. Bennett, J. Weber, W. Bendhafer, S. Champlot, The genetic identity of the earliest human-made hybrid animals the kungas of Syro-Mesopotamia, SCIENCE ADVANCES. Vol 8;2 (2022). DOI: 10.1126/sciadv.abm0218.
[6] A. Rovetta, I. Nasry, A. Helmi, The chariots of the Egyptian Pharaoh Tut Ankh Amun in 1337 B.C.: kinematics and dynamics, Mechanism and Machine Theory. 35 (2000) 1013-1031. https://doi.org/10.1016/S0094-114X(99)00049-X
[7] N. Scarlat, J-F. Dallemand, F. Monforti-Ferrario, V. Nita, The role of biomass and bioenergy in a future bioeconomy: Policies and facts, Environmental Development. 15 (2015) 3–34. https://doi.org/10.1016/j.envdev.2015.03.006
[8] European Environment Agency, A Roadmap for Moving to a Competitive Low Carbon Economy in 2050, COM (2011) 112.
http://eur-lex.europa.eu/LexUriServ/LexUriServ.do?uri=COM:2011:0112:FIN:EN:PDF
[9]https://ec.europa.eu/eurostat/statistics-explained/index.php?title=Wood_products_-_production_and_trade#Wood-based_industries (accessed 16 july 2023).
[10] https://inventaire-forestier.ign.fr/IMG/pdf/memento_2021.pdf (accessed 16 july 2023).
[11] D. Kohl, P. Link, S. Böhm. Wood as A Technical Material for Structural Vehicle Component, Procedia CIRP. 40 (2016) 557 – 561. doi: 10.1016/j.procir.2016.01.133.
[12] K. Sahoo, R. Bergman, S. Alanya-Rosenbaum, H. Gu, S. Liang. Life Cycle Assessment of Forest-Based Products: A Review, Sustainability. 11;17 (2019) 4722. https://doi.org/10.3390/su11174722.
[13] Marcus Lindner et al, Climate change impacts, adaptive capacity, and vulnerability of European forest ecosystems. Forest Ecology and Management. 259 (2010) 698–709. https://doi.org/10.1016/j.foreco.2009.09.023
[14] G.J. Harper, M.K. Steininger, C.J. Tucker, D. Juhn, F. Hawkins Fifty years of deforestation and forest fragmentation in Madagascar, Environnemental Conservervation. 34;4 (2007) 325-333. https://doi.org/10.1017/S0376892907004262.
[15] A. Andriamananjara et al, Land cover impacts on aboveground and soil carbon stocks in Malagasy rainforest, Agriculture, Ecosystems & Environment. 233 (2016) 1-15. https://doi.org/10.1016/j.agee.2016.08.030
[16] A.H. Rajemison. Proposition d'essences de substitution aux bois précieux en épuisement par la connaissance des propriétés du matériau bois : cas du palissandre de Madagascar : application en ameublement. PhD Thesis Toulouse (in french). http://thesesups.ups-tlse.fr/2318/
[17] P. Gillet, C. Vermeulen, L. Feintrenie, H. Dessard, C. Garcia, Quelles sont les causes de la déforestation dans le bassin du Congo ? Synthèse bibliographique et études de cas, Biotechnologie, Agronomie, Société et Environnement. 20 ;2 (2016) 183-194. https://doi.org/10.25518/1780-4507.13022

[18] U. Mantau, Wood Flows in Europe (EU27), Project Report Celle 2012. https://www.researchgate.net/publication/291034739_Wood_flows_in_Europe_EU_27

[19] F. Negro, R. Bergman, Carbon stored by furnishing wood-based products: An Italian case study, Maderas Ciencia y Tecnología. 21;1 (2019) 65-76. https://dx.doi.org/10.4067/S0718-221X2019005000106.
[20] R. Bergman, M. Puettmann, A. Taylor, K.E. Skog, The Carbon Impacts of Wood Products, Forest Product Journal. 64 (2014) 220–31. https://doi.org/10.13073/FPJ-D-14-00047.
[21] P. Leskinen et al, Substitution effects of wood-based products in climate change mitigation, From Science to Policy 7. European Forest Institute. https://doi.org/10.36333/fs07
[22] M-C Trouy, P. Triboulot, Matériau bois - Structure et caractéristiques, Techniques de l'ingénieur. 2019, pp.C925 v4. https://doi.org/10.51257/a-v4-c925.
[23] D. Guitard, Mécanique du matériau bois et composites, Cépaduès Editions, Toulouse, France 1987.
[24] I. Rahayu, L. Denaud, R. Marchal, W. Darmawan, Ten new poplar cultivars provide laminated veneer lumber for structural application. Annals of Forest Science. 72 (2015) 705–15. https://doi.org/10.1007/s13595-014-0422-0.
[25] J. Gáborík, K. Káčerová, Bending properties of laminated wood from juvenile poplar, Proc 2nd Int Sci Conf Woodwork Tech. Zalesina Croatia 11-15 Sept 2007 pp 233–40.
[26] F.F.P. Kollmann, W.A. Côté, Principles of Wood Science and Technology in Solid wood, Springer-Verlag, New York, 1968.
[27] P. Jodin, Le bois matériau d'ingénierie, ARBOLOR, Nancy, 1994. ISBN 2907086073.
[28] S. Girardon, L. Denaud, G. Pot, I. Rahayu, Modelling the effects of wood cambial age on the effective modulus of elasticity of poplar laminated veneer lumber, Annals of Forest Science. 73 (2016) 615–24. https://doi.org/10.1007/s13595-016-0569-y.
[29] J-F. Siau, Transport Processes in Wood, Springer-Verlag, New York, 1984. https://doi.org/10.1007/978-3-642-69213-0.
[30] J.M. Dinwoodie, Wood: Nature's cellular polymeric composite. Phys Technol 1978;9:185–91. https://doi.org/10.1088/0305-4624/9/5/302
[31] J. Bodig, B.A. Jayne, Mechanics of Wood and Wood Composites, Van Nostrand Reinhold, 1982.
[32] R.J. Ross, Wood handbook: wood as an engineering material, U.S. Department of Agriculture, Forest Service, Forest Products Laboratory, Madison WI, 2010. https://doi.org/10.2737/FPL-GTR-190.
[33] L.J. Gibson, M. F. Ashby, Cellular solids: structure and properties, Cambridge University Press, Cambridge, 1997. https://doi.org/10.1017/CBO9781139878326.
[34] Y. Aminanda, B. Castanié, J-J. Barrau, P. Thevenet, Experimental analysis and modeling of the crushing of honeycomb cores, Applied Composite Materials. 12 (2005) 213-227
[35] S. Holmberg, K. Persson, H. Petersson, Nonlinear mechanical behaviour and analysis of wood and fibre materials, Computer and Structures. 72 (1998) 459–80. https://doi.org/10.1016/s0045-7949(98)00331-9.
[36] M. Borrega, L.J. Gibson, Mechanics of balsa (Ochroma pyramidale) wood, Mechanic of Materials 84 (2015) 75-90. https://doi.org/10.1016/j.mechmat.2015.01.014.
[37] M. Renaud, M. Rueff, A.C. Rocaboy, Mechanical behaviour of saturated wood under compression Part 2: Behaviour of wood at low rates of strain some effects of compression on wood structure. Wood Science and Technolology 30 (1996) 237–243. https://doi.org/10.1007/BF00229346.
[38] C. Sola, B. Castanié, L. Michel, F. Lachaud, A. Delabie, E. Mermoz, On the role of kinking in the bearing failure of composite laminates, Composite Structures. 141 (2016) 184-193. https://doi.org/10.1016/j.compstruct.2016.01.058
[39] http://www-materials.eng.cam.ac.uk/mpsite/interactive_charts (accessed 16 july 2023).
[40] M.F. Ashby, D. CEBON, Materials selection in mechanical design, Le Journal de Physique IV. 1;3 1993 C7-1.

[41] M. Moutee, Modélisation du comportement mécanique du bois au cours du séchage, PhD Thesis, Université de Laval, Québec, 2006.
[41] P. Navi, F. Heger, Comportement thermo-hydromécanique du bois, Presses Polytechniques Romandes, Lausanne, 2005.
[42] B. Omnes, Modélisation micromécanique du comportement d'élastomères chargés, PhD Thesis, Université de Bretagne-Sud, Lorient, 2007.
[43] L.C. Palka, Predicting the effect of specific gravity, moisture content, temperature and strain rate on the elastic properties of softwoods, Wood Science and Technolology. 7 (1973) 127–41. https://doi.org/10.1007/BF00351155.
[44] J. Susainathan, F. Eyma, E. De Luycker, A. Cantarel, B. Castanié, Manufacturing and quasi-static bending behavior of wood-based sandwich structures, Composite Structures. 182 (2017) 487-504. https://doi.org/10.1016/j.compstruct.2017.09.034
[45] A.L. Shigo, How tree branches are attached to trunks, Canadian Journal of Botany. 63;8 (1985) 1391–1401. https://doi.org/10.1139/b85-193
[46] M. Hu, et al., Fibre directions at a branch-stem junction in Norway spruce: a microscale investigation using X-ray computed tomography. Wood Science and Technology. 56 (2022) 147–169. https://doi.org/10.1007/s00226-021-01353-y
[47] N. As, Y. Goker, T. Dundar, Effect of knots on the physical and mechanical properties of scots pine, Wood Research. 51 (2006) 51–58.
[48] V. Daval, G. Pot, M. Belkacemi, F. Meriaudeau, R. Collet, Automatic measurement of wood fiber orientation and knot detection using an optical system based on heating conduction, Optic Express. 23 (2015) 33529-33539. https://doi.org/10.1364/OE.23.033529.
[49] G. Ravenshorst, W. Gard, J.W. Van de Kuilen, Influence of slope of grain on the mechanical properties of tropical hardwoods and the consequences for grading, European Journal of Wood and Wood Products. 78 (2020) 915–21. https://doi.org/10.1007/s00107-020-01575-0.
[50] S-W. Hwang, T. Lee, H. Kim, H. Chung, J.G. Choi, H. Yeo, Classification of wood knots using artificial neural networks with texture and local feature-based image descriptors, Holzforschung. 76 (2022) 1–13. https://doi.org/10.1515/hf-2021-0051.
[51] B. Clair, B. Thibaut, Physical and mechanical properties of reaction wood, The biology of reaction wood. Springer Series in Wood Science, 2014, 171-200. https://doi.org/10.1007/978-3-642-10814-3_6
[52] Y. Erdil, A. Kasal , J.L. Zhang, H. Efe, T. Dizel, Comparison of Mechanical Properties of Solid Wood and Laminated Veneer Lumber Fabricated from Turkish Beech, Scotch Pine, and Lombardy Poplar, Forest Product Journal. 59 (2009) 55–60.
[53] H. Sasaki, A. Abdullahi, Lumber: Laminated Veneer, K. H. J. Buschow (Ed.), Encyclopedia of Materials: Science and Technology, Elsevier, Amsterdam, 2001, pp. 4678–4680. doi: 10.1016/B978-0-12-803581-8.01989-5
[54] M. Jakob et al. The strength and stiffness of oriented wood and cellulose-fibre materials: A review, Progress in Material Sciences. 125 (2022) 100916. https://doi.org/10.1016/j.pmatsci.2021.100916
[55] W. M. McKenzie, Fundamental analysis of the wood-cutting process, PhD Thesis. University of Michigan, 1961.
[56] John C. F. Walker, Primary Wood Processing, Principles and Practice, Springer Netherlands 2006. https://doi.org/10.1007/1-4020-4393-7.
[57] J. Fondronnier, J. Guillerm, Technologie du déroulage, Cahier du Centre technique du bois, ISSN 1979;5284937:64.

[58] I. Aydin, G. Colakoglu, S. Hiziroglu, Surface characteristics of spruce veneers and shear strength of plywood as a function of log temperature in peeling process, Internatinal Journal of Solids and Structures 43 (2006) 6140–7. https://doi.org/10.1016/j.ijsolstr.2005.05.034.

[59] R. Frayssinhes, Optimisation des paramètres de déroulage du douglas et modélisation des propriétés mécaniques de panneaux de LVL intégrant les données sylvicoles, PhD Arts et Metiers Institute of Technology, Cluny, France (2020).

[60] B. Thibaut, R. Marchal, Tranchage et déroulage, Mémento du forestier tropical, Quae, Versailles, 2015. https://doi.org/10.1515/hf-2020-0209.
[61] F.F.P. Kollmann, E.W. Kuenzi, A.J. Stamm, Principles of Wood Science and Technology : Wood based materials, Springer Berlin Heidelberg 1975. https://doi.org/10.1007/978-3-642-87931-9
[62] M. Pramreiter et al, Predicting strength of Finnish birch veneers based on three different failure criteria, Holzforschung; 75 (2021) 847–56. https://doi.org/10.1515/hf-2020-0209.
[63] M. Pramreiter et al. The Influence of Thickness on the Tensile Strength of Finnish Birch Veneers under Varying Load Angles. Forests 12 (2021) 87. https://doi.org/10.3390/f12010087.
[64] M. Lechner, P. Dietsch, S. Winter, Veneer-reinforced timber – Numerical and experimental studies on a novel hybrid timber product, Construction and Building Materials. 298 (2021) 123880. https://doi.org/10.1016/j.conbuildmat.2021.123880
[65] B. Palubicki, R. Marchal, J.-C. Butaud, L. E. Denaud, L. Bleron, R. Collet, G. Kowaluk, A Method of Lathe Checks Measurement; SMOF device and its software, European Journal of Wood and Wood Products 10 (2010) 151.

[66] P. Bekhta, S. Hiziroglu, O. Shepelyuk, Properties of plywood manufactured from compressed veneer as building material, Material and Design. 30 (2009) 947–53. https://doi.org/10.1016/j.matdes.2008.07.001
[67] J. Xavier, M. Oliveira, J. Morais, T. Pinto, Measurement of the shear properties of clear wood by the Arcan test, Holzforschung. 63 (2009) 217-225. https://doi.org/10.1515/HF.2009.034.
[68] J-C. Xavier, N.M. Garrido, M. Oliveira, J-L. Morais, P.P. Camanho, F. Pierron, A comparison between the Iosipescu and off-axis shear test methods for the characterization of Pinus Pinaster Ait, Composite Part A. 35 (2004) 827–40. https://doi.org/10.1016/j.compositesa.2004.01.013.
[69] A. Dietzel, H. Raßbach, R. Krichenbauer, Material Testing of Decorative Veneers and Different Approaches for Structural-Mechanical Modelling: Walnut Burl Wood and Multilaminar Wood Veneer, BioResources. 11 (2016) 7431–50. https://doi.org/10.15376/biores.11.3.7431-7450.
[70] A. Rohumaa, C.G. Hunt, M. Hughes, C.R Frihart, J. Logren, The influence of lathe check depth and orientation on the bond quality of phenol-formaldehyde – bonded birch plywood, Holzforschung. 67 (2013) 779–86. https://doi.org/10.1515/hf-2012-0161.
[71] W. Li, Z. Zhang, S. He, G. Zhou, C. Mei, The effect of lathe checks on the mechanical performance of LVL. European Journal of Wood and Wood Products 78 (2020) 545–54. https://doi.org/10.1007/s00107-020-01526-9.
[72] W. Leggate, R. McGavin, H. Bailleres. A guide to manufacturing rotary veneer and products from small logs. ACIAR Monograph. 2017
[73] G. Pot, L. E. Denaud, R. Colle, Numerical study of the influence of veneer lathe checks on the elastic mechanical properties of laminated veneer lumber (LVL) made of beech, *Holzforschung.* 69 (2015) 247-316. https://doi.org/10.1515/hf-2014-0011.

[74] W.E. Hillis, A.N. Rozsa, The Softening Temperatures of Wood, Holzforschung. 32 (1978) 68–73. https://doi.org/10.1515/hfsg.1978.32.2.68.

[75] L. Rautkari, M. Properzi, F. Pichelin, M. Hughes, Properties and set-recovery of surface densified Norway spruce and European beech, Wood Science and Technology. 44 (2010) 679–91. https://doi.org/10.1007/s00226-009-0291-0.

[76] P. Navi, F. Girardet, Effects of Thermo-Hydro-Mechanical Treatment on the Structure and Properties of Wood, Holzforschung. 54 (2000) 287–293. https://doi.org/10.1515/HF.2000.048.
[77] M. Gaff, M. Gašparík, Influence of Densification on Bending Strength of Laminated Beech Wood, BioResources. 10 (2015)1506–18. https://doi.org/10.15376/biores.10.1.1506-1518.
[78] M. Jakob, I. Czabany, S. Veigel, U. Müller, W. Gindl-Altmutter, Comparing the suitability of domestic spruce, beech, and poplar wood for high-strength densified wood, European Journal of Wood and Wood Products. 80 (2022) 859–76. https://doi.org/10.1007/s00107-022-01828-0.
[79] R. Kurt, M. Cil, Effects of press pressures on glue line thickness and properties of laminated veneer lumber glued with phenol formaldehyde adhesive, BioResources. 7 (2012) 5346–54. https://doi.org/10.15376/biores.7.4.5346-5354.
[80] F.A. Kamke, densified radiata pine for structural composites. Maderas Ciencia y Tecnología. 8 (2006) 83-92. https://doi.org/10.4067/S0718-221X2006000200002.
[81] A. Kutnar, F.A. Kamke, M. Sernek, The mechanical properties of densified VTC wood relevant for structural composites, Holz Als Roh- Werkst 66 (2008) 439–46. https://doi.org/10.1007/s00107-008-0259-z.
[82] Md. I. Shams, H. Yano, K. Endou, Compressive deformation of wood impregnated with low molecular weight phenol formaldehyde (PF) resin III: effects of sodium chlorite treatment. Journal of Wood Science. 51 (2005) 234–8. https://doi.org/10.1007/s10086-004-0638-y.
[83] I. Gavrilović-Grmuša, M. Dunky, M. Djiporović-Momčilović, M. Popović, J. Popović, Influence of Pressure on the Radial and Tangential Penetration of Adhesive Resin into Poplar Wood and on the Shear Strength of Adhesive Joints, BioResources. 11 (2016) 2238–55. https://doi.org/10.15376/biores.11.1.2238-2255.
[84] A.A. Marra, Technology of wood bonding: principles in practice, Van Nostrand Reinhold New York 1992.
[85] C.G. Hunt, C.R. Frihart, M. Dunky, A. Rohumaa, Understanding Wood Bonds–Going Beyond What Meets the Eye: A Critical Review. In: Mittal KL, editor. Prog. Adhes. Adhes. 1st ed., Wiley; 2019, p. 353–419. https://doi.org/10.1002/9781119625322.ch8.
[86] P. Wei, X. Rao, B.J. Wang, C. Dai, A modified theory of composite mechanics to predict tensile modulus of resinated wood, Wood Research. 60 (2015) 567-582.
[87] I. Gavrilović-Grmuša, M. Dunky, J. Miljković, M. Djiporović-Momčilović, Influence of the degree of condensation of urea-formaldehyde adhesives on the tangential penetration into beech and fir and on the shear strength of the adhesive joints. European Journal of Wood and Wood Products. 70 (2012) 655–65. https://doi.org/10.1007/s00107-012-0599-6.
[88] F.A. Kamke, J.N. Lee, Adhesive Penetration in Wood—a Review. Wood and Fiber Science. 39 (2007) 205–20.
[89] I. Gavrilović-Grmuša, M. Dunky, J. Miljković, M. Djiporović-Momčilović, Influence of the viscosity of UF resins on the radial and tangential penetration into poplar wood and on the shear strength of adhesive joints, Holzforschung. 66 (2012) 849–56. https://doi.org/10.1515/hf-2011-0177.
[90] P.F.S. Hass, Penetration behavior of adhesives into solid wood and micromechanics of the bondline, PhD Thesis. ETH Zurich, 2012.
[91] D. J Cown, Comparison of the Pilodyn and torsiometer methods for the rapid assessment of wood density in living trees, New Zealand Journal of Forestry Science. 8 (1978) 384-391

[92] F. Rinn, F-H. Schweingruber, E. Schär, RESISTOGRAPH and X-Ray Density Charts of Wood. Comparative Evaluation of Drill Resistance Profiles and X-ray Density Charts of Different Wood Species, Holzforschung. 50; 4 (1996) 303-311. https://doi.org/10.1515/hfsg.1996.50.4.303
[93] X. Wang, Acoustic measurements on trees and logs: a review and analysis. Wood Science and Technology. 47 (2013) 965–975. https://doi.org/10.1007/s00226-013-0552-9

[94] L. Schimleck, et al, Non-destructive evaluation techniques and what they tell us about wood property variation, Forests. 10(9) (2019) 728. https://doi.org/10.3390/f10090728
[95] U. Bergsten, J. Lindeberg, A. Rindby, R. Evans, Batch measurements of wood density on intact or prepared drill cores using x-ray microdensitometry, Wood Science and Technology. 35;5 (2001) 435-452. https://doi.org/10.1007/s002260100106
[96] V. Decoux, É. Varcin, J. M. Leban, Relationships between the intra-ring wood density assessed by X-ray densitometry and optical anatomical measurements in conifers. Consequences for the cell wall apparent density determination, Annals of forest science. 61 (2004)251-262. https://doi.org/10.1051/forest:2004018
[97] C. Freyburger, F. Longuetaud, F. Mothe, T. Constant, J. M. Leban, Measuring wood density by means of X-ray computer tomography, Annals of forest science. 66 (2009) 804. https://doi.org/10.1051/forest/2009071
[98] A. M. Beigzadeh, M. R. R. Vaziri, Z. Soltani, H. Afarideh, Design and improvement of a simple and easy-to-use gamma-ray densitometer for application in wood industry, Measurement. 138 (2019) 157-161. https://doi.org/10.1016/j.measurement.2019.02.017
[99] F. Divs, S. Szegedi, P. Raics, Local densitometry of wood by gamma back-scattering, Holz als Roh- und Werkstoff. 4;54 (1996) 279-281.
[100] B. Goy, P. Martin, J. M. Leban, The measurement of wood density by microwave sensor, Holz Als Roh-Und Werkstoff. 50 (1992) 163-166.
[101] B. Ahmed, Determination of Density and Moisture Content of Wood Using Terahertz Time Domain Spectroscopy, Doctoral dissertation, University of Northern British Columbia, 2014.
[102] M. Koch, S. Hunsche, P. Schumacher, M. C. Nuss, J. Feldmann, J. Fromm, THz-imaging: a new method for density mapping of wood, Wood Science and Technology. 32 (1998) 421–427. https://doi.org/10.1007/BF00702799
[103] A. Vander Vorst, A. Rosen, Y. Kotsuka, RF/microwave interaction with biological tissues Wiley-IEEE Press February 2006 ISBN: 978-0-471-75204-2
[104] E. Abbe, Neue Apparate zur Bestimmung des Brechungs und Zerstreuungsvermögens fester und flüssiger Körper, Jenaische Zeitschrift für Naturwissenschaft. Jena, Germany: Mauke's Verlag. 8. (1874) 96–174.
[105] J. F. Lutz, Wood Veneer: Log Selection, Cutting, and Drying, Forest Products Laboratory. Madison, WI, 1978.
[106] L. Tomppo, M. Tiitta, R. Lappalainen, Ultrasound evaluation of lathe check depth in birch veneer. European Journal of Wood and Wood Products. 67 (2009) 27–35. https://doi.org/10.1007/s00107-008-0276-y
[107] L.E. Denaud, L. Bléron, A. Ratlec, R. Marchal, Online control of wood peeling process: acoustical and vibratory measurements of lathe checks frequency, Annals of forest science. 64(2007) 569–575. https://doi.org/10.1051/forest:2007034
[108] B. Pałubicki, et al, A method of lathe checks measurement; SMOF device and its software. European Journal of Wood and Wood Products. 68 (2010) 151–159. https://doi.org/10.1007/s00107-009-0360-y
[109] T. Antikainen, J. Eskelinen, A. Rohumaa, T. Vainio, M. Hughes, Simultaneous measurement of lathe check depth and the grain angle of birch (Betula pendula Roth) veneers using laser trans-illumination imaging, Wood Science and Technology. 49 (2015) 591-605.
[110] R.L. Hankinson, Investigation of Crushing Strength of Spruce. at Varying Angles of Grain. Air Service Information. Circular No. 259, (1921) , U.S. Air Service.

[111] T. Wang, Y. Wang, R. Crocetti, M. Wålinder, In-plane mechanical properties of birch plywood, Construction and Building Materials. 340 (2022) 127852. https://doi.org/10.1016/j.conbuildmat.2022.127852
[112] E. A. Anderson, A. Koehler, Instruments for rapidly measuring slope of grain in lumber, Forest Product Laboratory. Madison, WI, 1955.
[113] J. Viguier, C. Bourgeay, A. Rohumaa, G. Pot, L. Denaud, An innovative method based on grain angle measurement to sort veneer and predict mechanical properties of beech laminated veneer lumber, Construction and Building Materials. 181 (2018) 146–55. https://doi.org/10.1016/j.conbuildmat.2018.06.050.
[114] R. Curti, B. Marcon, L. Denaud, R. Collet, Effect of Grain Direction on Cutting Forces and Chip Geometry during Green Beech Wood Machining, BioRessources. 13 (2018) 5491–5503.
[115] T. Ehrhart, R. Steiger, A. Frangi, A non-contact method for the determination of fibre direction of European beech wood (Fagus sylvatica L.), European Journal of Wood and Wood Products. 76 (2018) 925–35. https://doi.org/10.1007/s00107-017-1279-3.
[116] V. Bucur, Techniques for high resolution imaging of wood structure: a review, Measurement Science and Technology. 14 (2003) R91. https://doi.org/10.1088/0957-0233/14/12/R01.
[117] C. Bouvet, Mechanics of aeronautical composite materials, John Wiley & Sons, 2017.
[118] M. Okuma, Plywood properties influenced by the glue line, Wood Science and Technology. 10 (1976) 57–68. https://doi.org/10.1007/BF00376385.
[119] P. Wei, B.J. Wang, X. Wan, X. Chen, Modeling and prediction of modulus of elasticity of laminated veneer lumber based on laminated plate theory. Construction and Building Materials. 196 (2019) 437–42. https://doi.org/10.1016/j.conbuildmat.2018.11.137
[120] G. Pot, L. Denaud, R. Collet, Numerical study of the influence of veneer lathe checks on the elastic mechanical properties of laminated veneer lumber (LVL) made of beech, Holzforschung. 69 (2015) 337-345. https://doi.org/10.1515/hf-2014-0011.
[121] A. Tabiei, J. Wu, Three-dimensional nonlinear orthotropic finite element material model for wood, Composite Structures. 50 (2000) 143–9. https://doi.org/10.1016/S0263-8223(00)00089-1.
[122] Y. D. Murray, J. D. Reid, R. K. Faller, B. W. Bielenberg, and T. J. Paulsen, Evaluation of LS-DYNA wood material model 143, United States. Federal Highway Administration, Washington, 2005.
[123] J. Susainathan, F. Eyma, E. De Luycker, A. Cantarel, B. Castanié, Numerical modeling of impact on wood-based sandwich structures, Mechanics of Advanced Materials and Structures.
27 (2020) 1583–98. https://doi.org/10.1080/15376494.2018.1519619.
[124] H. Wang, K.R. Ramakrishnan, K. Shankar, Experimental study of the medium velocity impact response of sandwich panels with different cores, Material & Design. 99 (2016) 68‑82. https://doi.org/10.1016/j.matdes.2016.03.048.
[125] T. Maillot, V. Lapoujade, E. Grippon, B. Toson, N. Bardon, and J.-J. Pesque, Comparative Study of Material Laws Available in LS-DYNA® to Improve the Modeling of Balsa Wood, presented at the 13th International LS-DYNA Users Conference, Detroit, 2014.
[126] G. Baumann, U. Müller, R. Brandner, and F. Feist, A comparative study of material models for solid and laminated birch wood over wide ranges of strain, strain-rate and temperature, presented at the ECCOMAS 2022, Oslo, 2022.

[127] G. Baumann, U. Müller, S. Hartmann, C. Kurzböck, and F. Feist, Modelling solid wood in LS-Dyna Pros and Cons of Mat58, Mat126 and Mat143, presented at the IWCMM29, Dubrovnik, Croatia, 2019.
[128] M. Oudjene, M. Khelifa, Finite element modelling of wooden structures at large deformations and brittle failure prediction, Materials and Design. 30 (2009) 4081–7. https://doi.org/10.1016/j.matdes.2009.05.024.

[130] A. Makowski, Analytical Analysis of Distribution of Bending Stresses in Layers of Plywood with Numerical Verification, Drvna industrija. 70 (2019) 77–88. https://doi.org/10.5552/drvind.2019.1823.
[131] T. Akgul, A.C. Apay, E. Aydin, Y. Sumer, Study of Bending Strength and Numerical Modeling of Wooden and Plywood Frame Elements, Acta Physica Polonica A. 127 (2015) 1414–6. https://doi.org/10.12693/APhysPolA.127.1414.
[132] M. Merhar, Application of Failure Criteria on Plywood under Bending, Polymers. 13 (2021) 4449. https://doi.org/10.3390/polym13244449.
[133] M. Merhar, Determination of Elastic Properties of Beech Plywood by Analytical, Experimental and Numerical Methods, Forests. 11 (2020) 1221. https://doi.org/10.3390/f11111221.
[134] D. Zerbst, et al, Modelling Inhomogeneity of Veneer Laminates with a Finite Element Mapping Method Based on Arbitrary Grayscale Images, Materials 13 (2020) 2993. https://doi.org/10.3390/ma13132993.
[135] P.L. Clouston, F. Lam, Computational Modeling of Strand-Based Wood Composites, ASCE Journal of Engineering Mechanics. 127 (2001) 844-851. https://doi.org/10.1061/(ASCE)0733-9399(2001)127:8(844).
[136] J. Ek V. Norbäck, Modeling of laminated veneer lumber - A study of the material properties for thick structural elements. Master's Thesis. Chalmers University of Technology, 2020.
[137] B.P. Gilbert, H. Bailleres, H. Zhang, R.L. McGavin, Strength modelling of Laminated Veneer Lumber (LVL) beams. Construction and Building Materials. 149 (2017) 763–77.
[138] P.L. Clouston, F. Lam, A stochastic plasticity approach to strength modeling of strand-based wood composites, Composite Science and Technology. 62 (2002) 1381–95. https://doi.org/10.1016/S0266-3538(02)00086-6.
[139] M. Ardalany, M. Fragiacomo, P. Moss, Modeling of Laminated Veneer Lumber Beams with Holes Using Cohesive Elements, Journal of Structural Engineering. 142 (2016) 04015102. https://doi.org/10.1061/(ASCE)ST.1943-541X.0001338.
[140] A. El Moustaphaoui, A. Chouaf, K. Kimakh, M. Chergui, Determination of the onset and propagation criteria of delamination of Ceiba plywood by an experimental and numerical analysis, Wood Material Science & Engineering. 16 (2021) 325–35. https://doi.org/10.1080/17480272.2020.1737963.
[141] B.P. Gilbert, D. Dias-da-Costa, A. Lebée, G. Foret, Veneer-based timber circular hollow section beams: Behaviour, modelling and design, Construction and Building Materials. 258 (2020) 120380. https://doi.org/10.1016/j.conbuildmat.2020.120380.
[142] U. Müller, A. Sretenovic, A. Vincenti, W. Gindl, Direct measurement of strain distribution along a wood bond line. Part 1: Shear strain concentration in a lap joint specimen by means of electronic speckle pattern interferometry, Holzforschung 59 (2005) 300–6. https://doi.org/10.1515/HF.2005.050.
[143] E. Serrano, A numerical study of the shear-strength-predicting capabilities of test specimens for wood–adhesive bonds, International Journal of Adhesion and Adhesives. 24 (2004) 23–35. https://doi.org/10.1016/S0143-7496(03)00096-4.
[144] E.I. Saavedra Flores, K. Saavedra, J. Hinojosa, Y. Chandra, R. Das, Multi-scale modelling of rolling shear failure in cross-laminated timber structures by homogenisation and cohesive zone models, International Journal of Solids and Structures. 81 (2016) 219–232.

[145] F. Šebek, P. Kubík, M. Brabec, J. Tippner, Modelling of impact behaviour of European beech subjected to split Hopkinson pressure bar test, Composite Structures. 245 (2020) 112330.
[146] C. Bouvet, B. Castanié, M. Bizeul, J.-J. Barrau, Low velocity impact modelling in laminate composite panels with discrete interface elements, International Journal of Solids and Structures. 46 (2009) 2809–2821.

[147] P. Journoud, C. Bouvet, B. Castanié, F. Laurin, L. Ratsifandrihana, Experimental and numerical analysis of unfolding failure of L-shaped CFRP specimens, Composite Structures. 232 (2020) 111563. 10.1016/j.compstruct.2019.111563
[148] J. Serra, C. Bouvet, B. Castanié, C. Petiot, Experimental and numerical analysis of Carbon Fiber Reinforced Polymer notched coupons under tensile loading, Composite Structures. 181 (2017) 145–157.
[149] P. Journoud, C. Bouvet, B. Castanié, L. Ratsifandrihana, Experimental analysis of the effects of wrinkles in the radius of curvature of L-shaped carbon-epoxy specimens on unfolding failure, Composite Part A. 158 (2022) 106975. 10.1016/j.compositesa.2022.106975
[150] P. Journoud, C. Bouvet, B. Castanié, L. Ratsifandrihana, Numerical analysis of the effects of wrinkles in the radius of curvature of L- shaped CFRP specimens on unfolding failure, Composite Structures. 299 (2022) 116107. 10.1016/j.compstruct.2022.116107
[151] J. Susainathan, F. Eyma, E. De Luycker, A. Cantarel, B. Castanié, Experimental investigation of impact behavior of wood-based sandwich structures, Composites Part A. 109 (2018) 10–19
[152] J. Susainathan, F. Eyma, E. De Luycker, A. Cantarel, B. Castanié, Experimental investigation of compression and compression after impact of wood-based sandwich structures, Composite Structures. 220 (2019) 236–249.
[153] F. Neveu, C. Cornu, P. Olivier, B. Castanié, Manufacturing and impact behaviour of aeronautic overmolded grid-stiffened thermoplastic carbon plates, Composite Structures. 284 (2022) 115228. https://doi.org/10.1016/j.compstruct.2022.115228
[154] Y. Aminanda, B. Castanié, J.-J. Barrau, P. Thevenet, Experimental and numerical study of compression after impact of sandwich structures with metallic skins, Composites Science and Technology. 69 (2009) 50-59. https://doi.org/10.1016/j.compscitech.2007.10.045.
[155] B. Castanié, C. Bouvet, M. Ginot, Review of composite sandwich structure in aeronautic applications, Composites Part C. 1 (2020) 100004.

[156] M. Basha, A. Wagih, A. Melaibari, G. Lubineau, A.M. Abdraboh, M.A. Eltaher, Impact and post-impact response of lightweight CFRP/wood sandwich composites, Composite Structures. 279 (2022) 114766. https://doi.org/10.1016/j.compstruct.2021.114766.
[157] G. Palomba, G. Epasto, V. Crupi, Lightweight sandwich structures for marine applications: a review, Mechanics of Advanced Materials and Structures. 29 (2022) 4839–4864. doi: 10.1080/15376494.2021.1941448
[158] P. Wei, J. Chen, Y. Zhang, L. Pu, Wood-based sandwich panels: a review, Wood Research. 66 (2021) 875–90. https://doi.org/10.37763/wr.1336-4561/66.5.875890.
[159] E. Labans, K. Zudrags, K. Kalnins, Structural Performance of Wood Based Sandwich Panels in Four Point Bending, Procedia Engineering. 172 (2017) 628-633. https://doi.org/10.1016/j.proeng.2017.02.073.
[160] P. R. Oliveira, M. May, T. H. Panzera, S. Hiermaier, Bio-based/green sandwich structures: A review, Thin-Walled Structures. 177 (2022) 109426. https://doi.org/10.1016/j.tws.2022.109426.
[161] T.K. Demircioğlu, F. Balıkoğlu, O. İnal, N. Arslan, İ. Ay, A. Ataş, Experimental investigation on low-velocity impact response of wood skinned sandwich composites with different core configurations, Materials Today Communications, 17 (2018) 31-39. https://doi.org/10.1016/j.mtcomm.2018.08.003.

[162] E. Biblis, Analysis of wood-fiberglass composite beams within and beyond the elastic region, Forest Product Journal. 15 (1965) 81-88.
[163] T.L. Laufenberg, R.E. Rowlands, G.P. Krueger, Economic feasibility of synthetic fiber reinforced laminated veneer lumber (LVL), Forest Product Journal. 34 (1984) 15-22.
[164] M.P. Ansell, Hybrid wood composites-integration of wood with other engineering materials,

Wood Composites. 54 (2015) 411-426. https://doi.org/10.1016/B978-1-78242-454-3.00016-0
[165] P. Wei, B.J. Wang, D. Zhou, C. Dai, Q. Wang, S. Huang. Mechanical properties of poplar laminated veneer lumber modified by carbon fiber reinforced polymer. Bioresources, 8 (4) (2013), pp. 4883-4898, 10.15376/biores.10.4.7455-7465.
[166] F.J. Rescalvo, R. Duriot, G. Pot, A. Gallego, L. Denaud. Enhancement of bending properties of Douglas-fir and poplar laminate veneer lumber (LVL) beams with carbon and basalt fibers reinforcement. Construct. Build. Mater., 263 (2020), Article 120185, 10.1016/j.conbuildmat.2020.120185
[167] Z. Pengyi, S. Shijie, M.A. Chunmei. Strengthening mechanical properties of glulam with basalt fiber. Adv. Natural Sci., 4 (2) (2011), pp. 130-133.
[168] A. Zhou, R. Qin, C.L. Chow, D. Lau, Bond integrity of aramid, basalt and carbon fiber reinforced polymer bonded wood composites at elevated temperature, Composite Structures. 245 (2020) 112342. https://doi.org/10.1016/j.compstruct.2020.112342.
[169] A. P. Acosta, A.A. Xavier da Silva, R. de Avila Delucis, S. Campos Amico, Wood and wood-jute laminates manufactured by vacuum infusion, Journal of Building Engineering. 64 (2023) 105619. https://doi.org/10.1016/j.jobe.2022.105619.
[170] J. Jorda, et al, Investigation of 3D-Moldability of Flax Fiber Reinforced Beech Plywood, Polymers. 12 (2020) 2852. https://doi.org/10.3390/polym12122852
[171] B. Moezzipour, M. Ahmadi, A. Moezzipour, Physical and mechanical properties of reinforced ply wood with natural fibers, Journal of the Indian Academy of Wood Science 14 (2017) 70–73. https://doi.org/10.1007/s13196-017-0189-7
[172] Z.Q. Wang, X. N. Lu, X. J. Huang, Reinforcement of Laminated Veneer Lumber with Ramie Fibre, Advanced Materials Research. 332–334 (2011) 41–44.
[173] R. Karri, R. Lappalainen, L. Tomppo, R. Yadav, Bond quality of poplar plywood reinforced with hemp fibers and lignin-phenolic adhesives, Composites Part C. 9 (2022) 100299.
[174] F. Neveu, B. Castanié, P.Olivier, The GAP methodology: A new way to design composite structures, Materials & Design.172 (2019) 107755. https://doi.org/10.1016/j.matdes.2019.107755.
[175] M. Renaud, M. Rueff, A.C. Rocaboy, Mechanical behaviour of saturated wood under compression: part 1. Behaviour of wood at high rates of strain, Wood science and technology. 30 (1996) 153-64. https://doi.org/10.1007/BF00229346
[176] M. Neumann M, H. Jürgen H, Droste BO, Sylvius H. Compressive behaviour of axially loaded spruce wood under large deformations at different strain rates. European journal of wood and wood products. 2011 Aug 1;69(3):345-57. https://DOI:10.1007/s00107-010-0442-x
[177] S. Widehammar, Stress-strain relationships for spruce wood: Influence of strain rate, moisture content and loading direction, Experimental mechanics. 44 (2004) 44-8. https://doi.org/10.1007/BF02427975
[178] J. Buchar, S. Rolc, J. Lisy, J. Schwengmeier, Model of the wood response to the high velocity of loading, In Proceedings of the 19th International Symposium of Ballistics, Interlaken, Switzerland.
[179] V.L. Tagarielli, V.S. Deshpande, N.A. Fleck, The high strain rate response of PVC foams and end-grain balsa wood, Composites Part B. 39 (2008) 83-91.
https://doi.org/10.1016/j.compositesb.2007.02.005

[180] M. Vural, G. Ravichandran, Dynamic response and energy dissipation characteristics of balsa wood: experiment and analysis, International Journal of Solids and structures. 40 (2003) 2147-70. https://doi.org/10.1016/S0020-7683(03)00057-X
[181] G. J. Attwood, N. Butler, A. J. Neilson, Computer modelling of the impact performance of containers for the transport of radioactive materials, International Journal of Radioactive Materials Transport. 2 (1991) 33-39.

[182] N. Butler, Computer modelling of wood-filled impact limiters, Nuclear engineering and design. 150 (1994) 417-424.
[183] G. Eisenacher, et al., Dynamic crushing characteristics of spruce wood under large deformations, Wood science and technology. 47 (2013) 369–380. https://doi.org/10.1007/s00226-012-0508-5.
[184] T. Polocoser, F. Stoëckel, B. Kasal, Low-velocity transverse impact of small, clear spruce and pine specimens with additional energy absorbing treatments, Journal of Materials in Civil Engineering. 28 (2016). doi:10.1061/(ASCE)MT. 1943-5533.0001545
[185] R.M. Gutkowski, A. Shigidi, M.T. Abdallah, M.L Peterson, Dynamic impact load tests of a bridge guardrail system, MPC report. no. 07-188, Mountain-Plains Consortium, Fargo, ND, 37 pp (2007)
[186] T. Polocoșer, B. Kasal, F. Stöckel, State-of-the-art: intermediate and high strain rate testing of solid wood, Wood science and technology. 51 (2017) 1479–1534. DOI 10.1007/s00226-017-0925-6
[187] J.R. Keeton, Dynamic properties of small, clear specimens of structural-grade timber, U.S. Navy Civ Eng Lab. Technical report R-573, Y-F011-05-04-003, Port Hueneme, CA, United States, 50 pp (1968)
[188] W. Johnson, Historical and present day references concerning impact on wood, International Journal of Impact engineering. 4 (1986) 161-174.
[189] E. Jacques, et al., Influence of high strain rates on the dynamic flexural material properties of spruce–pine–fir wood studs. Canadian journal of civil engineering. 41 (2014) 56–64.
[190] M. Ding, W. K. Binienda, Characterization of Nonlinear Birchwood Model with Strain Rate Effect, Journal of Aerospace Engineering. 35 (2022). https://doi.org/10.1061/(ASCE)AS.1943-5525.0001415
[191] J. Wouts, G. Haugou, M. Oudjene, D. Coutellier, H. Morvan, Strain rate effects on the compressive response of wood and energy absorption capabilities – Part A: Experimental investigations, Composite Structures. 149 (2016)315-328. 10.1016/j.compstruct.2016.03.058
[192] J. Wouts, G. Haugou, M. Oudjene, H. Morvan, D. Coutellier, Strain rate effects on the compressive response of wood and energy absorption capabillities - Part B: Experimental investigation under rigid lateral confinement, Composite Structures. 204 (2018) 95-104. 10.1016/j.compstruct.2018.07.001
[193] S. Pang, Y. Liang, W. Tao, Y. Liu, S. Huan, H. Qin, Effect of the Strain Rate and Fiber Direction on the Dynamic Mechanical Properties of Beech Wood, Forests. 10 (2019) 881. 10.3390/f10100881
[194] X.T. Nguyen, S. Hou, T. Liu, X. Han, A potential natural energy absorption material – Coconut mesocarp: Part A: Experimental investigations on mechanical properties, International Journal of Mechanical Sciences. 115–116 (2016) 564–573. https://doi.org/10.1016/j.ijmecsci.2016.07.017.
[195] T. Liu, S. Hou, X.T. Nguyen, X. Han, Energy absorption characteristics of sandwich structures with composite sheets and bio coconut core, Composite Part B. 114 (2017) 328–338. https://doi.org/10.1016/j.compositesb.2017.01.035
[196] C. Lu, et al., The mystery of coconut overturns the crashworthiness design of composite materials, International Journal of Mechanical Sciences. 168 (2017) 105244. https://doi.org/10.1016/j.ijmecsci.2019.105244.
[197] R. Guélou, F. Eyma, A. Cantarel, S. Rivallant, B. Castanié, Crashworthiness of poplar wood veneer tubes, International Journal of Impact Engineering. 147 (2021) 103738. https://doi.org/10.1016/j.ijimpeng.2020.103738

[198] R. Guélou, F. Eyma, A. Cantarel, S. Rivallant, B. Castanié, Static crushing of wood based sandwich composite tubes, Composite Structures. 273 (2021) 114317. https://doi.org/10.1016/j.compstruct.2021.114317
[199] R. Guélou, F. Eyma, A. Cantarel, S. Rivallant, B. Castanié, Dynamic crushing of wood-based sandwich composite tubes, Mechanics of Advanced Materials and Structures. 29 (2022) 7004–7024. https://doi.org/10.1080/15376494.2021.1991533

[200] R. Guélou, F. Eyma, A. Cantarel, S. Rivallant, B. Castanié, A comparison of three wood species (poplar, birch and oak) for crash application, European Journal of Wood and Wood Products. 81 (2023) 125–141. https://doi.org/10.1007/s00107-022-01871-x
[201] R. Guélou, F. Eyma, A. Cantarel, S. Rivallant, B. Castanié, Static and dynamic crushing of sandwich tubes with a birch core and carbon skins, Proceedings of the 20th European Conference on Composite Materials: Composites Meet Sustainability. 2022, 5, pp. 33–38.
[202] R. Guélou, F. Eyma, A. Cantarel, S. Rivallant, B. Castanié, Static and dynamic crushing of sandwich tubes with composite skins and 3 plywood cores (poplar, birch and oak) Submitted to Int. J. of Crashworthiness.
[203] Y. Zhang, J. Wang, J. Lin, F. Zhang, X. Yan, Crushing mechanical responses of natural wood columns and wood-filled composite columns, Engineering Failure Analysis. 124 (2021) 105358. 10.1016/j.engfailanal.2021.105358
[204] Z. Naghizadeh, et al., Performance Comparison of Wood, Plywood, and Oriented Strand Board under High- and Low-Velocity Impact Loadings, Forest Products Journal. 71 (2021) 362–370. https://doi.org/10.13073/FPJ-D-21-00052
[205] D. Heyner, et al., Innovative concepts for the usage of veneer-based hybrid materials in vehicle structures, Proceedings of the Institution of Mechanical Engineers Part L. 235 (2021) 1302–11. https://doi.org/10.1177/1464420721998398
[206] M.Philippe, Dynamique des voies d'eau et de portage dans le processus de diffusion à grande distance des produits du Grand-Pressigny, APC Editions. Le phénomène Pressignien, N. Mallet, J. Pelegrin, C. Verjux Editors,p. 779-799 (2019).
https://www.academia.edu/42271692/Dynamique_des_voies_deau_et_de_portage_dans_le_processus_de_diffusion_%C3%A0_grande_distance_des_produits_du_Grand_Pressigny
[207] https://fr.wikipedia.org/wiki/Pirogue_de_Pesse (accessed 25th July 2023)
[208] B. Dubos, Les pirogues du lac de Sanguinet, Aquitania. 22 (2006) 7-53.
https://www.persee.fr/doc/aquit_0758-9670_2006_num_22_1_1145
[209] https://www.wonders-of-the-world.net/Pyramids-of-Egypt/Solar-boat-of-Khufu.php (accessed 25th July 2023).
[210] C. Ward, Boat-building and its social context in early Egypt: interpretations from the First Dynasty boat-grave cemetery at Abydos, Antiquity. 80 (2006) 118–129.
https://doi.org/10.1017/S0003598X00093303
[211] C. de Craecker-Dussart, Moyens d'orientation et de navigation des Vikings, marins accomplis en Atlantique Nord (fin VIIIe–XIe siècles), Le Moyen Age. CXXV (2019) 617- 650.
https://www.cairn.info/revue-le-moyen-age-2019-3-page-617.htm
[212] https://en.wikipedia.org/wiki/Vasa_(ship), (accessed 25th July 2023).
[213] https://www.sea.museum/whats-on/our-fleet/hmb-endeavour/ship-specifications (accessed 25th July 2023).
[214] https://fregate-hermione.com (accessed 25th July 2023).
[215]https://fr.wikipedia.org/wiki/Hermione_(frégate,_2014) (accessed 25th July 2023).
[216] https://www.chriscraft.com/our-story/heritage/ (accessed 25th July 2023).
[217]https://en.wikipedia.org/wiki/Wooden_boats_of_World_War_II (accessed 25th July 2023).
[218] https://spirityachts.com/ (accessed 25th July 2023).
[219] https://www.rm-yachts.com/ (accessed 25th July 2023).

[220] A. Elmendorf, Plywood and its Uses in Automobile Construction, SAE Transactions. 15 (1920) 863-884. https://www.jstor.org/stable/44717914

[221] https://tcct.com/news/2020/10/wood-it-will-return/ (accessed 25th July 2023).

[222] http://dfwelitetoymuseum.com/plywood-cars-and-hydraulic-drive-the-wartime-cars-of-ray-russell/ (accessed 25th July 2023).

[223] https://www.hotcars.com/these-drivable-cars-are-made-out-of-wood/ (accessed 25th July 2023).

[224] C. Cremonini, F. Negro, R. Zanuttini, Wood-based panels for land transport uses, Drewno. 58;195 (2015) 125-133. https://iris.unito.it/handle/2318/1550268

[225] http://www.italian.sakura.ne.jp/bad_toys/plywood_monocoque/ (accessed 25th July 2023).

[226] https://silodrome.com/marcos-gt-plywood-chassis/ (accessed 25th July 2023).

[227] https://www.motortrend.com/news/marcos-1600-gt-auction-sale-details-pictures (accessed 25th July 2023).

[228] https://silodrome.com/history-africar/ (accessed 25th July 2023).

[229] https://www.youtube.com/watch?v=zpvDkFL62qA&ab_channel=AfriCar (accessed 25th July 2023).

[230] Howard A. Africar, the development of a car for Africa. 1987 ISBN 1-870427-00-9

[231] https://www.youtube.com/watch?v=p4c9i250pc4&t=442s&ab_channel=MorganMotorCompany (accessed 25th July 2023).

[232] https://www.carthrottle.com/post/why-the-new-aluminium-frame-morgans-use-even-more-wood/ (accessed 25th July 2023).

[233] http://morganrebuild.co.uk/AshFrame.html (accessed 25th July 2023).

[234] https://en.wikipedia.org/wiki/Morgan_Motor_Company (accessed 25th July 2023).

[235] https://mag.toyota.co.uk/wooden-car-concept/ (accessed 25th July 2023).

[236] https://mag.toyota.co.uk/build-a-wooden-car/ (accessed 25th July 2023).

[237] https://www.woodcar.eu/ (accessed 25th July 2023).

[238] https://www.youtube.com/watch?v=EABG6uQCpak&t=788s&ab_channel=UlrichM%C3%BCller%3AHolz%7CWanderreiten%7CKultur (accessed 25th July 2023).

[239] G. Baumann, R. Brandner, U. Müller, A. Stadlmann, F. Feist, Comparative study on the temperature effect of solid birch wood and solid beech wood under impact loading, Materials. 14 (2021) 7616.

[240] U. Müller, et al., Crash simulation of wood and composite wood for future automotive engineering, Wood Material Science & Engineering. 15 (2020) 312–324. https://doi.org/10.1080/17480272.2019.1665581

[241] R.V.V. Petrescu, et al., History of Aviation-A Short Review, Journal of Aircraft and Spacecraft Technology. 1 (2017) 30-49. DOI: 10.3844/jastsp.2017.30.49

[242] https://www1.grc.nasa.gov/beginners-guide-to-aeronautics/wright-brothers-aircraft/ (accessed 25th July 2023).

[243] https://fr.wikipedia.org/wiki/Blériot_XI (accessed 25th July 2023).

[244] Peter J. Jakab. Wood to Metal: The Structural Origins of the Modern Airplane. Journal of Aircraft, vol 36, no 6, pp 914-918 Nov-Dec 1999 https://doi.org/10.2514/2.2551

[245] http://aviadejavu.ru/Site/Crafts/Craft33385.htm (accessed 25th July 2023).

[246] J. Bishop, Aerospace: A pioneer in structural adhesive bonding, Handbook of Adhesives and Sealants. 1 (2005) 215-347. https://www.sciencedirect.com/science/article/abs/pii/S1874569502800069

[247] https://fr.wikipedia.org/wiki/Hughes_H-4_Hercules (accessed 25th July 2023).

[248] https://en.wikipedia.org/wiki/Lockheed_Vega (accessed 25th July 2023).

[249] https://www.thisdayinaviation.com/4-july-1927/ (accessed 25th July 2023).

[250] A. Klemin, Aviation Surveyed, Scientific American. 170;5 (1944) 214-216. https://www.jstor.org/stable/10.2307/24997774

[251] Risbrudt C.D., Ross R.J., Blankenburg J.J., Nelson C.A. [2007]: Forest Products Laboratory supporting the nation's armed forces with valuable wood research for 90 years. Forest Products Journal 57 [1/2]: 7–14.

[252] Forest Products Laboratory (U.S.), Design of wood aircraft structures. U.S. Govt. Print. Off. (1944). Retrieved from 10.5479/sil.1018746.39088017549809

[253] Forest Products Laboratory (U.S.), Wood aircraft inspection and fabrication. U.S. Govt. Print. Off (1944). Retrieved from 10.5479/sil.1018745.39088017549767

[254] J. Bertolini, B. Castanié, J-J. Barrau, J-P. Navarro, C. Petiot, Multi-level experimental and numerical analysis of composite stiffener debonding. Part 2: Element and panel level, Composite Structures. 90 (2009), 392-403.

[255] https://fr.wikipedia.org/wiki/Yakovlev_Yak-1 (accessed 25th July 2023).

[256] https://fr.wikipedia.org/wiki/Heinkel_He_162 (accessed 25th July 2023).

[257]https://commons.wikimedia.org/wiki/File:%22WOOD_FLIES_TO_WAR%22_%28CARGO_PLANES_ARMY_PLYWOOD%29_-_NARA_-_516178.jpg (accessed 25th July 2023).

[258] http://stargazer2006.online.fr/aircraft/pages/variviggen.htm (accessed 25th July 2023).

[259]https://www.robin-aircraft.com/2016/06/selection-achat-et-preparation-de-nos-bois-aeronautiques/ (accessed 25th July 2023).

[260] https://www.robin-aircraft.com/2017/05/pourquoi-la-cellule-du-dr401-est-immortelle/ (accessed 25th July 2023).

[261] https://aura-aero.com/videos/de-bois-et-de-carbone/ (accessed 25th July 2023).

[262] https://www.avionsmauboussin.fr/en/ (accessed 25th July 2023).

[263] https://www.jpl.nasa.gov/blog/2013/11/ranger-impact-limiter

[264] W.J. Carley, Mars Entry and Landing Capsule. JPL Technical Memorandum. 33-236, 1965 https://ntrs.nasa.gov/api/citations/19670001420/downloads/19670001420.pdf

[265] A. C. Knoell. Environmental and Physical Effects on the Response of Balsa Wood as an Energy Dissipator. NASA Technical Report. No. 32-944, 1966. https://ntrs.nasa.gov/api/citations/19660020830/downloads/19660020830.pdf

[266] https://amorimcorkcomposites.com/en-us/ (accessed 25th July 2023).

[265] S. Petit, C. Bouvet, A. Bergerot, J-J. Barrau, Impact and compression after impact experimental study of a composite laminate with a cork thermal shield, Composites Science and Technology 67 (2007) 3286-3299.

[266] https://vintagespace.wordpress.com/2016/12/05/can-a-wood-heat-shield-really-work/ (accessed 25th July 2023).

[267] A.J.Ball, et al., The ExoMars Schiaparelli Entry, Descent and Landing Demonstrator Module (EDM) System Design, Space Science Review 218 (2022). https://doi.org/10.1007/s11214-022-00898-z

[268] G. Pinaud, et al., Exomars 2016: A preliminary postflight study of the entry module heat shield interactions with the martian atmosphere, 15th International Planetary Probe Workshop. Boulder, Colorado, US (2018). Found in researchgate.

[269] G. Pinaud, et al., Exomars mission 2016: A preliminary post-flight performance analysis of the heat shield during entry on Mars atmosphere, AIAA Scitech 2019 Forum. 7-11 January 2019. San Diego, California, paper AIAA 2019- 0244. https://doi.org/10.2514/6.2019-0244

[270] I. Sakraker, O. Chazot, J.P. Carvalho, Performance of cork-based thermal protection material P50 exposed to air plasma. An experimental study, CEAS Space Journal. 14 (2022) 377–393. https://doi.org/10.1007/s12567-021-00395-z

[271] https://www.youtube.com/watch?v=gtxYP9fLMmk (accessed 25th July 2023).

[272] https://www.space.com/wooden-satellite-lignosat-japan-2024 (accessed 25th July 2023).

[273] https://phys.org/news/2021-08-space-wooden-frontier.html (accessed 25th July 2023).

[274] https://phys.org/news/2023-05-space-magnolia-wooden-artificial-satellite.html (accessed 25th July 2023).

[275] https://www.wisaplywood.com/wisawoodsat/ (accessed 25th July 2023).

[276] https://phys.org/news/2021-06-esa-payloads-wooden-satellite.html (accessed 25th July 2023).

[277] https://anr.fr/Projet-ANR-21-CE43-0008 (accessed 25th July 2023).

[278] https://ica.cnrs.fr/boost/ (accessed 25th July 2023).